Rainfall Redistribution and Change of Water Quality in Tropical Forest Canopies: Patterns and Persistence

Alexander Zimmermann

A dissertation submitted to the Faculty of Mathematics and Natural Sciences at the University of Potsdam, Germany
for the degree of Doctor of Natural Sciences (Dr. rer. nat.) in Landscape Ecology and Soil Science.

March 2009

First Referee: Prof. Helmut Elsenbeer, University of Potsdam
Second Referee: Prof. Dirk Hölscher, University of Göttingen
Third Referee: Prof. Richard F. Keim, Lousiana State University

Table of contents

List of figures

List of tables

Abstract

Motivations and research objectives: During the passage of rain water through a forest canopy two main processes take place. First, water is redistributed; and second, its chemical properties change substantially. The rain water redistribution and the brief contact with plant surfaces results in a large variability of both throughfall and its chemical composition. Since throughfall and its chemistry influence a range of physical, chemical and biological processes at or below the forest floor the understanding of throughfall variability and the prediction of throughfall patterns potentially improves the understanding of near-surface processes in forest ecosystems. This thesis comprises three main research objectives. The first objective is to determine the variability of throughfall and its chemistry, and to investigate some of the controlling factors. Second, I explored throughfall spatial patterns. Finally, I attempted to assess the temporal persistence of throughfall and its chemical composition.

Research sites and methods: The thesis is based on investigations in a tropical montane rain forest in Ecuador, and lowland rain forest ecosystems in Brazil and Panama. The first two studies investigate both throughfall and throughfall chemistry following a deterministic approach. The third study investigates throughfall patterns with geostatistical methods, and hence, relies on a stochastic approach.

Results and Conclusions: Throughfall is highly variable. The variability of throughfall in tropical forests seems to exceed that of many temperate forests. These differences, however, do not solely reflect ecosystem-inherent characteristics, more likely they also mirror management practices. Apart from biotic factors that influence throughfall variability, rainfall magnitude is an important control. Throughfall solute concentrations and solute deposition are even more variable than throughfall. In contrast to throughfall volumes, the variability of solute deposition shows no clear differences between tropical and temperate forests, hence, biodiversity is not a strong predictor of solute deposition heterogeneity. Many other factors control solute deposition patterns, for instance, solute concentration in rainfall and antecedent dry period. The temporal variability of the latter factors partly accounts for the low temporal persistence of solute deposition. In contrast, measurements of throughfall volume are quite stable over time. Results from the Panamanian research site indicate that wet and dry areas outlast consecutive wet seasons. At this research site, throughfall exhibited only weak or pure nugget autocorrelation structures over the studies lag distances. A close look at the geostatistical tools at hand provided evidence that throughfall datasets, in particular those of large events, require robust variogram estimation if one wants to avoid outlier removal. This finding is important because all geostatistical throughfall studies that have been published so far analyzed their data using the classical, non-robust variogram estimator.

Kurzfassung

Motivation und Zielsetzung: Wenn Regen durch ein Kronendach fällt lassen sich zwei Prozesse beobachten: das Regenwasser wird umverteilt und die chemische Qualität des Wassers verändert sich erheblich. Die Prozesse im Kronenraum resultieren in einer hohen Variabilität des Bestandsniederschlags und dessen chemischer Zusammensetzung. Bestandsniederschlag beeinflusst eine Reihe von physikalischen, chemischen und biologischen Prozessen am Waldboden. Daher können Untersuchungen zur Variabilität und zu Mustern im Bestandsniederschlag helfen, bodennahe Prozesse besser zu verstehen. Diese Dissertation behandelt hauptsächlich drei Aspekte. Erstens, die Arbeit beschäftigt sich mit der Erfassung der Variabilität im Bestandsniederschlag und dessen chemischer Zusammensetzung, zudem werden Einflussfaktoren dieser Variabilität untersucht. Des Weiteren beschäftigt sich die Arbeit mit räumlichen Mustern des Bestandsniederschlagswassers, und drittens wird die zeitliche Stabilität des Bestandsniederschlags und dessen chemischer Zusammensetzung betrachtet.

Untersuchungsgebiete und Methoden: Diese Dissertation basiert auf Untersuchungen in einem tropischen Bergregenwald in Ecuador, sowie Studien in tropischen Tieflandregenwäldern in Brasilien und Panama. Die ersten zwei Studien untersuchen Bestandsniederschlag und dessen chemische Zusammensetzung mit Hilfe deterministischer Methoden. Die Arbeit in Panama nutzt geostatistische Methoden zur Beschreibung von Bestandsniederschlagsmustern und verfolgt somit einen stochastischen Ansatz.

Ergebnisse und Schlussfolgerungen: Die Variabilität des Bestandsniederschlages ist hoch; das heißt, die Menge des auf den Waldboden tropfenden Wassers kann sich je nach Standort stark unterscheiden. Diese räumliche Variabilität des Bestandsniederschlags ist in tropischen Wäldern höher als in vielen gemäßigten Waldökosystemen, was nicht allein auf verschiedenen Eigenschaften der Ökosysteme zurückzuführen ist. Vielmehr erklären sich die Unterschiede auch aus verschiedenen Waldnutzungen. Abgesehen von biologischen Faktoren beeinflusst die Regenmenge die Variabilität des Bestandsniederschlags erheblich. Die chemische Zusammensetzung des Bestandsniederschlags weist eine noch höhere Variabilität als der Bestandsniederschlag selbst auf. Unterschiede zwischen tropischen und gemäßigten Wäldern lassen sich hier allerdings nicht erkennen, weshalb die hohe Diversität tropischer Ökosysteme die Heterogenität der chemischen Zusammensetzung des Bestandsniederschlags nicht ausreichend erklärt. Eine Vielzahl anderer Faktoren kontrolliert deshalb die Variabilität der Bestandsniederschlagschemie, beispielsweise die Konzentration gelöster Stoffe im Regenwasser oder die Dauer von Trockenperioden. Deren hohe temporale Variabilität ist verantwortlich für die geringe zeitliche Stabilität von Depositionsmessungen. Im Gegensatz dazu ist die temporale Persistenz von Messungen der Bestandsniederschlagsmenge hoch. Insbesondere die Ergebnisse aus Panama zeigen, dass feuchte und trockene Messpunkte über einen Zeitraum von zwei Regenzeiten fortbestehen. Die räumlichen Bestandsniederschlagsmuster im letztgenannten Untersuchungsgebiet sind schwach bzw. weisen die Struktur eines reinen Nugget-Models auf. Die geostatistische Analyse zeigt, dass vor allem die Daten großer Regenereignisse eine robuste Modellierung des Variogramms erfordern, wenn die willkürliche Entfernung von Fernpunkten in den Daten vermieden werden soll. Dieses Resultat ist insbesondere deshalb von Bedeutung, da alle bisherigen Bestandsniederschlagsstudien den klassischen, nicht-robusten Schätzer benutzen, obwohl das Auftreten von Extremwerten in Bestandsniederschlagsdaten für viele Ökosysteme zu erwarten ist.

Acknowledgements

A short introduction to research on spatio-temporal patterns of throughfall and its chemical composition

1.1 Processes and definitions

When rainfall passes through a forest canopy it is divided into three fractions: interception loss, throughfall and stemflow. Interception loss is the proportion of rain that is captured by leaves, stems, branches and other vegetative cover and subsequently evaporates [*Dingman*, 1994]. Throughfall can be further partitioned into two components. The free throughfall component originates from rain falling in gaps without striking the canopy; it dominates small rains [*Gash*, 1979]. The proportion of rain that drips from the canopy represents the other throughfall component. Some of the rainfall, however, does not drip from leaves; instead it flows along twigs, branches, and eventually down the tree trunk. This proportion of water is defined as stemflow. If stemflow drips off before it reaches the forest floor, it is by definition termed throughfall again. This drip from branches or inclined tree trunks explains to some extent very large throughfall measurements [*Zimmermann et al.*, submitted].

Depending on the canopy structure, throughfall can be redistributed several times before it eventually reaches the forest floor. During this canopy passage the quality of the rain water changes due to various intra-crown processes such as foliar leaching, ion exchange processes, removal of dry deposition, and the assimilation and fixation of nutrients by leaf-dwelling organisms [e.g. *Parker*, 1983]. Depending on whether ions are predominately leached or washed off from the canopy we distinguish between endogenous and exogenous sources, respectively [*Whelan et al.*, 1998]. Potassium, for instance, typically exhibits a strong enrichment due to leaching [*Tukey*, 1970; *Parker*, 1983], whereas Cl^- originates from dry deposition as its foliar contents and leaching mobility are low [*Parker*, 1983]. Many solutes experience a pronounced enrichment in throughfall compared to their rainfall concentrations. However, some solutes such as NO_3^-, NH_4^+, and H^+ frequently show negative net throughfall ratios as they are retained in the canopy due to immobilization by active uptake or ion exchange processes [e.g. *Parker*, 1983; *Filoso et al.*, 1999].

Given the complex structure of many forest canopies, this short description already suggests that we can anticipate a high variability of both throughfall and its chemical composition. In this thesis I will explore this variability, determine some of its sources, and analyze emerging spatial and temporal patterns. At first, however, I will have a look at the

research that has been published in the last decades, examine some of the motivations, and inspect issues that warrant further research.

1.2 A little history, research motivations, and current problems

Research on spatio-temporal patterns of throughfall and its chemical composition has received considerable attention for decades [e.g. *Stout and McMahon*, 1961; *Helvey and Patrick*, 1965; *Kimmins*, 1973; *Lloyd and Marques*, 1988; *Beier et al.*, 1993; *Whelan et al.*, 1998; *Möttönen et al.*, 1999; *Raat et al.*, 2002; *Keim et al.*, 2005; *Staelens et al.*, 2006a]. Early studies mainly focused on the variability of throughfall volume and chemical composition to determine the minimum number of collectors that is required to estimate means with a given precision [*Helvey and Patrick*, 1965; *Kimmins*, 1973; *Lloyd and Marques*, 1988; *Kostelnik et al.*, 1989; *Puckett*, 1991]. This research initiated a debate on the reliability of earlier measurements as many studies during that time typically employed merely 5 to 10 collectors per plot [e.g. *Nye*, 1961; *Cronan*, 1980]. In his pioneering work, *Kimmins* [1973] provided the first evidence that throughfall volumes and throughfall chemistry display a high spatial variability. Accordingly, *Kimmins* [1973] concluded that due to widely varying sizes, numbers and arrangements of employed collectors it is "often unclear whether the number of collectors was in any way related to the observed variability in the study area" – a critique that still applies today.

Subsequent studies [e.g. *Beier et al.*, 1993; *Robson et al.*, 1994; *Whelan et al.*, 1998] aimed at detecting the sources of that variability; that is, whether or not canopy architecture predicts throughfall volumes and its chemistry. Next researchers started to take into account abiotic factors, such as rainfall magnitude, in an attempt to explain the large differences in the variability of throughfall measurements between events [e.g. *Rodrigo and Ávila*, 2001]. This research is of ongoing interest and numerous articles have been published that deal with some of these issues [e.g. *Staelens et al.*, 2006a]. Apart from the many interesting findings of those investigations, general comparisons remain problematic owing to the large variety of sampling schemes. Therefore, ideas that almost became paradigm, such as "tropical forests exhibit a higher variability in throughfall than many temperate forests" [e.g. *Jackson*, 1971; *Loescher et al.*, 2002] have yet to be evaluated with more data from unmanaged temperate, and a variety of tropical forest ecosystems. Moreover, it remains to be seen if this anticipated latitudinal gradient of throughfall variability holds true for throughfall chemistry.

The majority of studies mentioned so far use simple measures of variability (e.g. the coefficient of variation) as a first glance on throughfall and solute deposition patterns [e.g. *Whelan et al.*, 1998; *Raat et al.*, 2002; *Staelens et al.*, 2006a]. Several of these studies [e.g. *Whelan et al.*, 1998] attempt to explain the variability of their throughfall measurements with

variables such as canopy openness or leaf area index; i.e. they apply a deterministic approach. Since canopy characteristics are usually weak predictors of throughfall [*Loescher et al.*, 2002] and its chemistry [*Whelan et al.*, 1998], researchers increasingly started to use stochastic approaches. Geostatistical methods, for instance, provide an opportunity to describe random variation; that is, all variation which cannot be explained by a predicting variable.

The first throughfall studies that used geostatistics appeared three decades after the first research on throughfall variability had been published [*Bouten et al.*, 1992; *Loustau et al.*, 1992]. Computational constraints are not the only reason for this delay; instead, the slow transfer of knowledge from other disciplines such as mining [e.g. *Matheron*, 1962] may explain the late application of these methods in throughfall research. In the recent decade, the search for spatial patterns in throughfall gained considerable interest [*Bellot and Escarre*, 1998; *Möttönen et al.*, 1999; *Gómez et al.*, 2002; *Loescher et al.*, 2002; *Keim et al.*, 2005; *Staelens et al.*, 2006b; *Guevara-Escobar et al.*, 2007; *Zimmermann et al.*, submitted], whereas studies that apply geostatistical methods to analyze throughfall chemistry data do not exist yet. The main motivation for exploring throughfall patterns is their potential influence on a range of physical, chemical and biological processes at or below the forest floor. In fact, throughfall patterns effect soil water recharge [*Schume et al.*, 2003], seepage water and ion fluxes [*Manderscheid and Matzner*, 1995], decomposition of organic material [*Möttönen et al.*, 1999], root water uptake [*Bouten et al.*, 1992], and root growth [*Ford and Deans*, 1978]. Therefore, the understanding and prediction of throughfall patterns may improve the understanding of near-surface processes in forest ecosystems. This holds both for the spatial and the temporal domain as the influence of throughfall spatial patterns on processes at the forest floor critically depends on their temporal persistence [e.g. *Keim et al.*, 2005]. Hence, many researchers not only described the spatial variability of throughfall, but also examined the temporal stability of their measurements [e.g. *Staelens et al.*, 2006b; *Keim et al.*, 2005].

Unfortunately, large differences in sampling schemes and varying data analytical concepts hamper site comparisons. Moreover, several studies do not acknowledge the non-Gaussian nature of their throughfall data [e.g. *Bellot and Escarre*, 1998], or they apply sampling schemes that do not match the scale of the process in question [e.g. *Loescher et al.*, 2002]. Hence, some observations such as "canopy geometry accounts for the autocorrelation length in throughfall" [*Loescher et al.*, 2002] have to be verified yet.

The current problems and research questions highlighted in this introduction motivated me to write three articles. In the next chapter I provide a brief overview of my work and its links to other research in the field. This overview, however, is not meant to be a complete summary of my work; instead I try to explain how my research evolved through time.

Though all three articles deal with throughfall patterns they are quite different. The first two articles investigate both throughfall and throughfall chemistry following a

deterministic approach. The third article attempts to describe throughfall patterns with geostatistical methods, and hence, relies on a stochastic approach.

1.3 Patterns of throughfall and its chemical composition: Views from studies in Ecuador, Brazil and Panama

The first study in this thesis was conducted in a tropical montane rain forest in Ecuador during a three-month field campaign, which lasted from August to October 2005. (Chapter 2). The research site (4° 00' S 79° 05' W, 1950 m a.s.l.) (Fig. 1.1) is located in the south Ecuadorian Andes far away from marine influences and anthropogenic emission sources [*Wilcke et al.*, 2001]. In Ecuador, I focused my research on three main objectives. The first was the investigation of within-stand variability of throughfall and its chemical composition. Second, I was interested in the temporal persistence of throughfall volumes, solute concentrations, and solute deposition. Finally, I investigated within-event solute concentration dynamics in order to improve my understanding of leaching and washoff processes in this forest ecosystem.

Given the scarcity of comparable data from other tropical montane forests with respect to the spatial variability of throughfall [but see *Holwerda et al.*, 2006], and the lack of any data of the spatial variability of throughfall chemistry, I compared my data with those from a variety of tropical [*Lloyd and Marques*, 1988; *Lin et al.*, 1997; *Loescher et al.*, 2002] and temperate forest ecosystems [e.g. *Puckett*, 1991; *Pedersen*, 1992; *Beier et al.*, 1993; *Staelens et al.*, 2006a]. These comparisons revealed that the variability of throughfall was at the higher end compared with other tropical and temperate forest ecosystems, whereas the chemical variability was within the range of data obtained from temperate forest ecosystems. Epiphytes were partly responsible for the large variability of both throughfall and its chemical composition.

Another interesting and at that time surprising result was the high temporal stability of the throughfall measurements; and, although to a lesser extent, a detectable persistence of throughfall solute concentrations and deposition. In order to assess the persistence of my sampling points I used "time stability plots" [e.g. *Keim et al.*, 2005] and found that my throughfall measurements showed a relatively high temporal stability compared to a variety of temperate forests [*Raat et al.*, 2002; *Keim et al.*, 2005].

The data on within-event solute concentration dynamics revealed the influence of abiotic factors, i.e. rainfall intensity, on leaching and washoff processes. Moreover, the results showed that for the majority of solutes the low rainfall intensities, which are typical for many tropical montane forests [e.g. *Scatena*, 1990; *Fleischbein et al.*, 2006] do not deplete the large ion pools in the canopy. These findings are in contrast to recent observations from a lowland

tropical forest where throughfall solute concentrations showed depletion with progressing rainfall [*Germer et al.*, 2007]. The dataset from Ecuador, however, had its limitations as I sampled only 5 events. Therefore, I appreciated the opportunity to analyze a larger throughfall dataset that comprised 28 rainfall events and hence allowed a more profound analysis of the spatio-temporal variability of throughfall and its chemistry (Chapter 3).

The just mentioned 28 throughfall events were sampled in an open tropical rainforest (10° 18' S, 62° 52' W, 143 m a.s.l.) (Fig. 1.2) located in the northwestern Brazilian state of Rondônia. The throughfall measurements were conducted during two campaigns that covered the early wet season of 2004 and the peak of the wet season in 2005. The three main objectives of this study were to investigate the spatial variability of throughfall and solute deposition, to determine the influence of contrasting precipitation regimes (i.e. the differences between early and peak of the wet season), and to assess the temporal persistence of throughfall and ion deposition. The data from Brazil showed a lower spatial variability of throughfall compared to the results from Ecuador. Moreover, the data displayed a solute deposition variability which ranked on an intermediate position among a variety of temperate forest ecosystems [e.g. *Duijsings et al.*, 1986; *Beier et al.*, 1993; *Lawrence and Fernandez*, 1993; *Whelan et al., 1998*; *Raat et al.*, 2002; *Staelens et al.*, 2006a]. This result corroborated the findings from Ecuador.

For several solutes the deposition variability in the Brazilian forest exhibited interesting seasonal trends; that is, during the peak of the rainy season I detected a higher variability of solute deposition patterns. The antecedent dry period and rainfall solute concentrations correlated negatively with the variability of solute deposition, which to some extent explained the observed variations. These findings may have some relevance as the links between abiotic factors and solute deposition variability are not entirely understood yet [*Levia and Frost*, 2006]. Similar to the findings from Ecuador, I found a temporal persistence of throughfall over a period of several months and a relatively low persistence of solute deposition in the Brazilian forest.

So far, my studies comprised the investigation of the spatial variability and temporal persistence of throughfall, solute concentration, and solute deposition measurements (Chapter 2 and 3). These investigations revealed the influence of biotic and abiotic factors on the variability of throughfall and solute deposition. In the next study (Chapter 4) I focused on the estimation of throughfall spatial and temporal autocorrelations. For this investigation I applied variogram analysis and concentrated on throughfall only because geostatistical methods require sample sizes too large for a chemical analysis of all water samples. The study site is located on Barro Colorado Island, a 15 km^2 island in the Panama Canal (09° 09' N, 79° 51' W, 90 m a.s.l.) (Fig. 1.3). At this research site I used 220 collectors which were located in a 1-ha plot. Thanks to the help of my field assistants and Helmut Elsenbeer's efforts to catch even

the smallest storm we sampled 91 events during a 14-months period. This large dataset comprised 19926 observations and allowed not only the investigation of throughfall spatial and temporal patterns, but additionally provided the basis to deal with methodological issues.

During the exploratory data analysis I learned that the shape of throughfall frequency distributions changes with event size. Many of the analyzed events displayed large outliers, which can become a problem because common transformations cannot deal with them [*Kerry and Oliver*, 2007b]. My study provides evidence that if one wants to avoid the arbitrary decision of removing these outliers, robust variogram estimators offer a solution. All studies that have been published so far analyzed their data using the classical variogram estimator regardless of the distribution [*Loustau et al.*, 1992; *Bellot and Escarre*, 1998; *Möttönen et al.*, 1999; *Gómez et al.*, 2002; *Loescher et al.*, 2002; *Keim et al.*, 2005; *Staelens et al.*, 2006b; *Shachnovich et al.* 2008]. My work, however, indicates that the choice of the variogram estimator can have a strong influence on the semivariance estimates.

The throughfall data from the Panamanian study site displayed only weak or pure-nugget spatial autocorrelation structures, whereas I detected strong temporal autocorrelations. The application of variogram analysis to investigate temporal correlation of throughfall is a novelty and proved to be a valuable approach. It is particularly suitable for long-term datasets because the method separates between temporal lags, a benefit which outcompetes time stability plots. The Panamanian study clearly shows the need for large datasets and the necessity of a careful exploratory data analysis to investigate spatial and temporal patterns of throughfall.

Figure 1.1: View at the research area in the Ecuadorian montane forest (a). Note the landslides which are a typical landscape feature in this region. The high coverage of epiphytes is yet another prominent characteristic of the forest in the study area (b). View in the canopy at a throughfall sampling location (c), bulk throughfall collectors (d), and a bird's eye view on one of the sequential throughfall collectors (e). The latter collectors were used to determine within-event solute concentration dynamics. The gray PVC trough collects water, which then flows through a tipping bucket and finally enters the sampling bottles. As soon as one of them is completely filled, new water has to enter the next bottle.

Figure 1.2: View at the research area at the Brazilian study site (a). The region is characterized by a mosaic of pastures, secondary forests, and small old-growth forest remnants. The relatively high canopy openness (b and c) and the large number of palms are prominent characteristics of the old-growth forest. The next pictures (d and e) show the trough-type throughfall collectors used at the research site. Note the high density of small palms in the understory (e). The photographs (d) and (e) are used with kind permission of S. Germer.

Figure 1.3: Aerial view from Barro Colorado Island and Lake Gatun which is part of the Panama Canal (a). The island, a 15 km^2 nature reserve under the stewardship of the Smithsonian Tropical Research Institute, is dedicated to research and education. A close up view of the canopy in the research area (b), and a more detailed photograph of the canopy (c) show that deciduousness is a common phenomenon in the region. The throughfall plot is characterized by a highly variable understory that exhibits a mosaic of dense and relatively open patches (d). The next picture (e) shows stemflow which frequently dripped in the collectors and produced large throughfall volumes. The pictures (f) and (e) show throughfall collectors used in the study on Barro Colorado Island. The collectors are similar to the bulk throughfall sampling devices in Ecuador. The photograph (a) is used with kind permission of F. Bäse, and image (b) is printed with kind permission of Patrick Jansen.

Spatial and temporal patterns of throughfall quantity and quality in a tropical montane forest in Ecuador.

Alexander Zimmermann[1], Wolfgang Wilcke[2], Helmut Elsenbeer[1]

[1] Institute of Geoecology, University of Potsdam, Karl-Liebknecht-Str. 24-25, 14476 Potsdam, Germany

[2] Professorship of Soil Geography/Soil Science, Geographic Institute, Johannes Gutenberg University Mainz, 55099 Mainz, Germany

Abstract.   In forests, complex canopy processes control the change in volume and chemical composition of rain water. We hypothesize that (i) spatial patterns, (ii) the temporal stability of spatial patterns, and (iii) the temporal course of solute concentrations can be used to explore these processes. The study area at 1950 m above sea level in the south Ecuadorian Andes is far away from anthropogenic emission sources and marine influences. It received ca. 2200 mm of rain annually. We collected rain and throughfall on an event and within-event basis for five precipitation periods between August and October 2005 at up to 25 sites and analyzed the samples for pH and concentrations of K, Na, Ca, Mg, NH_4^+, Cl^-, NO_3^-, PO_4^{3-}, and total N (TN), P (TP), and organic C (TOC). Cumulative throughfall amounted to 79% of rainfall. Compared with other tropical forests, rainfall solute concentrations were low and throughfall solute concentrations similar. Volumes and solute concentrations of rainfall were spatially and temporally little variable. The spatial coefficient of variation for throughfall volumes was 53%, for solute concentrations 28–292%, and for deposition 33–252%. Temporal persistence of spatial patterns was high for throughfall volumes and varied among solutes. Spatial patterns of K, Mg and TOC concentrations in throughfall were highly persistent. The spatial patterns of throughfall fluxes were less stable than those of concentrations. During a monitoring time of 72 hours, solute concentrations in throughfall of selected rain events remained at a similar level indicating that the leachable element pool in the canopy was not exhausted. Our results demonstrate that the passage of rain through the canopy of a tropical montane forest in Ecuador results in a spatially heterogeneous throughfall pattern with a considerable stability during three months. There is a large leachable element pool in the canopy, which is not depleted by the typical light rain within 72 hours.

2.1 Introduction

The tropical Andes belong to the 25 hotspots of biodiversity on earth [*Myers et al.*, 2000]. In this region, the north Andean montane forests are the richest in plant species [*Henderson et al.*, 1991]. The diverse tree species composition, irregular shaped tree crowns and a multi-layered forest structure affect the redistribution of rainfall in these forests. Furthermore, epiphyte biomass and associated dead organic and mineral matter, which is abundant in tropical montane forests [*Bruijnzeel and Proctor*, 1995], influence spatial patterns of throughfall owing to an interplay of high water storage capacities [*Veneklaas and van Ek*, 1990; *Köhler et al.*, 2007] and the patchy distribution within the canopy [*Nadkarni et al.*, 2004]. Therefore, it seems likely that throughfall in tropical montane forests is particularly heterogeneous.

Several authors reported a high spatial variability of throughfall in tropical montane forests [e.g. *Cavelier et al.*, 1997; *Fleischbein et al.*, 2005; *Holwerda et al.*, 2006], which is attributed to a complex forest structure and to rainfall characteristics [e.g. *Scatena*, 1990]. For individual gauge catches, reported throughfall ranges between 0 – 107% [*Scatena*, 1990] or even 0 – 1000% [*Cavelier et al.*, 1997] of incident precipitation. Given that throughfall represents an important pathway of nutrients to the forest floor [*Parker*, 1983], the spatial variability in throughfall volume affects the spatial patterns of throughfall solute concentrations and deposition. Moreover, the living and dead biomass interacts with rain water during the passage through the canopy and creates a chemical variability of its own. Several authors investigated spatial patterns of throughfall chemistry in a variety of temperate and tropical forest ecosystems [e.g. *Seiler and Matzner*, 1995; *Lin et al.*, 1997; *Raat et al.*, 2002].

In the study area in Ecuador, *Wilcke et al.* [2001, 2002] found a considerable variation in base metal concentrations of throughfall among five sampling sites, which was correlated with soil fertility. If the heterogeneous spatial distribution of nutrient inputs to the soil were temporally stable, this would have an impact on soil fertility in the long term because of continuous local nutrient addition or leaching. Therefore, knowledge of the temporal stability of heterogeneous throughfall patterns is crucial to assess the ecological consequences of canopy processes.

We propose to use observations of within-event solute dynamics in throughfall to explore the complex interactions among throughfall deposition patterns, storage, and leaching of solutes from various canopy compartments (leaves, branches, epiphytes, organic and mineral accumulations). In analogy to published studies of spatial patterns of throughfall chemistry, most articles concern within-event rain and throughfall dynamics in temperate regions [e.g. *Parker*, 1983; *Lovett and Schaefer*, 1992; *Hambuckers and Remacle*, 1993;

Hansen et al., 1994; *Crockford et al.*, 1996] only a few studies deal with tropical environments [*Stallard and Edmond*, 1981; *Germer et al.*, 2007]. Within-event throughfall solute concentration dynamics can be highly variable, both between sampling sites and individual events [*Parker*, 1983]. Several authors reported decreasing concentrations that did not reach a constant level during the observation period [*Parker*, 1983; *Hansen et al.*, 1994], others observed more variable patterns [*Hambuckers and Remacle*, 1993; Hansen et al., 1994; *Crockford et al.*, 1996]. Rainfall intensity is an important control of leaching and washoff processes [*Lovett and Schaefer*, 1992; *Hansen et al.*, 1994; *Neary and Gizyn*, 1994]. Low precipitation intensities which seem to be characteristic for many tropical montane forests [*Veneklaas and van Ek*, 1990; *Clark et al.*, 1998; *Schellekens et al.*, 1999; *Fleischbein et al.*, 2006], enhance the contact time of rain water with plant tissue, which can increase ion concentrations in throughfall [*Lovett and Schaefer*, 1992; *Hansen et al.*, 1994].

The understanding of spatial and temporal patterns of throughfall is furthermore essential for a wide range of eco-hydrological problems such as: (1) the estimation of root water and nutrient uptake that is strongly affected by throughfall patterns [*Bouten et al.*, 1992], (2) flow path separation based on an event vs. pre-event water approach, with respect to the assumption that tracer concentrations of postulated end-members do not change during events [*Elsenbeer et al.*, 1995], and (3) the modeling of water and ion fluxes in forested watersheds [*Zirlewagen and von Wilpert*, 2001].

The objectives of our study were to investigate: (1) the spatial variability of throughfall volumes and solutes in a north Andean tropical montane forest, (2) its temporal stability, and (3) the within-event element concentrations in rain and throughfall.

We hypothesized that: (1) the spatial variability of throughfall and its chemical composition is particularly high compared with other forests because of its high biodiversity and epiphytism, (2) the temporal stability of the spatial pattern is high because of stable structures in the canopy (e.g. large epiphytes) that show only minor changes during our short term observation period, and (3) the element concentrations decrease with increasing rainfall because of exhausting element pools in the canopy.

2.2 Material and methods
2.2.1 Study area

The study site (4° 00' S 79° 05' W), near the research station Estación Científica de San Francisco (ECSF), is located on the eastern slope of the Cordillera Real between the cities of Loja and Zamora in the south Ecuadorian Andes (Figure 2.1). The area is subject to multidisciplinary research activities within the framework of the ecological special research group 402 (FOR 402) of the German Research Foundation (DFG). *Wilcke et al.* [2001]

selected three microcatchments on 30° – 50° steep slopes at an altitude of 1900 – 2200 m above sea level (a.s.l.) to study the chemical characteristics of water during the passage through the forest ecosystem. In Microcatchment 2, at an altitude of 1950 m a.s.l., we sampled throughfall, and rainfall in two adjacent clearings at a distance of less than 500 m.
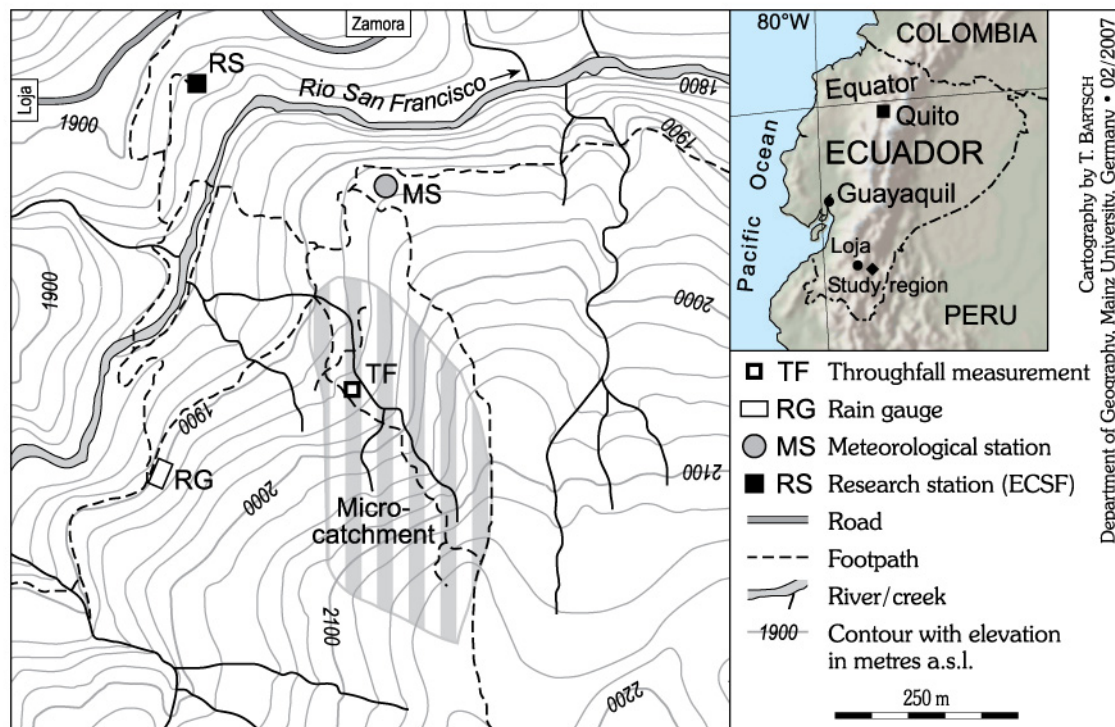
Figure 2.1: Location of the study area. The throughfall (TF) and the two rainfall (RG and MS) measurement sites are indicated.

Total rainfall averaged 2200 mm in a seven-year monitoring period from 1998 to 2005 [*Rollenbeck et al., 2007*]. Applying an event definition that separates discrete rainfall events by a dry period of at least two hours and based on a 1436 day study period (April 1998 to April 2002), the mean intensity and duration of events was 0.41 mm h^{-1} and 9.3 hours, respectively [*Fleischbein et al.*, 2006]. The annual precipitation shows a unimodal distribution with a maximum between April and July. The driest month is November with 70 mm on average. The mean annual temperature (1998 – 2000) at 1950 m a.s.l. was 16.2°C, the coldest month was July with a mean temperature of 14.9°C, the warmest month was November with a mean temperature of 17.3°C [*Emck*, unpublished]. The dominating soil types are Dystrudepts [*Soil Survey Staff*, 2003].

According to *Bruijnzeel and Hamilton* [2000], the forest is classified as lower montane rain forest. The forest has an upper 15 – 20 m-tall canopy storey with few emergents reaching 35 m, a lower 10 – 15 m-tall tree storey, and a <5 m-tall shrub storey. The coverage of the upper, second and shrub-vegetation layer is 50 – 60%, 10 – 50% and 50 – 80%, respectively [*Paulsch*, 2002]. Lauraceae, Rubiaceae, Melastomataceae and Euphorbiaceae are the most

important tree families of the area. The most abundant tree species between 1800 and 2200 m is Graffenrieda emarginata (Ruiz & Pav.) Triana (Melastomataceae) [*Homeier*, 2004]. The trees in our research area are densely covered with epiphytes. The epiphyte coverage (in %±SD) in the throughfall sampling area ranges in the five Johansson zones (JZ) [*Johansson*, 1974] between 18 ± 8 (JZ5) and 54 ± 19 (JZ2) for bryophytes, from 26 ± 5 (JZ1) to 36 ± 15 (JZ3 and 4) for lichens and from 10 ± 22 (JZ5) to 24 ± 17 (JZ3 and 4) for vascular epiphytes [*Fleischbein et al.*, 2005].

2.2.2 Field sampling

Rain and throughfall samples were collected from August to October 2005. We focused our sampling on precipitation events after dry spells and sampled for a predefined interval of 72 hours. Rainfall was sampled in two clearings (sampling sites indicated as RG and MS in Figure 2.1) with five collectors at each location. The collectors for event sampling consisted of a 2 l polyethylene sampling bottle and a funnel. The receiving area of each collector was 122 cm^2. A polyethylene net with 0.5 mm mesh width on the bottom of the funnel prevented contamination with particulate organic matter and insects. In addition, we used one trough-type collector with a collecting area of 3000 cm^2 for within-event rainfall sampling. The sequential sampler was equipped with a tipping bucket (100 ml tip capacity) logged by a Hobo Event Logger (Onset) with a resolution of 0.33 mm. The sequential sampler consisted of 10 connected bottles that partitioned events into predefined rainfall depth intervals of 3.74 ± 0.069 mm (mean ± SD). All rainfall collectors were installed on supports 1 m above ground. In order to reduce the influence of radiation, all sampling bottles were wrapped with Al foil, and a table tennis ball in the bulk collectors reduced evaporation. Throughfall was sampled on an event basis with 25 collectors located randomly in the 500 m^2 sampling area. Two trough-type collectors sampled throughfall sequentially. The bulk and sequential throughfall samplers were identical in construction to the rainfall sampling devices.

2.2.3 Laboratory analysis

Immediately after sample collection, we filtered aliquots through a 4 – 7 μm ashless white ribbon filter paper (Schleicher & Schuell). After filtration samples were frozen and stored in the dark. In an unfiltered aliquot we measured pH with a standard pH electrode (WTW pH 330i); this sub-sample was afterwards discarded due to the release of K by the pH electrode. After export of the aliquots from Ecuador to Germany in frozen state, the following parameters were determined: Concentrations of K, Na, Ca and Mg were analyzed with flame AAS (VARIAN AA240 FS), NH_4^+, NO_3^-, TN, PO_4^{3-}, TP and Cl^- were measured

with a continuous flow analyzer (CFA, BRAN & LÜBBE Autoanalyzer3), TOC concentrations were analyzed with an automatic TOC analyzer (ELEMENTAR high TOC II) and S concentrations were determined with inductively coupled plasma optical emission spectroscopy (ICP–OES, PerkinElmer Optima 3300 XL). The concentrations of organic N and P were calculated with equations 2.1 and 2.2, respectively.

$$TON = TN - \left(NO_3 \text{ - } N\right) - \left(NH_4 \text{ - } N\right) \tag{2.1}$$

$$TOP = TP - \left(PO_4 \text{ - } P\right) \tag{2.2}$$

2.2.4 Epiphytes above throughfall samplers

Six of the 25 bulk throughfall collectors received throughfall from an area with either thick moss mats (collectors 5 and 16) or arboreal bromeliads, which were situated on branches directly above (collectors 1, 6, 8 and 24). Above collector 6 and 24 we found big bromeliads (*Guzmania* spec., leaf lengths of up to 80 cm) characterized by the ability to store substantial volumes of water with their impounding foliage that functions as a tank [*Zotz and Thomas*, 1999]. Some of the bromeliads lived on and accumulated large amounts of dead organic matter on the host trees. The relative small receiving area of the bulk throughfall collectors allowed a clear determination if the collected water was in contact with big bromeliads and associated organic matter. In contrast, sequential throughfall samplers received a more integrated chemical signal due to their larger collecting area.

2.2.5 Data analysis
2.2.5.1 Event-based analysis

Volume-weighted means per event E (VWM_E) were used to express mean rain and throughfall solute concentration of individual events. The VWM_E per event was calculated as:

$$VWM_E = \left(\sum_{n=1}^{i} C_{i,E} V_{i,E} \right) \left(\sum_{n=1}^{i} V_{i,E} \right)^{-1} \tag{2.3}$$

for all sampled events, where $C_{i,E}$ and $V_{i,E}$ are the concentration and volume at collector i for event E. The volume-weighted standard deviation was calculated to determine the 95% confidence limits of the VWM_E [*Bland and Kerry*, 1998].

To compare the VWM_E solute concentrations of the five individual events with data in the literature we provided the mean (VWM_{E5}) and 95% confidence limits by bootstrapping the VWM_E's [*Efron and Tibshirani*, 1993]. We also calculated volume-weighted means per sampling point for the throughfall collectors (VWM_P) with equation 2.3, replacing the notation E with P for the sampling point and the notation i with E for events.

2.2.5.2 Spatial patterns of throughfall and temporal persistence

A series of studies [e.g. *Pedersen*, 1992; *Seiler and Matzner*, 1995; *Raat et al.*, 2002; *Staelens et al.*, 2006a] described the spatial variability of solute concentrations and ion deposition in throughfall with the spatial coefficient of variation (CV). Since the Shapiro-Wilk-statistic [*Shapiro and Wilk*, 1965] indicated that the majority of our solute concentration and deposition data did not match the normal distribution we provided the CV for comparison only and the median absolute deviation/median ratio (MAD/M from hereon) as an alternative measure of spatial variability. The CV and MAD/M of throughfall volumes and solute deposition are based on the amounts at each collector summed over the five events; CV and MAD/M of solute concentrations are based on VWM_P.

Several techniques were developed to analyze the temporal stability of the observed spatial patterns. *Raat et al.* [2002] applied a method first described by *Vachaud et al.* [1985] to analyze the temporal stability of throughfall characteristics:

$$\hat{\delta}_{i,E} = \left(\delta_{i,E} - \bar{\delta}_E \right)\left(\bar{\delta}_E \right)^{-1} \qquad (2.4)$$

where $\delta_{i,E}$ and $\hat{\delta}_{i,E}$ are the variable δ and the normalized variable δ at sampling point i of event E, and $\bar{\delta}_E$ is the mean of δ in event E.

Keim et al. [2005] used an alternative approach that considers the variance at the sampling point to analyze the persistence of high or low throughfall areas:

$$\tilde{\delta}_{i,E} = \left(\delta_{i,E} - \bar{\delta}_E \right)\left(s\delta_E \right)^{-1} \qquad (2.5)$$

where $\tilde{\delta}_{i,E}$ is the normalized variable δ at sampling point i of event E, $\bar{\delta}_E$ is the mean of δ in event E, and $s\delta_E$ its standard deviation. We used equation 2.5 to analyze the persistence of spatial patterns of throughfall volumes (T), solute concentrations (C) and solute deposition (D), but replaced $\bar{\delta}_E$ with the median of δ_E, $M\delta_E$, and $s\delta_E$ with the median absolute deviation of δ_E, $MAD\delta_E$:

$$\tilde{\delta}_{i,E} = \left(\delta_{i,E} - M\delta_E \right) \left(MAD\delta_E \right)^{-1} \qquad (2.6)$$

The plot of $\tilde{\delta}$ for each event and throughfall collector, ranked from minimum to maximum mean $\tilde{\delta}_{i,E}$, gives a visual interpretation of the deviation of a variable from the median for all sampling points. According to *Keim et al.* [2005], these time stability plots illustrate two types of persistence. First, extreme persistence refers to the deviation of the mean $\tilde{\delta}_{i,E}$ from the median in the region of the lower and upper quartiles of the ranked sampling points. Second, general persistence appears as the deviation of the mean $\tilde{\delta}_{i,E}$ in the interquartile range. Within this region single sampling points can be situated persistently above or below the median without being extremes [*Keim et al.*, 2005]. We used 95% confidence intervals of the mean $\tilde{\delta}_{i,E}$ as the criterion of persistence; other authors applied ± 1 standard deviation as a weaker criterion [*Raat et al.*, 2002; *Staelens et al.*, 2006a].

In order to interpret the spatial patterns of T, C, and D and their temporal persistence, we analyzed:

(1) The ranking pattern of sampling points with respect to the mean $\tilde{\delta}_{i,E}$. In particular we examined if the ranking positions of collectors that received throughfall from areas with thick moss mats or big arboreal bromeliads (collectors 1, 5, 6, 8, 16 and 24) could be expected by chance. Thereby we assigned each ranking position a number 1...*n*, and compared the sum of observed ranking positions with its confidence intervals that were estimated by a random sample algorithm after re-sampling for 10.000 times.

(2) The correlations between C and D, and among C, D and T, respectively.

In the remainder of the paper we replaced δ with T, C, and D for throughfall volumes, solute concentrations and solute deposition, respectively. The low sample volumes of collectors 6, 18 and 24 precluded chemical analysis, which is why we excluded these sampling points from our data analysis. Values below the detection limit were taken as zero for calculations. We used S-PLUS [*Insightful Corporation*, 2001a, b] for all data analysis.

2.3. Results and discussion
2.3.1 Event characteristics

The total incident rainfall from August 17 to October 31 2005 was 225 mm, which is below the mean for this period in the previous 7 years of 260 mm (range: 198 – 316 mm) (Data provided by R. Rollenbeck and M. Richter). During the sampling period we collected 111 mm rainfall. The sampled events had low intensities and were characterized by relatively dry antecedent conditions (Table 2.1).

Table 2.1: Event characteristics.

Event Number	Date (start)	Rainfall (mm) Mean ± SD	Throughfall (mm) Mean ± SD	MaxI10 (mm/h)	MaxI30 (mm/h)	MaxI60 (mm/h)	Index3 (mm)	Index7 (mm)
1	25.08.2005	24.2 ± 1.7	20.2 ± 9.9	12.0	9.3	7.0	4.0	4.3
2	12.09.2005	19.7 ± 1.6	12.9 ± 8.7	4.0	2.0	2.0	16.3	25.3
3	28.09.2005	12.6 ± 1.8	9.2 ± 6.5	10.0	8.0	5.7	7.0	7.0
4	14.10.2005	18.5 ± 1.3	14.0 ± 7.5	16.0	6.7	5.3	0.0	20.0
5	29.10.2005	35.6 ± 1.4	31.1 ± 26.0	16.0	10.0	5.7	3.0	4.7

MaxI10, MaxI30 and MaxI60 are the maximum 10, 30 and 60 minute rainfall intensities, respectively. Index3 and Index7, is the 3 and 7-day antecedent wetness index, the sum of precipitation for the previous three and seven days, respectively.

2.3.2 Mean rain and throughfall solute concentrations

The VWM_{E5} concentrations in rainfall for all solutes but NO_3^- and H^+ were at the lower end of values reported from various sites in South and Central American tropical montane and lowland forests (Fig. 2.2, Table 2.2). The concentrations of NH_4^+, Mg, Cl^- and TOC were even significantly lower, except when compared to Reserva Ducke (TOC not comparable) in Central Amazonia [*Forti and Moreira-Nordemann*, 1991]. Similar low concentrations in rainfall for most elements were measured during a one year sampling campaign in the study area by *Wilcke et al.* [2001]. They found that the solute concentrations were at the lower end of values reported by *Forti and Neal* [1992b] for various tropical rain forests and by *Hafkenscheid* [2000] for a range of lower montane rain forests in Central and South America. The detected concentrations in rainfall during our short term study matched observed patterns of the long term monitoring. The low concentrations of most solutes in rainfall result from the large distance to the sea and to anthropogenic emission sources [*Wilcke et al.*, 2001]. The high DOC concentrations observed in Brazil [*Germer et al.*, 2007; Table 2.2) coincided with biomass burning in the area and associated high DOC concentrations in aerosols [*Andreae et al.*, 1988]. In rain water at two montane rain forest sites in Colombia elevated SO_4^{2-} concentrations were the result of SO_2 release from a nearby volcano [*Veneklaas*, 1990]. The high Na^+ concentrations in Panama were explained by the proximity of the Caribbean Sea [*Cavelier et al.*, 1997].

While rainfall VWM_{E5} concentrations were at the lower end of reported values, solute concentrations in throughfall except H^+ were more within the range of reported values from
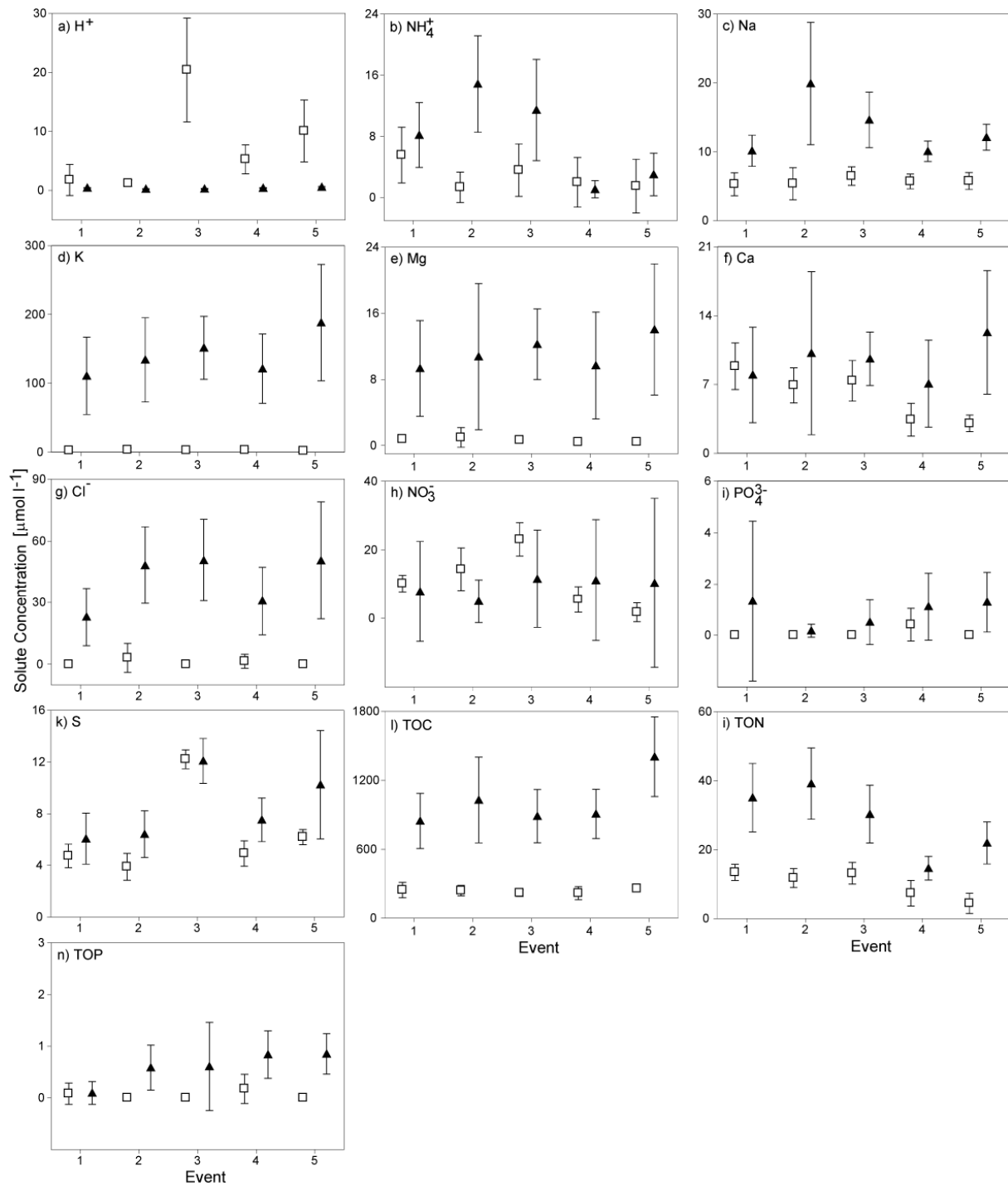
Figure 2.2: Rainfall (empty boxes) and throughfall (solid triangles) VWM_E solute concentrations for (a) H^+, (b) NH_4^+, (c) Na, (d) K, (e) Mg, (f) Ca, (g) Cl^-, (h) NO_3^-, (i) PO_4^{3-}, (k) S, (l) TOC, (m) TON and (n) TOP plotted for individual events. The error bars indicate the 95% confidence limits.

other tropical montane and lowland forests, though K concentrations were at the upper end of this range (Table 2.3). Again, as for rainfall solute concentrations, *Wilcke et al.* [2001] found a similar pattern when they compared element concentrations measured during a one year

sampling in the area with values reported by *Forti and Neal* [1992b] and *Hafkenscheid* [2000] for various tropical rain and montane forests.

VWM_E solute concentrations showed a significant enrichment after the passage through the canopy for K, Na, Mg (except event 2, not significant), Cl^-, TON and TOC; NH_4^+, Ca and PO_4^{3-} showed significant enrichment in one, TOP in two events (Figure 2.2). For most events, VWM_E H^+ concentrations in throughfall were significantly depleted because of buffering in the canopy (except event 1, not significant). The strong increase in K concentrations after the interaction of rain water with the forest canopy has frequently been observed and is attributed to the high leachability of K from the leaf tissue [*Tukey*, 1970; *Parker*, 1983]. Most elements showed enrichment after rainfall passed through the canopy; during some events, however, we observed lower VWM_E concentrations in throughfall (though not statistically significant) for NH_4^+, Ca, NO_3^- and S. Both negative and positive balances of NH_4^+ and NO_3^- between throughfall and rainfall are often reported [e.g. *Forti and Moreira-Nordemann*, 1991; *Filoso et al.*, 1999; *Liu et al.*, 2002; *Zeng et al.*, 2005]; reports of canopy uptake of Ca are less frequent [*Jordan et al.*, 1980; *Langusch et al.*, 2003].

2.3.3 Spatial patterns of throughfall

A comparison with studies conducted in a variety of temperate and tropical forest ecosystems (Table 2.4) reveals that the variability of throughfall volumes at our study site is at the higher end of the reported values and similar to the spatial variability in a lower montane rain forest in Puerto Rico [*Holwerda et al.*, 2006] and a tropical rain forest in Brazil [*Lloyd and Marques*, 1988]. *Cavelier et al.* [1997] noticed, based on a comparison with data from *Lloyd and Marques* [1988], that the distribution of throughfall is more heterogeneous in tropical montane cloud forests than in lowland rain forests owing to the interplay of a more irregular canopy height and a reduction in tree stature and leaf area index. The results of our study did not match this pattern. On the basis of Table 2.4 we suggest that the spatial variability mainly depends on the canopy complexity (the number of species per area, the age structure of the forest, and the arrangement of trees influence this complexity) and rainfall depth of the collected events [*Rodrigo and Àvila*, 2001; *Keim et al.*, 2005] regardless of the type of forest. Epiphytes may play a crucial role with respect to spatial patterns of throughfall because of their high water storage capacity [*Veneklaas and van Ek*, 1990] although *Fleischbein et al.* [2005] did not detect a strong effect of epiphytes on interception loss in the study forest. However, *Holwerda et al.* [2006] attributed the high variability in the lower montane rain forest in Puerto Rico partly to past hurricane damages and to the influence of palms. The latter can strongly affect the distribution of throughfall in the canopy [*Germer et al.*, 2006]. These examples demonstrate that a high spatial variability can occur for various reasons, which is

Table 2.2: Rainfall solute concentrations and lower (LCL) and upper (UCL) confidence limits (where provided by the authors) in µmol per liter for this and selected South and Central American tropical montane and lowland forests. For Na and K it was assumed that the monovalent cation and for Ca and Mg the divalent cation were the only species in solution.

Forest type[1], Site	H^+ (pH) mean	LCL	UCL	n	NH_4^+ mean	LCL	UCL	n	Na^+ mean	LCL	UCL	n	K^+ mean	LCL	UCL	n	Mg^{2+} mean	LCL	UCL	n	Ca^{2+} mean	LCL	UCL	n
LMRF, Ecuador[a]	7.8 (5.5)	2.3	14.5	5	2.8	1.6	4.3	5	5.7	5.4	6.1	5	2.7	2.2	3.2	5	0.7	0.5	0.8	5	5.9	4.0	7.9	5
LMRF, Columbia[b]	(4.4)	–	–	50	61.7	53.7	69.6	50	49.6	41.8	57.4	50	9.6	7.3	11.9	50	6.3	5.4	7.2	50	11.9	9.9	13.9	50
LMRF, Venezuela[c]	(4.6)	–	–	36	–	–	–	–	12.1	–	–	36	5.5	–	–	36	21.1	–	–	36	9.6	–	–	36
LMRF, Costa Rica[d]	(5.0)	–	–	102	3.6	–	–	102	27.4	–	–	102	2.3	–	–	102	2.9	–	–	102	4.5	–	–	102
LMRF, Panama[e]	–	–	–	–	–	–	–	–	78.7	–	–	18	9.8	–	–	18	4.8	–	–	20	19.8	–	–	20
UMRF, Columbia[f]	(4.4)	–	–	50	55.2	48.1	62.3	50	47.7	39.9	55.5	50	12.2	9.9	14.5	50	7.0	5.9	8.1	50	12.6	10.6	14.6	50
UMRF, Jamaika[g]	(5.5)	–	–	17	9.3	6.0	12.6	17	29.1	22.4	35.9	17	6.9	5.2	8.6	17	2.9	2.2	3.5	17	7.2	4.3	10.2	17
LRF, Columbia[b]	13.6 (5.0)	9.5	17.7	35	11.5	8.6	14.4	35	20.0	17.5	22.5	35	9.0	6.4	11.6	35	2.8	2.2	3.4	35	6.8	6.0	7.6	35
LRF, Brazil[i]	(6.3)	–	–	–	24.0	13.0	34.9	–	7.0	5.9	8.1	39	13.1	8.2	17.9	37	4.3	2.9	5.8	39	25.4	20.1	30.7	39
LRF, Brazil[k1]	–	–	–	29	2.4	1.1	3.7	18	3.1	1.3	4.9	18	0.6	0.3	0.9	18	0.3	0.1	0.5	18	2.4	1.4	3.4	18
LRF, Brazil[k2]	(4.7)	–	–	–	8.6	-2.9	20.0	11	9.6	0.7	18.4	11	3.6	0.9	6.3	11	0.8	0.1	1.4	11	3.1	1.5	4.7	11

[1] Abbreviations are: LMRF: lower montane rain forest, UMRF: upper montane rain forest and LRF: lowland rain forest.

[a] Present study; [b] Veneklaas [1990], study site at 2550 m altitude; [c] Steinhardt [1979]; [d] Clark et al. [1998]; [e] Cavelier et al. [1997]; [f] Veneklaas [1990], study site at 3370 m altitude; [g] Hafkenscheid [2000]; [h] Tobón et al. [2004]; [i] Germer et al. [2007]; [k1] Forti and Moreira-Nordemann [1991], data refers to wet season; [k2] Forti and Moreira-Nordemann [1991], data refers to dry season.

Table 2.2 continued:

Forest type[1], Site	Cl⁻ mean	LCL	UCL	n	NO₃⁻ mean	LCL	UCL	n	PO₄³⁻ mean	LCL	UCL	n	S[2] mean	LCL	UCL	n	TOC[3] mean	LCL	UCL	n
LMRF, Ecuador[a]	0.9	0.0	2.2	5	11.0	5.0	17.9	5	0.1	0.0	0.2	5	6.4	4.4	9.3	5	236.5	223.5	249.5	5
LMRF, Columbia[b]	25.8	21.8	29.8	50	–	–	–	–	1.1	0.9	1.3	50	38.6	34.9	42.3	50	–	–	–	50
LMRF, Costa Rica[d]	–	–	–	–	3.6	–	–	102	0.1	–	–	102	–	–	–	102	–	–	–	–
LMRF, Panama[e]	27.7	–	–	16	–	–	–	–	0.6	–	–	16	11.7	–	–	16	–	–	–	20
UMRF, Columbia[f]	26.4	21.3	31.5	50	–	–	–	–	1.1	0.9	1.3	50	36.1	32.7	39.6	50	–	–	–	50
UMRF, Jamaika[g]	32.2	23.6	40.7	17	4.3	2.8	5.8	17	0.1	0.1	0.2	17	4.1	2.5	5.7	17	–	–	–	17
LRF, Columbia[b]	25.4	21.2	29.6	35	6.4	5.0	7.8	35	0.3	0.2	0.4	35	36.9	28.3	45.5	35	328.3	281.9	374.7	35
LRF, Brazil[i]	11.4	8.8	13.9	38	4.1	2.4	5.8	37	–	–	–	–	4.5	2.7	6.4	27	591.8	375.0	808.6	37
LRF, Brazil[k1]	7.7	0.7	14.8	18	–	–	–	–	–	–	–	–	3.0	-0.4	6.5	18	–	–	–	–
LRF, Brazil[k2]	11.8	3.9	19.8	11	–	–	–	–	–	–	–	–	7.2	1.8	12.7	11	–	–	–	–

1) Abbreviations are: LMRF: lower montane rain forest, UMRF: upper montane rain forest and LRF: lowland rain forest.

2) Values for S refer to total S in our study and SO_4^{2-} in the literature.

3) Values in the literature refer to DOC.

a) Present study; b) Veneklaas [1990], study site at 2550 m altitude; c) Steinhardt [1979]; d) Clark et al. [1998]; e) Cavelier et al. [1997]; f) Veneklaas [1990], study site at 3370 m altitude; g) Hafkenscheid [2000]; h) Tobón et al. [2004]; i) Germer et al. [2007]; k1) Forti and Moreira-Nordemann [1991], data refers to wet season; k2) Forti and Moreira-Nordemann [1991], data refers to dry season.

Note: TON and TOP values were not compared due to missing references in the literature, the mean, LCL and UCL (in µmol l⁻¹) are: 10.1, 6.8, 13.0 and 0.1, 0.0, 0.1 for TON and TOP, respectively.

Table 2.3: Throughfall solute concentrations and lower (LCL) and upper (UCL) confidence limits (where provided by the authors) in µmol per liter for for this and selected South and Central American tropical montane and lowland forests. For Na and K it was assumed that the monovalent cation and for Ca and Mg the divalent cation were the only species in solution.

Forest type[1], Site	H+ (pH)				NH4+				Na+				K+				Mg2+				Ca2+			
	mean	LCL	UCL	n	mean	LCL	UCL	n	mean	LCL	UCL	n	mean	LCL	UCL	n	mean	LCL	UCL	n	mean	LCL	UCL	n
LMRF, Ecuador[a]	0.4 (6.5)	0.3	0.5	5	7.7	3.3	12.2	5	13.4	10.5	16.9	5	141.3	119.8	166.4	5	10.2	8.6	11.9	5	9.4	7.9	11.0	5
LMRF, Columbia[b]	(5.6)	–	–	50	82.6	72.0	93.2	50	63.0	54.7	71.3	50	131.4	116.9	146.0	50	23.7	21.5	26.0	50	36.5	33.3	39.6	50
LMRF, Venezuela[c]	(5.6)	–	–	36	–	–	–	–	20.3	–	–	–	200.3	–	–	36	18.5	–	–	36	19.0	–	–	36
LMRF, Costa Rica[d]	(5.7)	–	–	102	5.0	–	–	102	89.2	–	–	102	89.0	–	–	102	17.7	–	–	102	30.9	–	–	102
LMRF, Panama[e]	–	–	–	–	–	–	–	–	258.9	–	–	–	73.4	–	–	18	14.2	–	–	20	39.7	–	–	20
UMRF, Columbia[f]	(4.4)	–	–	50	69.8	61.9	77.8	50	52.9	46.0	59.8	50	71.1	63.7	78.5	50	24.2	21.3	27.1	50	39.5	34.8	44.3	50
UMRF, Jamaika[g]	(5.9)	–	–	17	13.6	9.9	17.2	17	47.4	38.7	56.1	17	39.4	31.0	47.8	17	9.1	6.9	11.2	17	12.5	9.1	15.8	17
LRF, Columbia[h1]	12.2 (5.2)	9.4	15.1	35	27.6	20.7	34.5	35	24.0	22.2	25.8	35	32.4	27.0	37.8	35	8.1	7.2	9.0	35	8.8	8.4	9.2	35
LRF, Columbia[h2]	10.9 (5.5)	5.1	16.7	35	35.7	20.4	51.0	35	28.0	26.5	29.5	35	45.0	32.6	57.4	35	7.6	6.7	8.4	35	9.5	8.8	10.2	35
LRF, Columbia[h3]	16.3 (5.3)	6.8	25.8	35	32.2	19.8	44.6	35	28.0	25.5	30.5	35	44.1	33.8	54.4	35	9.0	8.0	9.9	35	10.2	9.3	11.0	35
LRF, Columbia[h4]	6.8 (5.5)	5.2	8.4	35	32.2	24.1	40.3	35	26.0	24.7	27.2	35	41.4	33.9	48.9	35	14.3	12.5	16.0	35	15.0	13.9	16.0	35
LRF, Brazil[i]	(6.3)	–	–	–	21.7	10.8	32.6	–	13.0	9.2	16.8	42	109.7	87.9	131.5	40	12.0	8.8	15.2	42	21.6	17.5	25.7	40
LRF, Brazil[k1]	–	–	–	–	4.7	3.2	6.1	–	10.6	8.6	12.6	16	6.6	5.2	8.1	16	3.7	2.8	4.5	16	5.1	4.0	6.2	16
LRF, Brazil[k2]	–	–	–	–	6.1	3.8	9.5	–	29.0	24.2	35.9	10	25.1	20.5	29.6	10	10.9	9.1	12.6	10	10.2	8.2	12.1	10

[1] Abbreviations are: LMRF: lower montane rain forest, UMRF: upper montane rain forest and LRF: lowland rain forest.

[a] Present study; [b] *Veneklaas* [1990], study site at 2550 m altitude; [c] *Steinhardt* [1979]; [d] *Clark et al.* [1998]; [e] *Cavelier et al.* [1997]; [f] *Veneklaas* [1990], study site at 3370 m altitude; [g] *Hafkenscheid* [2000]; [h1-4) *Tobón et al.* [2004], h1-4 refers to four adjacent research areas: sedimentary plain, high terrace, low terrace and flood plain, respectively; [i] *Germer et al.* [2007]; [k1) *Forti and Moreira-Nordemann* [1991], data refers to wet season; [k2) *Forti and Moreira-Nordemann* [1991], data refers to dry season.

Table 2.3 continued:

Forest type[1], Site	Cl^-				NO_3^-				PO_4^{3-}				S[2]				TOC[3]			
	mean	LCL	UCL	n	mean	LCL	UCL	n	mean	LCL	UCL	n	mean	LCL	UCL	n	mean	LCL	UCL	n
LMRF, Ecuador[a]	40.7	30.1	50.2	5	9.7	7.3	11.7	5	0.9	0.5	1.3	5	8.5	6.5	10.6	5	1016.0	875.9	1219.0	5
LMRF, Columbia[b]	55.3	47.0	63.6	50	–	–	–	–	2.9	2.4	3.4	50	38.6	34.9	42.3	50	–	–	–	–
LMRF, Costa Rica[d]	–	–	–	–	2.9	–	–	102	0.9	–	–	102	–	–	–	–	–	–	–	–
LMRF, Panama[e]	63.5	–	–	16	3.1	–	–	–	–	–	–	16	8.6	–	–	16	–	–	–	20
UMRF, Columbia[f]	46.9	39.3	54.5	50	–	–	–	–	1.1	0.9	1.3	50	83.3	74.5	92.0	50	–	–	–	–
UMRF, Jamaika[g]	53.9	43.4	64.3	17	1.4	0.3	2.5	17	0.2	0.2	0.3	17	14.0	9.2	18.8	17	–	–	–	–
LRF, Columbia[h1]	22.9	21.2	24.5	35	23.7	17.2	30.1	35	1.0	0.4	1.6	35	59.0	52.1	66.0	35	459.6	436.4	482.8	35
LRF, Columbia[h2]	38.1	33.5	42.7	35	16.6	11.3	22.0	35	0.7	0.5	1.0	35	77.5	62.0	93.0	35	558.1	511.7	604.5	35
LRF, Columbia[h3]	35.6	32.2	39.0	35	33.2	21.7	44.8	35	1.1	0.6	1.7	35	84.9	65.9	103.8	35	558.1	525.6	590.6	35
LRF, Columbia[h4]	40.6	36.5	44.8	35	39.0	17.9	60.2	35	1.5	0.2	2.9	35	70.1	53.7	86.5	35	525.3	497.4	553.1	35
LRF, Brazil[i]	31.4	24.2	38.5	41	8.7	5.7	11.8	42	–	–	–	–	5.3	3.7	7	–	1354.0	1031.0	1678.0	40
LRF, Brazil[k1]	10.3	8.5	12.1	16	–	–	–	–	–	–	–	–	4.6	3.8	5.5	16	–	–	–	–
LRF, Brazil[k2]	21.0	17.3	24.7	10	–	–	–	–	–	–	–	–	11.8	10.2	13.4	10	–	–	–	–

[1] Abbreviations are: LMRF: lower montane rain forest, UMRF: upper montane rain forest and LRF: lowland rain forest.

[2] Values for S refer to total S in our study and SO_4^{2-} in the literature.

[3] Values in the literature refer to DOC.

[a] Present study; [b] *Veneklaas* [1990], study site at 2550 m altitude; [c] *Steinhardt* [1979]; [d] *Clark et al.* [1998]; [e] *Cavelier et al.* [1997]; [f] *Veneklaas* [1990], study site at 3370 m altitude; [g] *Hafkenscheid* [2000]; [h1-4] *Tobón et al.* [2004], h1-4 refers to four adjacent research areas: sedimentary plain, high terrace, low terrace and flood plain, respectively; [i] *Germer et al.* [2007]; [k1] *Forti and Moreira-Nordemann* [1991], data refers to wet season; [k2] *Forti and Moreira-Nordemann* [1991], data refers to dry season.

Note: TON and TOP values were not compared due to missing references in the literature, the mean, LCL and UCL (in µmol l⁻¹) are: 28.3, 20.2, 35.8 and 0.6, 0.3, 0.8 for TON and TOP, respectively.

why spatial patterns of throughfall volumes can be ecosystem-independent. Moreover, the various sampling techniques of the studies compared in Table 2.4 are certainly responsible for some of the observed differences [*Thimonier*, 1998].

Table 2.4: Spatial patterns of throughfall amount in this and thirteen other studies expressed as the coefficient of variation (CV, in %) and the MAD/median (MAD/M) ratio (in %). Both measures are provided for this study (MAD/M ratio in brackets), for the other studies there is only the CV available. The ranges of CVs in *Puckett* [1991] and *Keim et al.* [2005] refer to single events and CVs in *Whelan et al.* [1998] are for individual collection periods of 9 to 17 days length.

Reference	TF collectors		Forest type [1]	CV (MAD/M)
	N	A (cm²)		
Present study	25	122	LMRF	53 (49)
Clark et al. 1998	20	20	LMRF	29
Holwerda et al. 2006	30	100	LMRF	48
Keim et al. 2005	94	9	Douglas fir stand	14–22
			Mixed hardwood forest	30–38
			Mixed conifer forest	39–65
Lin et al. 1997[a]	18	942	Moist subtropical forest	13
Lloyd and Marques 1988[b]	36	127	LRF	54
Loescher et al. 2002	36	95	LRF	24
Pedersen 1992[c]	30	121	Sitka spruce stand	22
Puckett 1991	50	182	Mixed hardwood forest	12–18
Raat et al. 2002	24	320	Douglas fir stand	21
Rodrigo and Àvila 2001[a] [d]	36	79	Holm oak forest	21
Seiler and Matzner 1995	100	106	Norway spruce stand	3
Staelens et al. 2006a[e]	12	460	Mixed hardwood forest	18
Whelan et al. 1998	39	177	Norway spruce stand	7–16

[1] Abbreviations are: LMRF: lower montane rain forest, LRF: lowland rain forest.
[a] CV based on mean volumes, [b] Throughfall measured at 494 sampling positions with 36 roving gages over a one year period, calculation of CV follows *Holwerda et al.* [2006], [c] Mean of CV's of three even-aged Sitka spruce forests, [d] Mean of CV's of two adjacent holm oak forests, [e] CV refers to the leafed period.

In analogy to throughfall volumes, most solutes showed a high spatial variability (Table 2.5). The MAD/M ratio of VWM_P is very high for NO_3^- and PO_4^{3-} due to a spatial pattern of low solute concentrations (often below detection limit) for the majority of sampling points and few patches with high concentrations. For K, Mg, Ca, TOP and Cl^- we found a MAD/M ratio in the range of $62 - 77$, H^+, NH_4^+, TOC, TON and S had a lower ratio in the range of $38 - 52$ and the lowest spatial variability showed Na with a ratio of 27. The spatial variability of solute deposition decreased compared to the variability of solute

concentrations for most of the solutes; only H^+, NH_4^+, Na and TOP showed a higher MAD/M ratio for deposition rates than for concentrations.

To our knowledge there are no other studies that reported the spatial variability of throughfall chemistry of tropical montane forests. Moreover, a study conducted in a tropical rainforest [*Forti and Neal*, 1992a] is unfortunately not comparable with respect to sample size requirements. Hence, we compare our data based on CVs for both, concentrations and ion fluxes, with studies conducted in temperate coniferous forests [*Pedersen*, 1992; *Beier et al.*, 1993; *Seiler and Matzner*, 1995; *Whelan et al.*, 1998; *Raat et al.*, 2002], deciduous forests [*Puckett*, 1991; *Staelens et al.*, 2006a] and a subtropical forest [*Lin et al.*, 1997]. The comparison reveals that the spatial variability of K, Mg, Ca, Cl^-, NO_3^- and S is higher at our study site. The spatial variability of H^+ and NH_4^+ is at the upper end, and the variability of Na is within the range of the reported values. The other solutes (PO_4^{3-}, TOC, TON, TOP) were not compared as too few studies provided spatial CVs for these solutes.

We attribute the high spatial variability of both throughfall volumes and solutes to:

(1) A complex canopy structure due to a high diversity of tree species and the occurrence of tree ferns; an irregular canopy height partly as a result of steep slopes; and a high epiphyte load on the host trees [*Fleischbein et al.*, 2005].

(2) Stable structures in the canopy that cause temporally persistent patterns with respect to throughfall volumes and solute concentrations. Epiphytes are partly responsible for the generation of these patterns (see section 2.3.4).

(3) Low rainfall intensities and volumes (Table 2.1). In connection to this, several authors found that throughfall shows higher spatial variation for small events [*Scatena*, 1990; *Bouten et al.*, 1992; *Rodrigo and Àvila*, 2001].

Most CVs of solute concentrations exceeded those for solute deposition rates (Table 2.5) which is in part the result of negative correlations (except H^+, ρ: 0.67, p<0.01) between VWM_P solute concentrations and throughfall volumes (Table 2.6). Negative correlations between throughfall volumes and solute concentrations are frequently reported and indicate dilution effects [e.g. *Raat et al.*, 2002]. VWM_P solute concentrations were positively correlated with each other, except for H^+ and the correlation between NH_4^+ and S (Table 2.6). In general, correlations among most solutes were strong with the exception of NH_4^+; TOP, and PO_4^{3-}. A different pattern was observed for correlations among solute deposition rates and the throughfall magnitude. Most correlations were not significant. Strong correlations, however, existed between throughfall volumes and H^+, Na and NO_3^- deposition rates. Furthermore there were weak but significant correlations between throughfall volumes and NH_4^+, TON and PO_4^{3-} deposition. Few correlations among solute deposition were strong, e.g, among K, Mg, Ca, and Cl^- and between K and S.

Table 2.5: Spatial patterns of the chemical composition of throughfall in this and eight other studies expressed as the coefficient of variation (CV, in %) and the MAD/median (MAD/M) ratio (in %). Both measures are provided for this study (MAD/M in brackets), for the other studies there is only the CV available. The abbreviations C and D indicate if values are based on concentrations or ion deposition, respectively. Ranges of CVs in *Puckett* [1991] refer to single events and CVs from *Whelan et al.* [1998] are for individual collection periods of 9 to 17 days length. CVs in *Pedersen* [1992] refer to three even-aged Sitka spruce forests. For Na and K it was assumed that the monovalent cation and for Ca and Mg the divalent cation were the only species in solution.

Reference	Present study		Beier et al. 1993	Lin et al. 1997	Pedersen 1992	Puckett 1991	Raat et al. 2002	Seiler and Matzner 1995	Staelens et al. 2006a		Whelan et al. 1998	
TF collectors N	22		20	18	30	50	25	100	12		39	
A (cm²)	122		178	942	121	182	320	106	460		177	
Forest type	Tropical lower montane forest		Norway spruce	Moist subtropical forest	Sitka spruce	mixed hardwood forest	Douglas fir	Norway spruce	Beech		Norway spruce	
	C[c]	D	D	C[c]	C[d]	C	D	C[d]	C[c]	D	C	D
H⁺	52	(52)	55	59	17-34	15-53	–	35	13	28	–	–
NH₄⁺	55	(38)	44	18	29-53	19-177	26	24	37	23	38-175	31-170
Na⁺	28	(27)	45	16	33-47	24-63	26	42	26	11	–	–
K⁺	99	(62)	32	19	25-34	36-68	18	30	26	13	17-52	11-43
Mg²⁺	156	(73)	44	26	34-47	19-64	19	34	31	17	–	–
Ca²⁺	125	(74)	44	–	31-44	15-73	20	33	29	14	–	–
Cl⁻	110	(73)	42	19	33-47	23-82	22	61	28	13	25-62	18-57
NO₃⁻	292	(148)	39	18	26-37	14-33	19	29	25	14	32-56	23-63
PO₄³⁻	252	(148)	–	–	48-65	–	–	–	–	–	–	–
S[a]	73	(38)	41	13	28-47	7-32	26	38	30	16	25-52	23-44
TOC	54	(39)	–	–	–	–	–	–	–	–	–	–
TON[b]	45	(43)	–	–	–	–	–	24	–	–	–	–
TOP	113	(77)	–	–	–	–	–	–	–	–	–	–

Table 2.5 continued:

[a] Values for S refer to total S in our study and SO_4^{2-} in the literature.

[b] Value from *Seiler and Matzner* [1995] refers to DON.

[c] CVs in *Lin et al.* [1997], *Staelens et al.* [2006a] and this study based on volume-weighted means.

[d] CVs in *Pedersen* [1992] and *Seiler and Matzner* [1995] refer to time-average concentrations.

Table 2.6: Spearman rank correlation coefficients (ρ) for throughfall amounts (TF) and volume-weighted mean (VWMP) solute concentrations (values upper right) and solute deposition (values lower left), n=22, * p<0.05, ** p<0.01.

TF	H^+	NH_4^+	Na	K	Mg	Ca	Cl^-	NO_3^-	PO_4^{3-}	S	TOC	TON	TOP	
1	.67**	-.25	-.59**	-.50*	-.40	-.42	-.47*	-.79**	-.52*	-.37	-.55*	-.52*	-.48*	TF
.86**	1	-.25	-.65**	-.83**	-.66**	-.66**	-.84**	-.64**	-.72**	-.62**	-.56*	-.58**	-.61**	H^+
.47*	.43*	1	.23	.13	.07	.13	.25	.42	.19	-.05	.29	.26	.11	NH_4^+
.81**	.58**	.42	1	.63**	.60**	.60**	.69**	.61**	.53*	.45*	.46*	.46*	.29	Na
.07	-.26	-.15	.27	1	.80**	.78**	.87**	.57**	.66**	.81**	.78**	.77**	.48*	K
.02	-.26	-.18	.19	.74**	1	.97**	.75**	.67**	.42	.69**	.66**	.77**	.30	Mg
.00	-.29	-.18	.17	.65**	.95**	1	.81**	.69**	.46*	.62**	.69**	.80**	.33	Ca
-.02	-.38	.01	.28	.79**	.74**	.74**	1	.52*	.72**	.64**	.69**	.68**	.58**	Cl^-
-.75**	-.76**	-.28	-.54*	.17	.42	.47*	.22	1	.38	.43	.61**	.85**	.29	NO_3^-
-.43*	-.58**	-.23	-.17	.50*	.31	.29	.60**	.30	1	.64**	.42	.37	.56*	PO_4^{3-}
.42	.11	.04	.43*	.78**	.64**	.54*	.59**	-.19	.32	1	.65**	.57**	.38	S
.26	.14	.07	.22	.64**	.43	.42	.35	.06	.07	.61**	1	.90**	.24	TOC
.51*	.35	.23	.35	.38	.38	.35	.24	-.12	-.14	.43*	.56*	1	.24	TON
-.06	-.21	-.30	-.10	.45*	.30	.25	.50*	-.04	.40	.35	.04	.03	1	TOP

Similar correlation patterns among solute concentrations were found by others [e.g. *Whelan et al.*, 1998; *Raat et al.*, 2002; *Staelens et al.*, 2006a]. Interestingly, ions with different sources (e.g. K with endogenous sources, i.e. foliar leaching and Cl^- with exogenous sources, i.e. dry deposition) were strongly correlated, whereas other solutes showed only weak correlations (e.g. NH_4^+ and Cl^-, both solutes have exogenous sources). *Whelan et al.* [1998] suggested that similar spatial patterns among solutes with apparently different sources emerge because foliar leaching and dry deposition are both influenced by the density and architecture of the canopy. This might also be a consequence of electroneutrality because K^+ is the dominating cation in throughfall and Cl^- the dominating anion (Table 2.3).

The weak correlations between NH_4^+ and all other solutes can be explained by low solute concentrations (also detected for TOP and PO_4^{3-}); in particular, in event 4 and 5 over 50% of the samples showed concentrations below the detection limit, which caused weak spatial patterns. In addition, NH_4^+ showed a somewhat higher variability in throughfall concentrations among events (Figure 2.2), which further weakened the spatial patterns.

2.3.4 Temporal persistence of spatial throughfall patterns

A time stability plot of throughfall volumes (Figure 2.3) indicates extreme persistence of both dry (e.g. collectors 6, 18, 24, 5, and 16) and wet (e.g. collectors 20, 21, 23, 14 and 3) sampling points. Among the five driest sampling points four (collectors 6, 24, 5, and 16) received throughfall from an area with either thick moss mats (collectors 5 and 16) or vascular

epiphytes such as arboreal bromeliads (collectors 6 and 24). The agglomeration of the latter sampling points in a negative direction from the median (except collector 8) is not likely to occur by chance (random sample algorithm, p<0.05). There were two sampling points (collectors 8 and 20) that showed a higher variability of $\tilde{T}_{i,E}$, with $T_{i,E}$ extremes of up to 395% of the median throughfall magnitude. The receiving area of the five sampling points, which collected the highest throughfall volumes, was characterized by a more open canopy without big bromeliads that can store water in tank structures [*Zotz and Thomas*, 1999]. *Veneklaas and van Ek* [1990] described a similar pattern in that gauges below branches or trunks with abundant epiphyte loads had high interception values; interestingly, they found that during the wettest periods the gauge catch changed and showed characteristics similar to that of drip points. This phenomenon was observed for collector 8 in event 5 during this study. Mean $\tilde{T}_{i,E}$ was significantly different than zero for 68% of the collectors (Figure 2.3), thus throughfall volumes at individual sampling positions were not randomly distributed over time. The proportion of sampling points in this study that deviated consistently in one direction from the median seems to be high compared to 31 – 46% detected in two coniferous forests and one deciduous forest in the Pacific Northwest, USA [*Keim et al.*, 2005] and 48% (based on the standard deviation) measured in a Douglas fir stand in the Netherlands [*Raat et al.*, 2002].

Figure 2.3: Time stability plot of throughfall water normalized to zero median and unit variance. The collectors are plotted along the horizontal axis and ranked by their means, $\tilde{T}_{i,E}$. Error bars indicate the 95% confidence limits. Note: Collectors 1, 5, 6, 8, 16 and 24 received throughfall from areas with either thick moss mats or arboreal bromeliads, which were situated on branches directly above.

Time stability plots of solute concentrations (Figure 2.4) and deposition (Figure 2.5) were calculated for H^+, Na, K, Mg, Ca, Cl^-, S, TOC and TON. The other solutes showed at least in one event for half of the sampling points concentrations below the detection limit, which ruled out the calculation of $\tilde{C}_{i,E}$ and $\tilde{D}_{i,E}$ with equation 2.6. The sampling points showed low general persistence for most of the solute concentrations (H^+, Na, Mg, Ca,
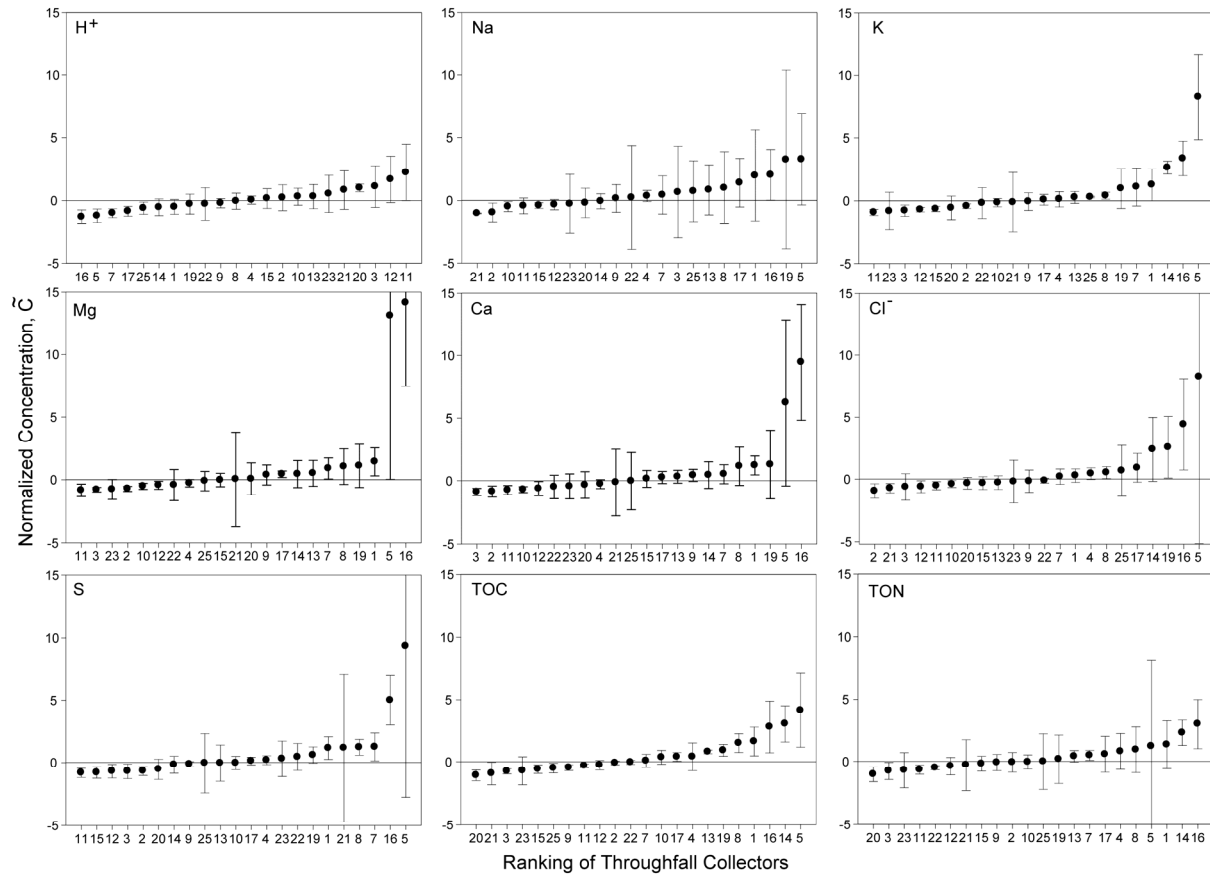
Figure 2.4: Time stability plot of throughfall solute concentrations normalized to zero median and unit variance. The collectors are plotted along the horizontal axis and ranked by their means, $\tilde{C}_{i,E}$. Error bars indicate the 95% confidence limits. Note: Collectors 1, 5, 8 and 16 received throughfall from areas with either thick moss mats or arboreal bromeliads, which were situated on branches directly above.

Cl^-, S and TON). A somewhat higher general persistence was detected for K and TOC concentrations, whereas the latter solute showed the greatest general persistence. Extreme persistence was detected for all solutes with more sampling points that deviated consistently in a negative direction from the median. The ranking of collectors by their mean $\tilde{C}_{i,E}$ (Figure 2.4) indicates a clear pattern in that sampling points with moss mats or bromeliads (collectors 1, 5, 8, 16) are agglomerated in a positive direction from the median and occupy the extreme ranking positions (for H^+ the agglomeration is in the negative direction from the median). This pattern is valid for all solutes and not likely to occur by chance (random sample algorithm, for H^+ and Cl^- p<0.05, all other solutes p<0.01). Mean $\tilde{C}_{i,E}$ were significantly different than zero for $23 - 68\%$ of the collectors (Figure 2.4, Table 2.7); K, Mg and TOC showed the most distinctive patterns.

The former patterns diminished with respect to K, Mg, S, TOC and TON solute deposition (cf. Figure 2.4 and 2.5; Table 2.7) in that general and extreme persistence were weaker or partly not detectable; for H^+, Na, Ca and Cl^- we detected either a higher
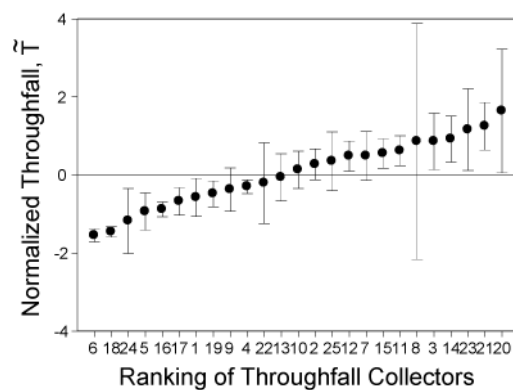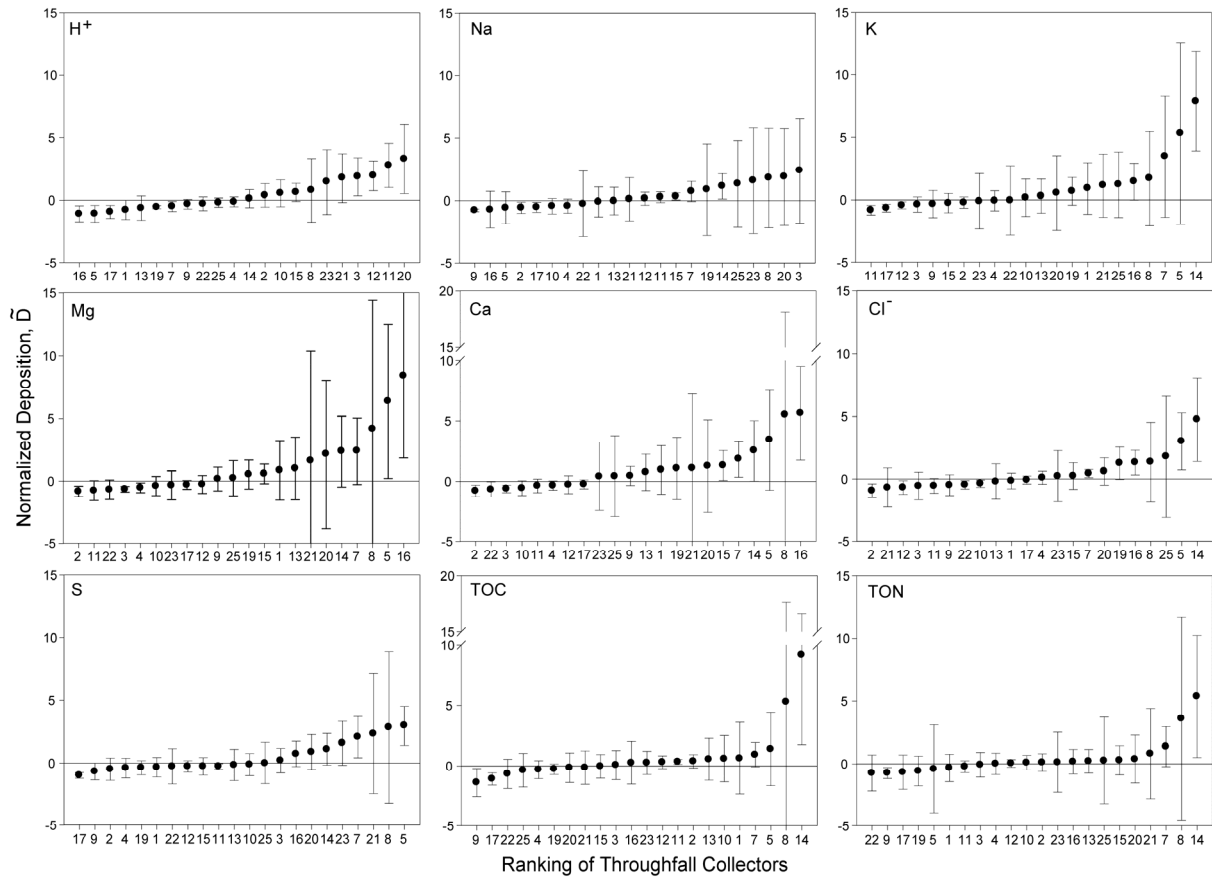
Figure 2.5: Time stability plot of throughfall solute deposition normalized to zero median and unit variance. The collectors are plotted along the horizontal axis and ranked by their means, $\tilde{D}_{i,E}$. Error bars indicate the 95% confidence limits. Note: Collectors 1, 5, 8 and 16 received throughfall from areas with either thick moss mats or arboreal bromeliads, which were situated on branches directly above.

Table 2.7: Proportion of collectors (in %) with mean normalized concentration (C) and mean normalized deposition (D) significantly different than zero (α=0.05).

Element	C	D
H^+	27	46
Na	23	23
K	50	18
Mg	46	23
Ca	32	32
Cl^-	36	36
S	41	23
TOC	68	18
TON	32	9

extreme persistence (H^+) or similar time stability patterns (Na, Ca and Cl^-). Furthermore, sampling points with moss mats or bromeliads were not for all solutes agglomerated in a direction from the median, only for K, Mg, Ca and TOC deposition did we detect an

agglomeration pattern that is not likely to occur by chance (random sample algorithm, for K and TOC, p<0.05; for Mg and Ca, p<0.01). Despite the somewhat weaker time stability patterns of solute deposition (in comparison to the detected patterns of solute concentrations), the proportion of collectors that showed a mean $\tilde{D}_{i,E}$ significantly different from zero for H^+, Na, Ca, Mg, and Cl^- was higher than values reported from temperate coniferous and deciduous forests [*Raat et al.*, 2002; *Staelens et al.*, 2006a]; K and S showed slightly lower values when compared with the data from *Staelens et al.* [2006a].

2.3.5 Temporal variability between events

The comparison of both rain and throughfall VWM_E solute concentrations between events showed no significant differences for most elements (Figure 2.2). We interpret the low temporal variability of rainfall VWM_E solute concentrations as a result of the overall low solute concentrations (in particular observed for NH_4^+, K, Mg, Cl^-, PO_4^{3-} and TOP). Conditions that favor low dust transport and stable wind directions during our short term observation period may explain the observed low solute concentrations in rainfall. Long-term data, however, show variable solute concentrations in rainfall [*Wilcke et al.*, 2001] and occasional high dust loads depending on the prevailing wind direction [*Wilcke*, unpublished]. The small differences between events in throughfall are potentially a result of several rainfall and biotic characteristics. First, all events studied had relative low intensities and magnitudes (Table 2.1), therefore the critical volume of water [*Neary and Gizyn*, 1994] required to remove all dry deposition from the foliage was perhaps not reached. Hence, a distinct dilution effect of throughfall water that is reflected in lower element concentrations at all sampling points was not likely to occur. This assumption is also supported by the within-event chemistry patterns (see section 3.6). Second, big epiphytes and accumulated dead organic matter are leached and consequently contribute to the enrichment of rainfall water [*Nadkarni*, 1986]; hence, a dilution effect of throughfall water is possibly weakened in places where big epiphytes and associated dead organic matter are dominant.

2.3.6 Within-event patterns

There were no clear temporal trends in volumes and solute concentrations of rainfall during the 72 monitored hours (Figure 2.6). The absence of within-event solute concentration dynamics was also observed for two wet season events in the western Amazon Basin [*Stallard and Edmond*, 1981]. Rainfall within-event solute concentration dynamics of certain elements seem to depend on site-specific conditions. Initially high solute concentrations that decreased during later event stages occurred for Ca^{2+}, Na^+ and Cl^- at locations near the sea [*Hansen*
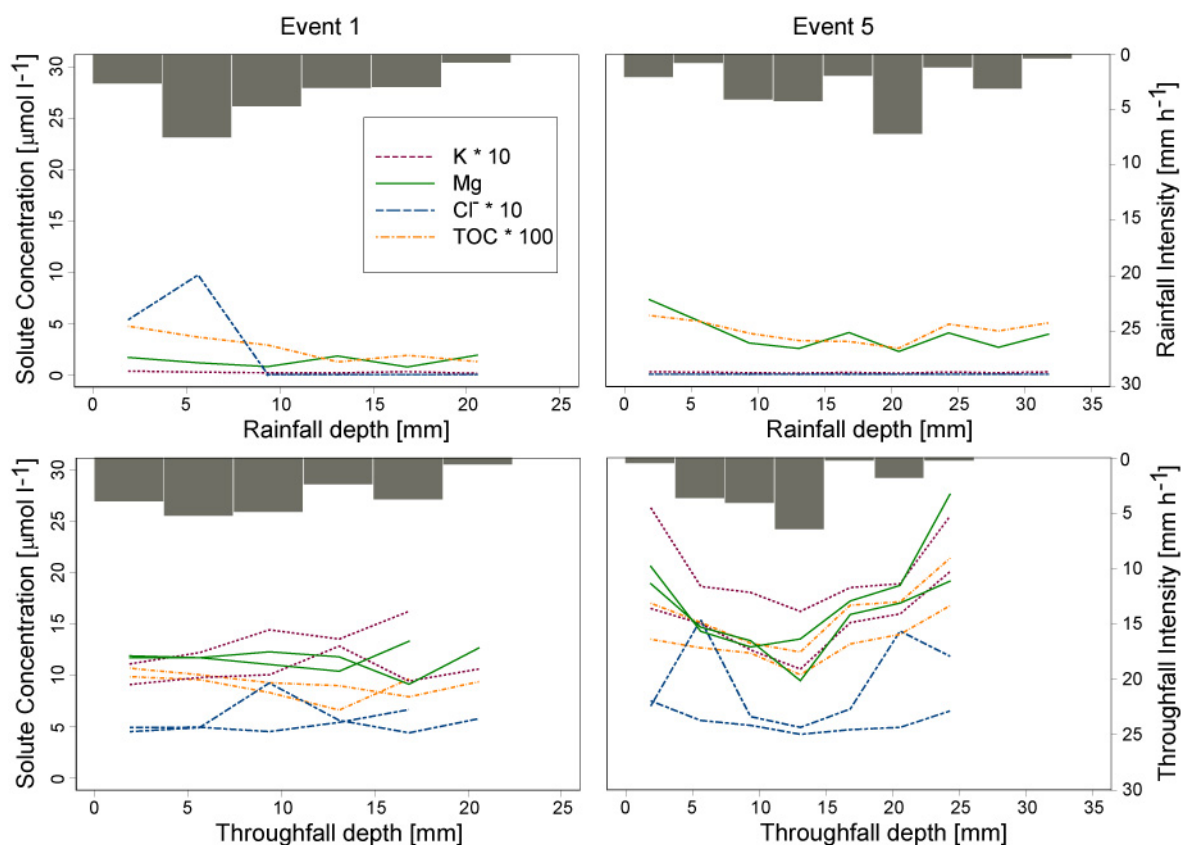
Figure 2.6: Selected within-event solute concentrations dynamics in rain and throughfall for K, Mg, Cl^- and TOC. The left and right panel refer to event 1 and 5, respectively. The solute concentrations of K, Cl^- and TOC are scaled for matters of comparison, scaling factors given in the legend. Throughfall within-event dynamics are shown for two individual sampling locations. The bars illustrate the rain and throughfall intensity, respectively. Event 1 and 5 were selected for this illustration because of their greater magnitude and hence higher sample number compared to the other events, for more details on event characteristics see Table 2.1.

et al., 1994], for NH_4^+ and SO_4^{2-} in agricultural areas [*Hansen et al.*, 1994], and for NH_4^+, K^+, NO_3^-, SO_4^{2-} and DOC in a Brazilian lowland forest influenced by widespread biomass burning [*Germer et al.*, 2007]. In contrast, in regions far away from marine inputs and anthropogenic emissions, within-event solute concentrations seem to show less distinct patterns. At such remote continental sites, the duration of the dry period before the rain event [*Hansen et al.*, 1994], the rainfall magnitude, and biogenic emissions of elements such as K [*Guyon et al.*, 2003] may influence within-event solute concentration dynamics in rainfall. Within-event throughfall solute concentration showed variable patterns. As shown in Figure 2.6 for K, Mg, Cl^- and TOC, we did not, for most solutes and events, detect decreasing concentrations that resulted in constant low concentration levels in later event stages. The concentration patterns of K, Mg, S and TOC varied little between the two within-event sampling sites. In addition, variations among events in the within-event patterns of K, Mg, S and TOC can be partly explained by different throughfall intensities. The change in

throughfall intensity was significantly correlated with the response of solute concentrations, i.e. increasing rainfall intensity decreased the variation in solute concentrations (Figure 2.7).

The concentration patterns of Na, Ca, Cl^-, TON and TOP were highly variable between events and sampling sites. The only common characteristic of within-event concentration dynamics of these solutes is that either concentrations fluctuated (e.g. Cl^-, Figure 2.6) or increased in later event stages. NH_4^+, NO_3^- and PO_4^{3-} concentrations varied without a clear trend within events, which might be partly a consequence of the low solute concentrations with 35, 78 and 59% of the samples below detection limit, respectively. H^+ concentrations decreased gradually with proceeding rainfall in all events as a consequence of buffering. There was no significant correlation of solute concentrations with throughfall intensity indicating that dilution/concentration effects did not control solute concentrations. Our results indicated that rainfall did not exhaust leachable ion pools in the canopy within the monitored 72 hours.
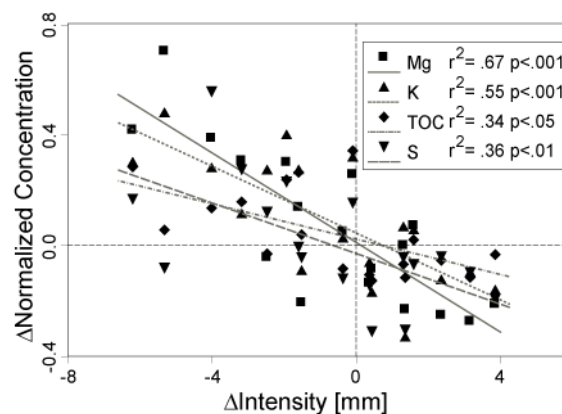
Figure 2.7: Relationships between change in throughfall intensity (Δ Intensity) and response of K, Mg, S and TOC concentrations (Δ Concentration) for the within-event sampling at one of the sampling sites (5 events, number of within-event samples = 23). The concentrations were normalized to the mean solute concentration of the particular events to allow a direct comparison between solutes. Regression lines based on least squares, the proportion of variance explained by the linear model and the level of significance is indicated.

In summary, we attribute the observed within-event solute concentration patterns to: (1) Low rainfall intensities that lead to an incomplete removal of dry deposition and to slow washoff processes. Accordingly, leachable canopy ion pools were never emptied except for NH_4^+, NO_3^- and PO_4^{3-} pools, which showed frequently a complete depletion in later event stages. In addition, low rainfall intensities result in longer contact times of rain water with the canopy surface and therefore higher ion concentrations [*Lovett and Schaefer*, 1992; *Hansen et al.*, 1994]. In contrast to our observations, in a Brazilian lowland rain forest constant low throughfall concentration levels were observed during intense and long lasting rains in later

event stages, indicating a strong depletion of ion pools (mainly derived from dry deposition, *Germer et al.*, 2007].

(2) The slow wetting of organic matter (which supports the growth of large epiphytes and is in turn replenished by them, *Köhler et al.*, 2007] and subsequent leaching and wash-off processes may partly explain the fluctuating solute concentrations during some events (e.g. *TOC* concentrations, Figure 2.6). This assumption is supported by our findings that below thick moss mats and big bromeliads throughfall element concentrations are high compared to the median concentration level in a particular event (Figure 2.4). The relevance of the latter process is stressed by the fact that epiphyte mats, organic matter, and mineral dust accumulate in large quantities in the canopy of tropical montane forests [*Nadkarni et al.*, 2004; *Köhler et al.*, 2007].

2.4. Conclusions

(1) The spatial variability of throughfall quantity and quality of the studied Ecuadorian montane forest was at the higher end of tropical forests but not consistently higher than at other tropical forest sites. This suggests that plant diversity and throughfall heterogeneity are not linearly correlated.

(2) The observed spatial pattern was temporally stable during the three-months observation period. Thus, canopy structures controlling the throughfall pattern seem to be stable at least at the scale of a few weeks.

(3) Rainfall intensity and cumulative volume was in all five monitored events too low to deplete the large leachable ion pools in the canopy of the studied forest during 72 hours. This might be typical of tropical montane forests with their usually light rainfall, strong epiphytism, and associated soil-like matter accumulations in the canopy.

2.5 Acknowledgments

Spatio–temporal patterns of throughfall and solute deposition in an open tropical rain forest.

Alexander Zimmermann[1], Sonja Germer[1], Christopher Neill[2], Alex V. Krusche[3], Helmut Elsenbeer[1]

[1] Institute of Geoecology, University of Potsdam, Karl-Liebknecht-Str. 24-25, 14476 Potsdam, Germany

[2] The Ecosystems Center, Marine Biological Laboratory, Woods Hole, MA 02543, USA

[3] CENA, University of São Paulo, PO BOX 96, 13.400–970 Piracicaba, S.P., Brazil

Abstract   The brief interaction of precipitation with a forest canopy can create a high spatial variability of both throughfall and solute deposition. We hypothesized that (i) the variability in natural forest systems is high but depends on system-inherent stability, (ii) the spatial variability of solute deposition shows seasonal dynamics depending on the increase in rainfall frequency, and (iii) spatial patterns persist only in the short-term. The study area in the north-western Brazilian state of Rondônia is subject to a climate with a distinct wet and dry season. We collected rain and throughfall on an event basis during the early wet season (n=14) and peak of the wet season (n=14) and analyzed the samples for pH and concentrations of NH_4^+, Na^+, K^+, Ca^{2+}, Mg^{2+}, Cl^-, NO_3^-, SO_4^{2-} and DOC. The coefficient of variation for throughfall based on both sampling intervals was 29%, which is at the lower end of values reported from other tropical forest sites, but which is higher than in most temperate forests. Coefficients of variation of solute deposition ranged from 29 to 52%. This heterogeneity of solute deposition is neither particularly high nor particularly low compared with a range of tropical and temperate forest ecosystems. We observed an increase in solute deposition variability with the progressing wet season, which was explained by a negative correlation between heterogeneity of solute deposition and antecedent dry period. The temporal stability of throughfall patterns was low during the early wet season, but gained in stability as the wet season progressed. We suggest that rapid plant growth at the beginning of the rainy season is responsible for the lower stability, whereas less vegetative activity during the later rainy season might favor the higher persistence of "hot" and "cold" spots of throughfall quantities. The relatively high stability of throughfall patterns during later stages of the wet season may influence processes at the forest floor and in the soil. Solute deposition patterns showed less clear trends but all patterns displayed a short-term stability only. The weak stability of those patterns is apt to impede the formation of solute deposition-induced biochemical microhabitats in the soil.

3.1 Introduction

During the passage of rain water through a forest canopy two main processes take place: first, water is redistributed, and second, its quality changes due to foliar leaching, removal of dry deposition and the assimilation of nutrients by leaf-dwelling organisms. The brief interaction of precipitation with the phyllosphere can create a high spatial variability of both throughfall and solute deposition [*Kimmins*, 1973; *Kostelnik et al.*, 1989; *Puckett*, 1991; *Beier et al.*, 1993; *Whelan et al.*, 1998; *Zimmermann et al.*, 2007]. Since throughfall is an important pathway of nutrients to the forest floor [Parker, 1983], particularly in tropical forest ecosystems on strongly weathered soils [*Bruijnzeel*, 1991], emerging spatial patterns in throughfall potentially control processes at the forest floor and in the soil. Several studies found effects of throughfall patterns on the spatial distribution of soil water content [*Schume et al.*, 2003], root water uptake [*Bouten et al.*, 1992], root growth [*Ford and Deans*, 1978] and annual seepage water fluxes [*Manderscheid and Matzner*, 1995]. *Raat et al.* [2002], however, could not directly relate throughfall patterns with soil water content, mainly because of forest floor thickness and drainage. The strength of the relationship between throughfall patterns and spatial processes at or below the forest floor critically depends not only on the spatial variability of the throughfall characteristic but also on its spatio-temporal stability [*Keim et al.*, 2005].

The majority of studies on throughfall patterns took place in temperate forests; only a few studies dealt with the spatial variability of throughfall in tropical forests [*Lloyd and Marques*, 1988; *Loescher et al.*, 2002; *Holwerda et al.*, 2006]. Hence, the overall knowledge is fragmentary particularly with respect to ion flux patterns and their temporal stability. In tropical forests, throughfall volumes seem to show a broader frequency distribution than in most managed temperate forest stands with typical ranges of 0 – 200 % of incident precipitation compared to 0 – 100 % relative throughfall, respectively [*Lloyd and Marques*, 1988; *Holwerda et al.*, 2006]. In this context, *Zimmermann et al.* [2007] reported a very high spatial variability of solute deposition in a tropical montane forest.

Studies from temperate forests indicate that spatial patterns of throughfall might persist over several events [*Keim et al.*, 2005]. Other researchers detected a temporal stability of throughfall and solute deposition even at seasonal timescales [*Raat et al.*, 2002; *Staelens et al.*, 2006a, b].

Meteorological event characteristics such as the rainfall magnitude, intensity and duration are known to influence throughfall patterns [*Levia and Frost*, 2006]. While some researchers found that high rainfall magnitudes decrease the spatial variability of throughfall [*Bouten et al.*, 1992; *Rodrigo and Àvila*, 2001; *Staelens et al.*, 2006b] no consensus has been reached regarding the role of the precipitation intensity [*Levia and Frost*, 2006]. The

influence of meteorological conditions on solute deposition patterns is largely unknown [*Levia and Frost*, 2006]. *Lovett et al.* [1999] and *Raat et al.* [2002], however, noted that dry deposition increases the spatial variability of solute deposition. Since large parts of tropical forests are exposed to biomass burning [*Andreae et al.*, 2004], elevated dry deposition [*Andreae et al.*, 1990] might influence the spatial variability of solute deposition patterns in those forests.

The understanding of throughfall spatial patterns and its temporal stability is important for a wide range of eco – hydrological applications such as: (1) modeling of water and ion fluxes in forested watersheds [*Zirlewagen and von Wilpert*, 2001], (2) investigation of plant / soil-nutrient interactions, which may explain the distribution of trees [*John et al.*, 2007], and (3) research on the distribution of micro-, meso- and macrofauna at or in the soil, which show higher abundance under moist conditions [*Levings and Windsor*, 1984, 1996; *Kaspari and Weiser*, 2000].

The objectives of our study were to investigate: (1) the spatial variability of throughfall and solute deposition in an open tropical rain forest, (2) the influence of contrasting precipitation regimes and rainfall characteristics on these patterns, and (3) the temporal stability of the spatial patterns throughout the wet season. We hypothesized that:

(1) The spatial variability of throughfall and its chemical composition is high but does not exceed the variability in structurally diverse and comparably stable forest ecosystems (the seasonality of leaf production is a factor that influences this stability).

(2) The spatial variability of throughfall solute deposition differs between early and later stages of the wet season, because meteorological characteristics such as the rainfall frequency change markedly throughout the wet season.

(3) The temporal stability of the spatial pattern is high in the short term but not throughout the wet season.

3.2 Methods
3.2.1 Research area

The study was conducted in Rancho Grande (10° 18' S, 62° 52' W, 143 m a.s.l.) in the northwestern Brazilian state of Rondônia. Mean annual temperature and precipitation for the years 1984–2003 were 27°C and 2300 mm, respectively [*Germer et al.*, 2006]. The precipitation regime shows an unimodal distribution with a maximum between December and March and a pronounced dry period from June to August. Soils in the area are classified as Kandiudults [*Soil Survey Staff*, 2003; *Zimmermann et al.*, 2006]. The primary vegetation is classified as open tropical rainforest (Floresta Ombrófila Aberta) with a high abundance of palms [*Pires and Prance*, 1986]. Tree density for the size class of > 5 cm dbh (diameter at

breast height) is 813 ha $^{-1}$, including 108 palms. The most common tree species in the latter size class are *Brosimum gaudichaudii* Trécul (Moraceae) and *Protium sp.*, (Burseraceae). Among palms (Arecaceae), *Iriartea deltoidea* Ruiz & Pav. and *Orbignya phalerata* Mart. are the most abundant.

3.2.2 Field sampling

Rain and throughfall samples were collected on an event basis in the early wet season from September to November 2004 (n=14 events) and during the peak of the wet season from January to the beginning of April 2005 (n=14 events) (EWS and WS, respectively, from hereon). Rainfall events were defined as follows: at least 0.508 mm recorded in 30 minutes, events were separated by two hours without rain. Rainfall measurement and sampling were conducted in a pasture at a distance of 400 m from the forest. A tipping bucket rain gauge (Hydrological Services P/L, Liverpool Australia) with a resolution of 0.254 mm and a Campbell Scientific data logger recorded precipitation at 5-minute intervals. Rainfall was sampled with a trough-type collector. The collector, installed 1 m above ground, consisted of a PVC pipe with a receiving area of 980 cm^2, which was connected via flexible tubing to a 20 liter canister. A fine nylon mesh pre-leached with de-ionized water between trough and tubing prevented contamination with organic material and insects. In order to minimize dry deposition in the EWS, the trough was rinsed daily with de-ionized water on days without precipitation. In the WS dry deposition was expected to be low.

Throughfall was sampled with 20 collectors, which were identical in construction to the rainfall sampling device. The collectors were distributed throughout a 1.37 ha catchment with a maximum distance of 140 m between collectors. The sampling sites were chosen at random, but with a view towards minimizing disturbance instead of a strictly random distribution. After each event troughs were cleaned of organic material. We measured rain and throughfall volumes and collected samples two hours after each event, or alternatively the next morning for events that ended later than 9:00 PM. Samples were collected in 1 L Nalgene polyethylene bottles, which were pre-washed with dilute (5%) *HCl* and then rinsed with de-ionized water.

3.2.3 Laboratory analysis

Immediately after sample collection we measured pH of an unfiltered aliquot with an Orion pH meter (model 250A+). A 50 ml aliquot for cation/anion analysis was filtered through 0.7 μm pre-ashed glass fiber fine filters (Whatman). After filtration samples were stored in acid washed polyethylene bottles, preserved with thymol and frozen. For *DOC*

analysis we filtered another 50 ml and stored samples in pre-combusted, acid washed 30 ml glass vials with acid washed Teflon lid liners. DOC samples were preserved with $HgCl_2$ at a final concentration of 300 μmol l^{-1} and refrigerated. Concentrations of NH_4^+, Na^+, K^+, Ca^{2+}, Mg^{2+}, Cl^-, SO_4^{2-} and NO_3^- were analyzed with a Dionex ion chromatograph (model DX-500). A Shimadzu total carbon analyzer (model TOC 5000A) was used to measure DOC concentrations by combustion at 720°C and detection of the evolved CO_2 in a non-dispersive infrared gas analyzer. The detection limits were (in μmol l^{-1}): NH_4^+=2.77, Na^+=2.17, K^+=1.28, Ca^{2+}=1.25, Mg^{2+}=2.06, Cl^-=1.41, SO_4^{2-}=0.52, NO_3^-=0.81 and DOC=10. Analytical variability of solute concentrations was always less than 10%. Sample blanks of de-ionized water that passed through the PVC collectors were below detection limits.

3.2.4 Data analysis
3.2.4.1 Solute concentrations and deposition

Volume-weighted means per event E (VWM_E) were used to express mean throughfall solute concentration of individual events. The VWM_E per event was calculated as:

$$VWM_E = \left(\sum_{n=1}^{i} C_{i,E} V_{i,E} \right) \left(\sum_{n=1}^{i} V_{i,E} \right)^{-1} \qquad (3.1)$$

for all sampled events, where $C_{i,E}$ and $V_{i,E}$ are the concentration and volume at collector i for event E. To compare rain and throughfall solute concentrations of the EWS and WS we provided means of these sampling periods and 95% confidence limits by bootstrapping [Efron and Tibshirani, 1993] the throughfall VWM_E's and the measured rainfall solute concentrations.

The analysis of spatial patterns and their temporal persistence is based on fluxes. The solute flux (solute deposition is used synonymously) at collector i, D_i, was calculated as:

$$D_i = \sum_{n=1}^{E} \left(C_{i,E} \cdot V_{i,E} \right) \qquad (3.2)$$

3.2.4.2 Spatial variability of throughfall and solute deposition

Seiler and Matzner [1995], *Raat et al.* [2002], and *Staelens et al.* [2006a, b] described the spatial variability of throughfall and ion deposition with the coefficient of variation (CV). Since the Shapiro-Wilk-Statistic [*Shapiro and Wilk*, 1965] suggested Gaussian behavior for the majority of our throughfall flux data, we too, expressed the spatial variability by the CV.

To understand the main factors that influence the variability of throughfall quantities (T) and solute deposition (D), we calculated non-parametric Spearman rank correlation coefficients between the CVs of throughfall quantity and solute deposition (n = 28 events) and a set of rainfall event characteristics such as gross precipitation (P_G), solute concentration in precipitation ($P_{G\ conc.}$), antecedent dry period (ADP), amount of precipitation of previous 3 and 7 days ($Index_3$ and $Index_7$, respectively), mean precipitation intensity (mean I) and maximum 30 minute precipitation intensity ($maxI_{30}$).

3.2.4.3 Temporal persistence of spatial patterns

Several techniques have been developed to analyze the temporal stability of spatial patterns [*Vachaud et al.*, 1985; *Raat et al.*, 2002]. *Keim et al.* [2005] considered the variance of the sampling points to describe the persistence of high or low throughfall areas:

$$\tilde{\delta}_{i,E} = \left(\delta_{i,E} - \bar{\delta}_E \right) \left(s\delta_E \right)^{-1} \tag{3.3}$$

where $\tilde{\delta}_{i,E}$ and $\delta_{i,E}$ are the normalized variable δ and the variable δ at sampling point i of event E, respectively, $\bar{\delta}_E$ is the mean of δ in event E, and $s\delta_E$ its standard deviation. We used equation 3.3 to analyze the persistence of spatial patterns of throughfall and solute deposition, but replaced $\bar{\delta}_E$ with the median of δ_E, $M\delta_E$, and $s\delta_E$ with the median absolute deviation of δ_E, $MAD\delta_E$, because our data frequently did not match the normal distribution if analyzed on an event basis:

$$\tilde{\delta}_{i,E} = \left(\delta_{i,E} - M\delta_E \right) \left(MAD\delta_E \right)^{-1} \tag{3.4}$$

The plot of $\tilde{\delta}$ for each event and throughfall collector, ranked from minimum to maximum mean $\tilde{\delta}_{i,E}$, shows the deviation of a variable from the median for all sampling points. These time stability plots illustrate two types of persistence [*Keim et al.*, 2005]. First, extreme persistence refers to the deviation of the mean $\tilde{\delta}_{i,E}$ from the median in the region of the lower and upper quartiles of the ranked sampling points (Figure 3.1). Second, general persistence appears as the deviation of the mean $\tilde{\delta}_{i,E}$ in the interquartile range. Within this region, single sampling points can be situated persistently above or below the median without being extremes [*Keim et al.*, 2005]. We used 95% confidence limits of the mean $\tilde{\delta}_{i,E}$ as the criterion of persistence; other authors applied $\pm$ 1 standard deviation as a weaker criterion [*Raat et al.*,

2002; *Staelens et al.*, 2006a, b]. In the remainder of the paper we replaced δ with T and D for the amount of throughfall and solute deposition, respectively.
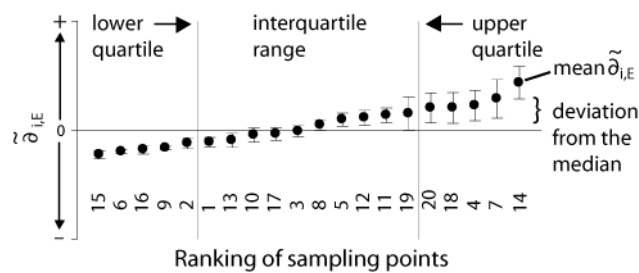
Figure 3.1: Characteristics of a time stability plot. The plot shows $\tilde{\delta}_{i,E}$, the deviation of a variable δ from the median for each sampling point i and all events E. Sampling points are ranked from minimum to maximum mean $\tilde{\delta}_{i,E}$. The bars indicate 95% confidence intervals. Data points pertaining to the lower or upper quartile are deemed extreme as long as their confidence intervals do not overlap with the median line. Data points falling into the interquartile range, but with confidence intervals not including the median are considered generally persistent, while those with confidence intervals including the median are not persistent.

In addition to time stability plots, we calculated Spearman rank correlation coefficients (r_s) of all possible event pairings (n=91 for EWS and WS, respectively) for throughfall and solute deposition. We then examined whether r_s could be modeled as a function of the temporal lag between events (Δ day). The latter analysis is a technique to investigate the change of a spatial pattern through time, given that Δ day is a significant predictor for r_s. To explain the variation in the Spearman rank correlation coefficients we tested if the inclusion of meteorological event characteristics (P_G, ADP, Index$_3$, Index$_7$, mean I and maxI$_{30}$) as additional independent variables could improve the model. For choosing the best model we performed a stepwise model selection using the Akaike information criterion [*Venables and Ripley*, 2002].

We used S-PLUS [*Insightful Corporation*, 2001a, b] and R Version 2.6.0 [*R Development Core Team*, 2007] for data analysis.

3.3 Results
3.3.1 Event characteristics

The total incident rainfall from September 16th to November 17th 2004 (EWS) was 383 mm and from January 22nd to April 3rd 2005 (WS) we measured 779 mm. Precipitation in the EWS is close to the mean of 373 mm for this period in the previous 20 years, whereas during the WS the amount of rain is slightly below the 20 year mean of 834 mm. During the EWS we collected 351 mm and during the WS 430 mm of incident rainfall. The sampled events

showed a broad range of rainfall magnitudes, storm intensities and antecedent wetness conditions (Table 3.1). For the antecedent dry period (ADP) and the antecedent wetness index of the previous three days (Index$_3$), we detected significantly shorter dry periods and higher antecedent rainfall in the WS, respectively (p<0.01, Wilcoxon rank sum test). All other event characteristics showed no significant differences between both sampling periods.

Table 3.1: Event characteristics, P$_G$: gross precipitation, mean I: mean precipitation intensity, maxI$_{30}$: maximum 30 minute precipitation intensity, ADP: antecedent dry period, Index$_3$ and Index$_7$ are the 3 and 7 day antecedent wetness index, a sum of all precipitation for the previous 3 and 7 days, respectively.

Event	Date	P$_G$	mean I	max I$_{30}$	ADP	Index$_3$	Index$_7$
	dd-mm-yy	mm	mm/h	mm/h	h	mm	mm
1	16-09-04	21.3	7.3	21.8	339	0.0	0.0
2	25-09-04	27.2	29.6	48.3	227	0.0	0.0
3	29-09-04	7.9	13.5	15.2	26	2.5	40.1
4	07-10-04	25.7	30.8	46.7	73	0.3	2.3
5	12-10-04	31.2	20.8	51.3	43	1.8	27.7
6	21-10-04	33.3	33.3	44.2	22	0.8	8.6
7	24-10-04	10.4	2.8	12.2	67	1.0	35.1
8	27-10-04	4.3	3.2	5.1	72	0.3	45.0
9	30-10-04	19.8	29.7	38.6	64	4.3	15.0
10	04-11-04	45.5	10.1	58.9	26	4.6	27.9
11	10-11-04	31.0	6.1	37.6	88	0.0	103.6
12	11-11-04	6.4	1.9	3.6	26	31.2	89.2
13	14-11-04	63.8	6.1	47.2	7	6.6	39.6
14	17-11-04	23.6	31.5	46.7	70	1.0	102.6
15	22-01-05	78.2	15.9	64.0	15	1.0	4.3
16	24-01-05	23.1	46.2	46.2	48	79.0	81.0
17	31-01-05	29.5	35.4	43.7	26	23.6	73.4
18	04-02-05	15.2	26.1	30.0	73	0.0	79.5
19	11-02-05	37.8	3.9	33.5	42	59.7	70.6
20	19-02-05	30.5	19.3	43.7	23	49.8	55.1
21	23-02-05	34.9	9.3	32.0	44	24.4	106.2
22	27-02-05	31.8	6.7	42.7	22	6.1	67.8
23	02-03-05	11.7	2.5	5.6	12	57.7	101.1
24	05-03-05	57.7	21.6	73.7	24	6.6	76.7
25	14-03-05	20.6	5.6	13.2	15	5.1	14.2
26	18-03-05	10.7	25.6	21.3	11	28.2	52.6
27	28-03-05	33.5	2.6	6.6	2	5.8	9.7
28	02-04-05	14.5	2.9	9.7	20	3.0	38.4

3.3.2 Rain and throughfall quality

For the majority of solutes we detected differences of concentrations in rain and throughfall between EWS and WS (Figure 3.2). The drier pre-event conditions during the EWS coincided with significantly higher solute concentrations in rain and throughfall compared to the WS, with the exception of H^+, Na^+, Cl^- and DOC. For Na^+ and Cl^- we detected significant differences only in throughfall, and for DOC only in rainfall, whereas H^+ concentrations showed no seasonal variation.

Interestingly, we detected during the EWS only for K^+, Mg^{2+} and DOC a significant enrichment of throughfall compared to rainfall, while during the WS all solutes but Na^+ and Ca^{2+} showed significantly higher concentrations in throughfall (Figure 3.2). For H^+ we did not observe significant depletion, which indicates little buffering in the canopy. In some events we observed canopy uptake of NH_4^+, Ca^{2+} and NO_3^-. Concentrations of Ca^{2+} in rainfall exceeded those in throughfall in 16 events, NH_4^+ showed the latter phenomenon in eight events, and NO_3^- only twice during this study.
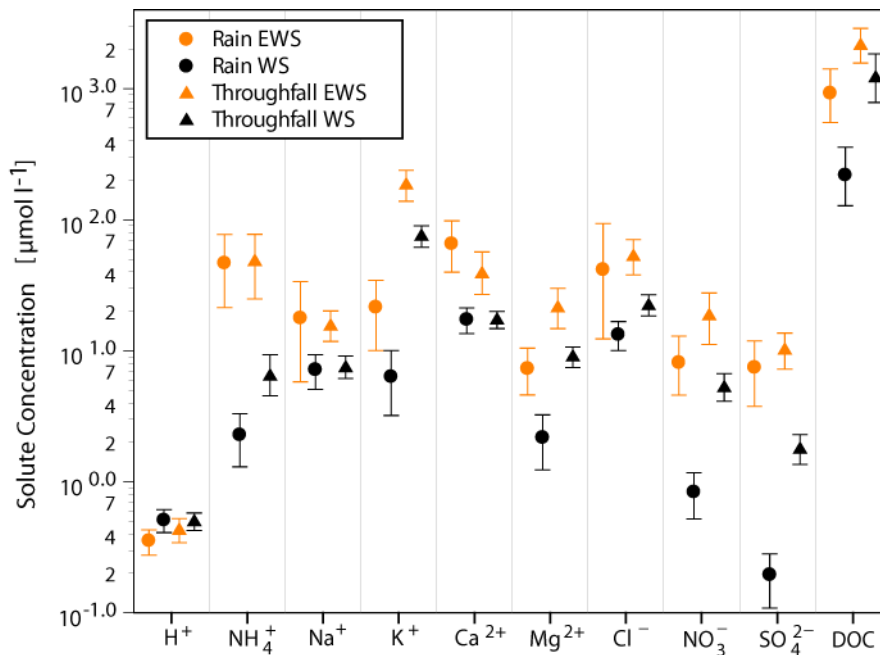
Figure 3.2: Solute concentration dynamics in rain and throughfall between the early (EWS, n=14 events) and peak of the wet season (WS, n=14 events). The bars indicate 95% confidence intervals.

3.3.3 Spatial patterns of throughfall and solute deposition

The spatial variability of throughfall deposition based on both EWS and WS was highest for SO_4^{2-}, Cl^-, NO_3^- and DOC. Throughfall volumes, NH_4^+ and Ca^{2+} showed relatively low CVs (Table 3.2). The ratios of maximum to minimum catch in the collectors for the whole study period were high for K^+, SO_4^{2-}, Cl^-, NO_3^- and DOC. For the latter solutes, we found ratios between 4.6 and 6.3.

The patterns of throughfall amount and most solutes, except for Na^+, Ca^{2+} and Mg^{2+}, showed a higher spatial variability in the WS than in the EWS (Table 3.2). A comparison of CVs on an event basis (Figure 3.3), however, indicated a significant increase in variability from the EWS to the WS only for the deposition patterns of DOC and SO_4^{2-} (Wilcoxon rank sum test, p<0.001 and p<0.05, respectively). The spatial patterns of NH_4^+, K^+, Cl^-, SO_4^{2-} and DOC were significantly correlated to pre-event conditions (Table 3.3) in that an increase of rainfall prior to an event and a decrease of the antecedent dry period coincided with an increase of the spatial variability of throughfall solute deposition patterns

(though Cl^- deposition patterns were significantly correlated only with ADP). Moreover, the spatial variability of SO_4^{2-} and DOC deposition patterns were negatively correlated with the solute concentration in rainfall. Beside the influence of antecedent wetness conditions and rainfall chemistry, we found significant negative correlations between rainfall intensities and the spatial variability of throughfall quantity, H^+ and Cl^- deposition.

Table 3.2: Spatial patterns of throughfall volume and solute deposition expressed as the coefficient of variation (CV, %, n=20), and the maximum /minimum ratio for the early wet season (EWS, n=14 events), peak of the wet season (WS, n=14 events) and throughout the rainy season (EWS and WS, n=28 events), respectively.

Variable	EWS		WS		EWS and WS	
	CV	Max/min	CV	Max/min	CV	Max/min
Water	26	2.9	35	3.9	29	2.6
H^+	39	4.1	52	6.8	43	4.2
NH_4^+	29	2.5	60	7.4	29	2.5
Na^+	42	3.6	41	5.8	38	4.1
K^+	39	4.5	48	4.6	40	4.6
Ca^{2+}	35	4.6	31	2.9	31	3.2
Mg^{2+}	40	4.5	38	3.8	38	4.0
Cl^-	50	5.6	54	6.8	48	6.0
NO_3^-	42	4.5	78	11.9	47	4.6
SO_4^{2-}	48	5.8	71	9.8	52	6.3
DOC	35	4.1	73	12.1	44	4.6

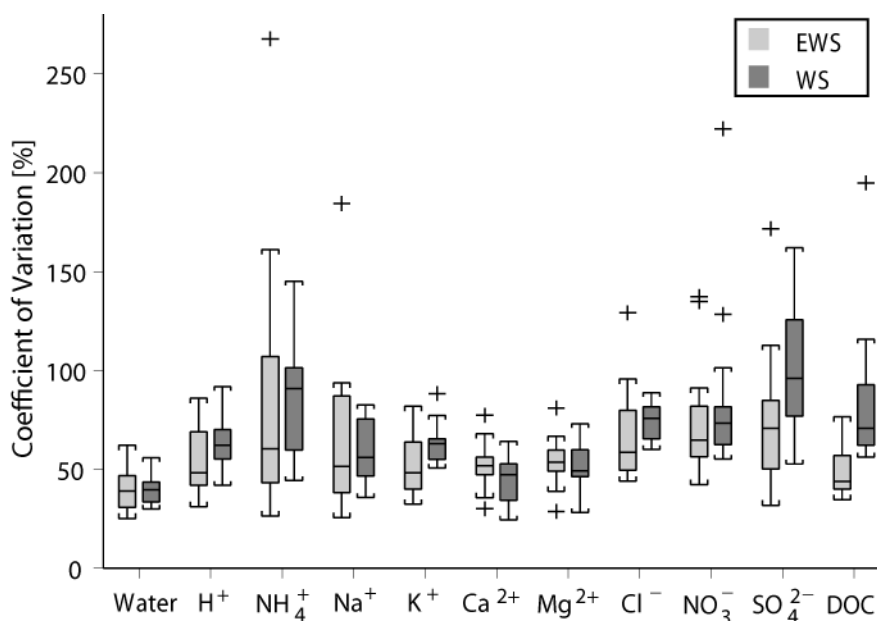Figure 3.3: Box plot comparison of the spatial coefficient of variation (CV, %, n=20) for throughfall and solute deposition during the early wet season (EWS, n=14 events) and peak of the wet season (WS, n=14 events). The length of each box represents the interquartile range, the horizontal bar the median, and the crosses indicate data points further away from the quartile than 1.5 times the interquartile range.

Table 3.3: Spearman rank correlation coefficients between the spatial variability of throughfall variables expressed by the coefficient of variation (CV, EWS and WS, n=28 events, n=20) and gross precipitation (P_G), solute concentration in precipitation ($P_{G\ conc.}$), antecedent dry period (ADP), amount of precipitation of previous 3 and 7 days ($Index_3$ and $Index_7$, respectively), mean precipitation intensity (mean I) and maximum 30 minute precipitation intensity ($maxI_{30}$). Only solutes that showed significant correlations are shown.

CV	P_G	$P_{G\ conc.}$	ADP	$Index_3$	$Index_7$	mean I	max I_{30}
Water	-0.40*	n.a.	n.a.	n.a.	n.a.	-0.49*	-0.59**
H^+	–	–	–	–	–	-0.57**	-0.60**
NH_4^+	–	–	-0.42*	0.56**	0.54**	–	–
K^+	–	–	-0.46*	0.55**	0.60**	–	–
Cl^-	–	–	-0.40*	–	–	–	-0.41*
NO_3^-	0.39*	–	–	–	–	–	–
$SO_4^{2-\ a)}$	–	-0.57*	-0.46*	0.39*	0.53**	–	–
DOC	–	-0.61**	-0.51**	0.71***	0.63**	–	–

n.a.: not applicable, – not significant, * p<0.05, ** p<0.01, *** p<0.001
[a)] n=19 events with $P_{G\ conc.}$ data

3.3.4 Temporal persistence of spatial throughfall patterns

Time stability plots of throughfall (Figure 3.4) indicate extreme persistence of both dry (e.g. collectors 2, 6 and 16) and wet (e.g. collectors 7, 14 and 20) sampling points. During both EWS and WS mean normalized throughfall was significantly different from zero for 65% of the collectors, thus throughfall volumes at individual sampling positions were not randomly distributed over time. The comparison of throughfall time stability plots between EWS and WS (Figure 3.4) showed that the ranking position of individual collectors can change substantially, in particular wet sampling points showed a lower stability (e.g. collectors 4, 17 and 19). The stability of the spatial pattern (based on r_s) during the EWS is restricted to short-term periods of about a month. In contrast, we still detected significant correlations (p<0.05) among events after more than two months during the WS (Figure 3.5). The temporal lag between events (Δ day) is a strong predictor for the stability of the spatial pattern during the EWS, whereas during the WS, meteorological variables such as the $maxI_{30}$, play a more important role. The relative importance of Δ day vs. meteorological event parameters is clearly illustrated by the slope of the two-parameter-plane in the respective direction, i.e. the steeper the slope, the more important the given parameter as a predictor of r_s (Figure 3.5).
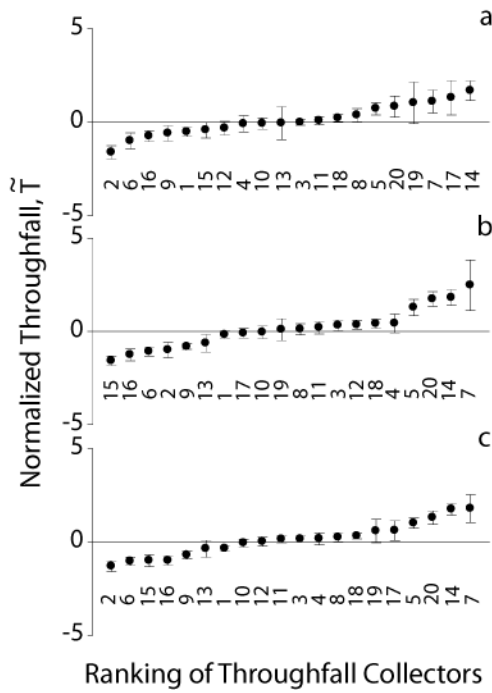
Figure 3.4: Time stability plots of throughfall normalized to zero median and unit variance for a) the early wet season (EWS, n=14 events), b) the peak of the wet season (WS, n=14 events), and c) throughout the rainy season (EWS and WS, n= 28 events). The collectors are plotted along the horizontal axis and ranked by their means, $\tilde{T}_{i,E}$. The bars indicate 95% confidence intervals.
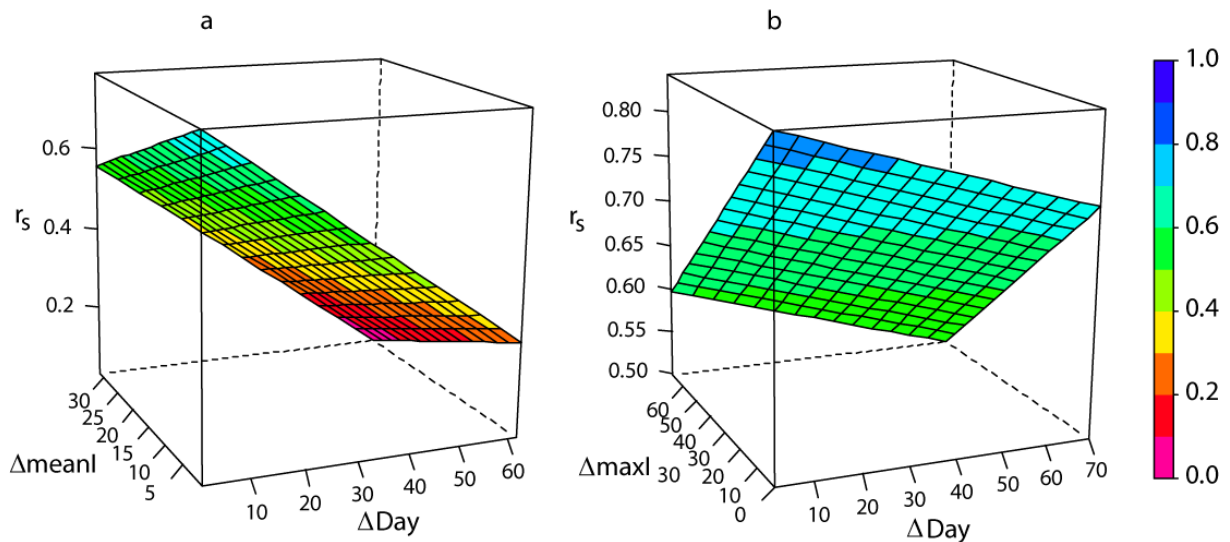
Figure 3.5: The stability of throughfall patterns during a) the early wet season (EWS) and b) peak of the wet season (WS). The stability of the spatial pattern between events is expressed with Spearman rank correlation coefficients (r_s), significance is given if r_s>0.45 (n=20, α=0.05). The planes illustrate predictions of r_s by linear models of the form $z = ax + by + c$ using the variables temporal lag between events (Δ day) and absolute differences between events of either the mean rainfall intensity (Δ meanI) or the maximum 30 minute intensities (Δ maxI$_{30}$). The proportion of variance explained and the level of significance for the EWS and WS model are r^2= 0.42, p= $3.14*10^{-11}$ and r^2= 0.31, p= $9.60*10^{-8}$, respectively. The colors of the planes indicate distinct levels of r_s, see color key for corresponding values. Note: the perspective on both graphs is identical.

Time stability plots of throughfall solute deposition (Figure 3.6) showed extreme persistence for the majority of solutes, only NH_4^+ and DOC deposition patterns displayed a somewhat weaker persistence during the WS. For Mg^{2+} and H^+ we found a distinct general persistence during the EWS and WS, respectively. The other solutes showed either a weak or no detectable pattern of general persistence.
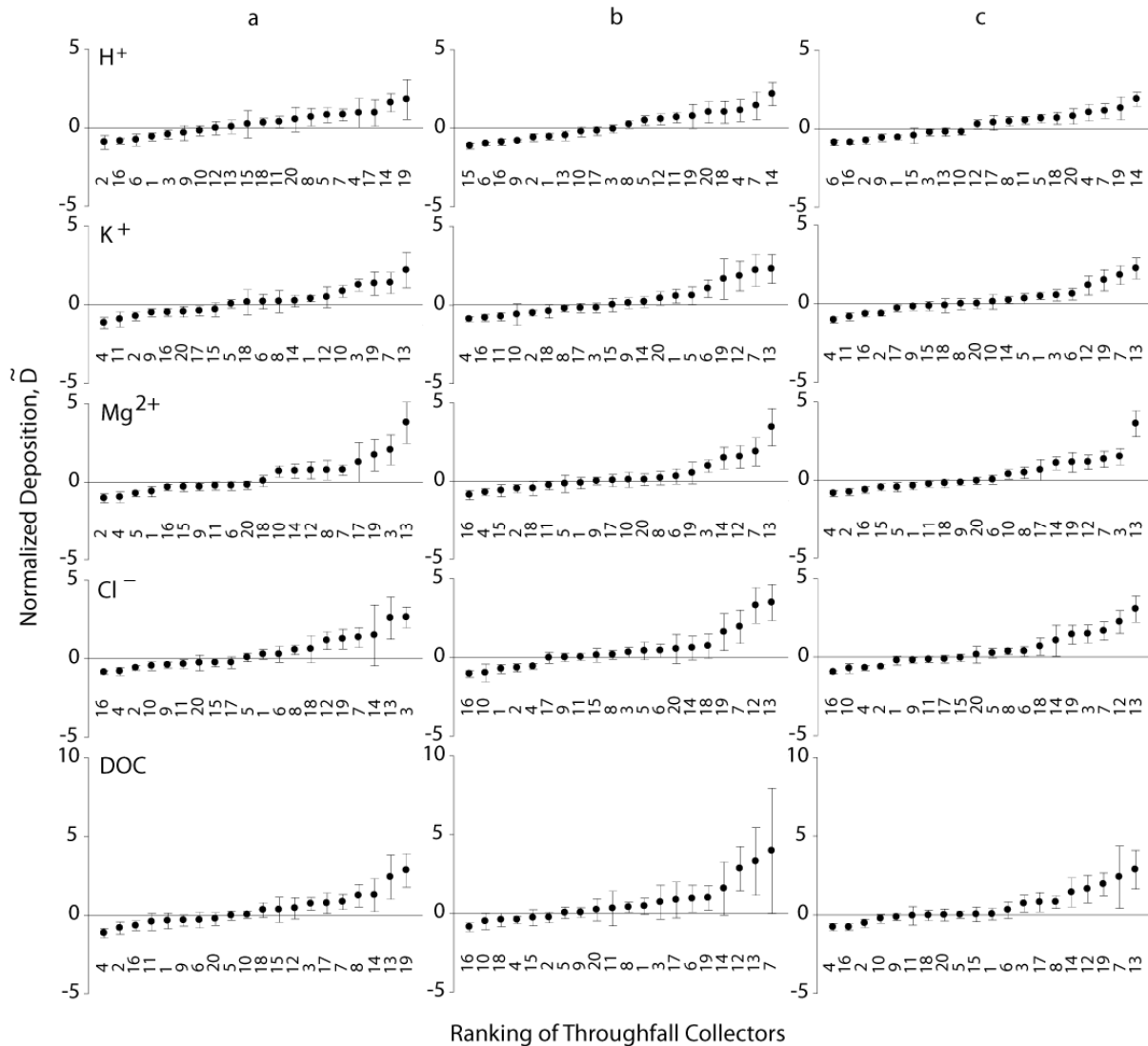
Figure 3.6: Selected time stability plots for H^+, K^+, Mg^{2+}, Cl^- and DOC deposition normalized to zero median and unit variance for a) the early wet season (EWS, n = 14 events), b) the peak of the wet season (WS, n=14 events) , and c) throughout the rainy season (EWS and WS, n = 28 events). The collectors are plotted along the horizontal axis and ranked by their means, $\tilde{D}_{i,E}$. The bars indicate 95% confidence intervals.

The analysis of Spearman rank correlation coefficients among events (r_s) indicated that all but Mg^{2+}, Ca^{2+} and Cl^- solute deposition patterns showed a low temporal stability during the EWS, whereas we detected patterns of higher stability for H^+, K^+ and Cl^-

during the WS (Figure 3.7). In analogy to throughfall, the relative importance of Δ day decreased as a predictor of r_s during the progressing wet season for most solutes, whereas meteorological event characteristics gained in influence (Table 3.4, Figure 3.7). Exceptions are NH_4^+ and SO_4^{2-} for which Δ day showed either more influence or no change, respectively. Some of the models applied to predict r_s explained only a low proportion of the variance ($r^2 < 0.25$ for NH_4^+, Na^+, Mg^{2+} and SO_4^{2-}), whereas others had more explanatory power, particularly during the EWS (r^2 ranged between 0.45 and 0.51 for H^+, K^+ and NO_3^-).

3.4 Discussion
3.4.1 Rain and throughfall quality

The increasing rainfall frequency with the progressing wet season and biomass burning, which is most widespread at the end of the dry season [*Artaxo et al.*, 2002], result in a marked difference of atmospheric aerosol concentrations between the dry and wet season [*Artaxo et al.*, 2002; *Guyon et al.*, 2003]. Decreasing aerosol concentrations throughout the wet season are related to decreasing solute concentrations in rain and throughfall [*Andreae et al.*, 1990; *Germer et al.*, 2007], which explains the observed solute concentration dynamics (Figure 3.2). According to *Germer et al.* [2007], high enrichment ratios of NH_4^+, NO_3^-, SO_4^{2-} and DOC between EWS and WS in rainfall at our research site indicate that biomass burning is an important source, K^+ showed a lower EWS/WS-ratio because biogenic emissions can be high during the WS [*Guyon et al.*, 2003].

The high leachability of K^+ from leaf tissue [*Tukey*, 1970; *Parker*, 1983] results in the strong increase of K^+ concentrations after the passage of rain water through the canopy (Figure 3.2). The observed negative and positive balances of NH_4^+ and NO_3^- between rain and throughfall are frequently reported [*Forti and Moreira-Nordemann*, 1991; *Filoso et al.*, 1999; *Liu et al.*, 2002; *Laclau et al.*, 2003; *Zeng et al.*, 2005; *Staelens et al.*, 2007]. Whether NH_4^+ and NO_3^- are leached from or retained by the canopy mainly depends on concentration gradients between rainfall and the vegetation [*Filoso et al.*, 1999]. Results from *Germer et al.* [2007] are in line with this finding and show that during the EWS NH_4^+ and NO_3^- were frequently retained by the canopy at our site, whereas leaching was dominant in the WS. Reports of Ca^{2+} uptake in the canopy are less common [*Jordan et al.*, 1980; *Langusch et al.*, 2003]. Calcium retention in the canopy at our site was dependent on Ca^{2+} concentrations in rainfall regardless of sampling period [*Germer et al.*, 2007], which suggests a canopy exchange mechanism by diffusion.
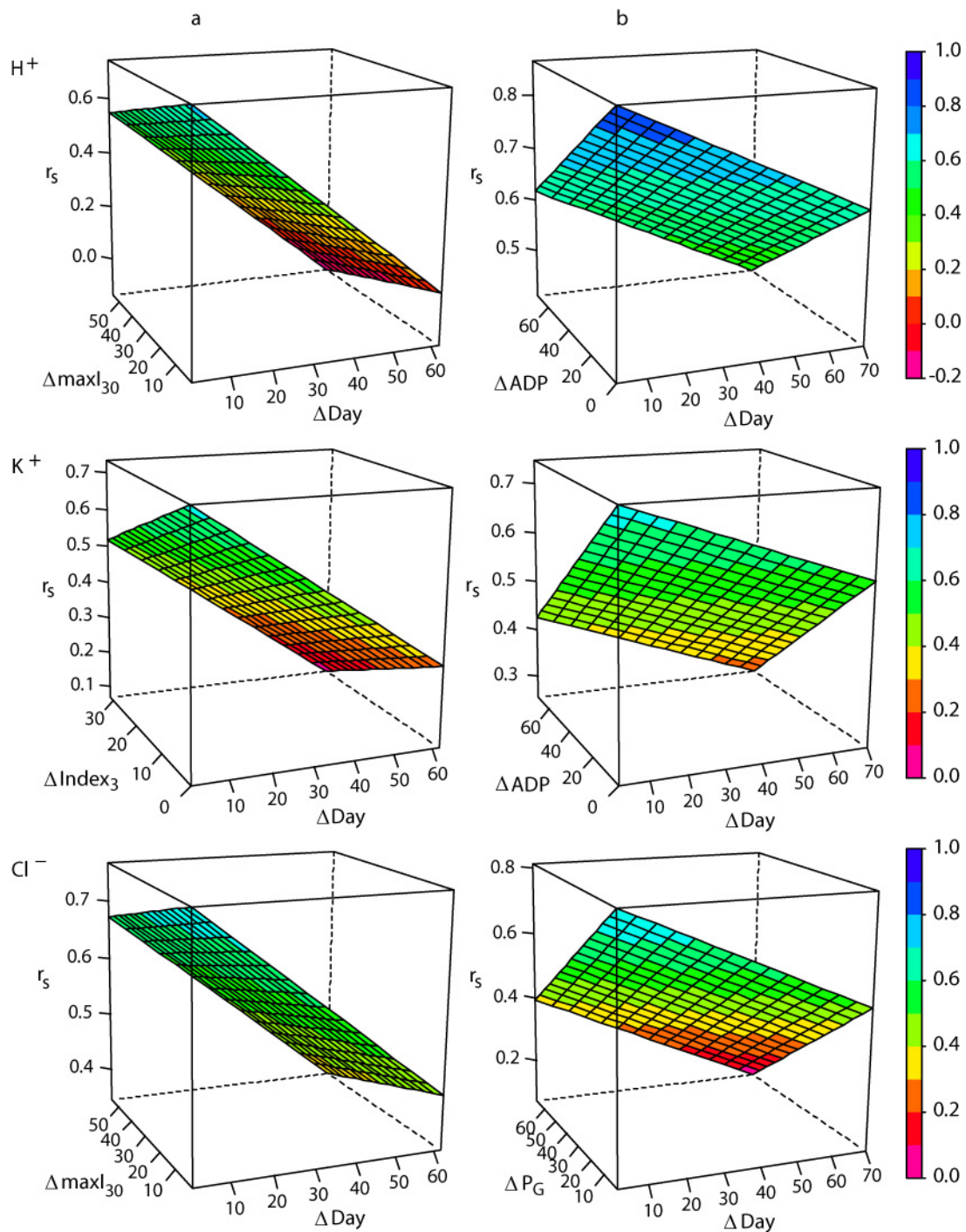
Figure 3.7: The stability of solute deposition patterns for selected solutes during a) the early wet season (EWS) and b) peak of the wet season (WS). The stability of the spatial pattern between events is expressed with Spearman rank correlation coefficients (r_s), significance is given if $r_s > 0.45$ (n = 20, α=0.05). The planes illustrate predictions of r_s by linear models of the form z = ax + by + c, predictor variables are the temporal lag between events (Δ day, d) and a set of meteorological event parameters (absolute differences between events, Δ). Abbreviations are: P_G (mm), gross precipitation, ADP, antecedent dry period (h), $maxI_{30}$, maximum 30 minute precipitation intensity (mm h^{-1}) and $Index_3$, amount of precipitation of previous 3 days (mm). The colors of the planes indicate distinct levels of r_s, see color key for corresponding values. Note: the perspective on the graphs is identical.

62

Table 3.4: Models applied for predicting Spearman rank correlation coefficients (r_s) among events during the early wet season (EWS, n = 14 events) and peak of the wet season (WS, n = 14 events) with the predictor variables temporal lag between events (ΔDay), and a set of meteorological parameters (absolute differences between events): gross precipitation (ΔP_G), antecedent dry period (ΔADP), amount of precipitation of previous 3 and 7 days (ΔIndex$_3$ and ΔIndex$_7$), mean precipitation intensity (ΔmeanI), and 30 minute precipitation intensity (ΔmaxI30).

Solute	EWS	WS
H^+	ΔDay*** + ΔmaxI30**	ΔADP*** + ΔDay***
NH_4^+	ΔIndex$_7$***	ΔDay* + ΔADP*
Na^+	ΔDay***	ΔmeanI***
K^+	ΔDay*** + ΔIndex$_3$***	ΔADP*** + ΔDay*
Mg^{2+}	ΔDay*** + ΔP_G*	−
Ca^{2+}	ΔDay***	−
Cl^-	ΔDay*** + ΔmaxI30°	ΔP_G*** + ΔDay***
NO_3^-	ΔDay***	ΔP_G*** + ΔADP*
SO_4^{2-}	ΔDay*** + ΔP_G**	ΔDay* + ΔADP*
DOC	ΔDay*** + ΔIndex$_3$***	ΔIndex$_3$*** + ΔP_G*

The level of significance per predictor is indicated by either ° $p<0.1$, * $p<0.05$, ** $p<0.01$, *** $p<0.001$.

3.4.2 Global comparison of spatial patterns in throughfall
3.4.2.1 Throughfall quantity

A comparison with a variety of temperate and tropical forests (Table 3.5) reveals that the spatial variability of throughfall based on both EWS and WS at our study site is (1) higher than in all temperate forests with the exception of an old, uneven-aged, mixed conifer forest in the Pacific Northwest, USA [*Keim et al.*, 2005], which showed a similar spatial variability, and (2) at the lower end of values reported from other tropical lowland and montane rain forests. On the basis of Table 3.5, we suggest that the variability of throughfall quantity depends on the following factors.

(1) Biotic factors influence the variability of throughfall by way of canopy complexity [*Crockford and Richardson*, 2000; *Loescher et al.*, 2002; *Levia and Frost*, 2006]. This complexity is determined by the number of crown-architecture types of canopy plants, the age structure of the forest and the arrangement of trees. Throughfall in forest plantations with a high stand density showed low coefficients of variation [*Raat et al.*, 2002], whereas *Zimmermann et al.* [2007] linked very heterogeneous throughfall patterns to the high water storage capacity of epiphytes after dry spells.

Table 3.5: Spatial patterns of throughfall amount in this and eighteen other studies expressed as the coefficient of variation (CV, in %).

Reference	Collectors		Forest type [a]	CV
	n	A (cm^2)		
This study	20	980	LRF	29
Lloyd and Marques 1988[b]	36	127	LRF	54
Loescher et al. 2002	36	95	LRF	24
Vernimmen et al. 2007[b]	18	100	LRF	36
Vernimmen et al. 2007[b]	20	100	LRF, tall heath forest	27
Vernimmen et al. 2007[b]	20	100	LRF, stunted heath forest	31
Clark et al. 1998	20	20	LMRF	29
Holwerda et al. 2006	30	100	LMRF	48
Zimmermann et al. 2007	25	122	LMRF	53
Lin et al. 1997[c]	18	942	Moist subtropical forest	13
Carlyle-Moses et al., 2004[d]	38	661	Red oak stand	17
Duijsings et al. 1986	11	350	Oak-beech forest	8
Keim et al. 2005[e]	94	9	Mixed hardwood forest	30–38
Puckett 1991	50	182	Mixed hardwood forest	12–18
Rodrigo and Àvila 2001[c) f)]	36	79	Holm oak forest	21
Staelens et al. 2006a[e) g)]	12	460	Beech	18
Keim et al. 2005	94	9	Douglas fir stand	14–26
Keim et al. 2005	94	9	Mixed conifer forest	39–65
Lawrence and Fernandez 1993[h]	40	342	Spruce-fir forest	24
Pedersen 1992[i]	30	121	Sitka spruce stand	22
Raat et al. 2002	24	320	Douglas fir stand	21
Seiler and Matzner 1995	100	106	Norway spruce stand	3
Whelan et al. 1998	39	177	Norway spruce stand	7–16

The ranges of CVs in *Puckett* [1991] and *Keim et al.* [2005] refer to single events and CVs in *Whelan et al.* [1998] are for individual collection periods of 9 to 17 days length.

[a] Abbreviations are: LRF: lowland rain forest and LMRF: lower montane rain forest.

[b] Throughfall measured with roving gauges. *Lloyd and Marques* [1988] measured at 494 sampling points over a one year period; the calculation of CV follows *Holwerda et al.* [2006]. *Vernimmen et al.* [2007] measured over a one year period and relocated gauges after approximately seven events.

[c] CV based on mean volumes.

[d] CV based on pooled data of two adjacent red oak stands.

[e] CV refers to the leafed period.

[f] Mean of CV's of two adjacent holm oak forests.

[g] Collectors were placed below a single beech tree.

[h] Value refers to the median coefficient of variation of 23 sampling months.

[i] Mean of CV's of three even-aged Sitka spruce forests.

(2) Abiotic factors strongly influence the spatial heterogeneity of throughfall quantity [*Levia and Frost*, 2006]. The influence of rainfall depth is most thoroughly documented, with a consensus that low rainfall magnitudes result in a higher spatial variability of throughfall quantity [*Bouten et al.*, 1992; *Rodrigo and Àvila*, 2001; *Keim et al.*, 2005; *Staelens et al.*, 2006b].

Above all, design criteria such as temporal extent, number of sampling points and spatial extent strongly influence the analysis of spatial patterns. Several studies observed that the CV decreases to a constant level with either an increasing number of sampling occasions [*Holwerda et al.*, 2006] or, in case of a roving gauge arrangement, with an increasing number of relocations [*Vernimmen et al.*, 2007]. Furthermore, the spatial extent is of crucial importance, because CVs obtained from small plots are in general less meaningful as they do not integrate over the full range of canopy structures. Large sampling plots (> 1ha), however, encounter the problem that small-scale variations in rainfall magnitude could mask biotic-controlled throughfall patterns.

3.4.2.2 Solute deposition

While the spatial variability of throughfall amount is frequently reported, studies that examine spatial patterns of throughfall solute deposition are far less common. In addition, sampling designs and collection periods are very different, which is why comparability is further restricted. With these constraints in mind, we compared our data with temperate and tropical forest ecosystems and found that, although the forest at our research site shows a heterogeneous structure [*Lu*, 2005], the CVs of solute deposition rank on intermediate positions among the other studies (Table 3.6).

(1) CVs for most solutes were higher than values reported from managed temperate forest stands, exceptions were one Norway spruce forest [*Beier et al.*, 1993] where the variability of H^+, NH_4^+, Na^+, Ca^{2+} and Mg^{2+} deposition exceeded the values in this study, and a spruce-fir forest [*Lawrence and Fernandez*, 1993] that showed higher CVs for most solutes.

(2) CVs for all solutes but Na^+ and SO_4^{2-} were lower than in a tropical montane rain forest [*Zimmermann et al.*, 2007]. To allow an unbiased comparison with respect to the number of sampling occasions [n=5 events in *Zimmermann et al.*, 2007] we took random sub-samples of five events from our EWS data. This comparison still indicated a higher variability of most solute deposition patterns in the lower montane rain forest.

The high spatial variability of solute deposition reported by *Beier et al.* [1993] is likely the result of the sampling design because they sampled along four randomly selected transects below single trees at fixed distances from the tree trunk including sampling positions under open sky. Two of the other temperate conifer forest sites included in the comparison [*Whelan*

et al., 1998; *Raat et al.*, 2002] were relatively young forest stands with a homogeneous structure. Since foliar leaching and dry deposition are both influenced by the density and architecture of the canopy [*Whelan et al.*, 1998] a homogenous vegetation structure would explain the relatively low spatial variability. In contrast to the former sites, the spruce-fir stand showed a more heterogeneous canopy structure due to a selective logging history and a previous spruce–budworm (*Chloristoneura fumiferana* Clem.) infestation of balsam firs that resulted in some canopy gaps [*Lawrence and Fernandez*, 1993]. In addition, the latter disturbance increased the proportion of dead wood, which might contribute to highly variable solute deposition patterns. The low spatial variability reported by *Staelens et al.* [2006a] presumably originates from the sampling below a single beech tree, though *Duijsings et al.* [1986] measured similar values in a mixed oak–beech forest.

Table 3.6: Spatial patterns of throughfall solute deposition in this and seven other studies expressed as the coefficient of variation (CV, %).

Reference		This study	Zimmermann et al. 2007	Duijsings et al. 1986	Staelens et al. 2006a[b]	Beier et al. 1993	Lawrence & Fernandez 1993 [c]	Raat et al. 2002	Whelan et al. 1998[d]
Collectors	n	20	22	11	12	20	40	25	39
	A (cm^2)	980	122	350	460	178	342	320	177
Forest type[a]		LRF	LMRF	Oak-beech	Beech	Norway spruce	Spruce-fir	Douglas fir	Norway spruce
H$^+$		43	73	28	28	55	41	–	–
NH$_4^+$		29	60	15	23	44	74	26	31-170
Na$^+$		38	33	17	11	45	52	26	–
K$^+$		40	68	21	13	32	56	18	11-43
Mg^{2+}		38	92	13	17	44	74	19	–
Ca^{2+}		31	89	14	14	44	65	20	–
Cl$^-$		48	76	11	13	42	48	22	18-57
NO$_3^-$		47	252	9	14	39	76	19	23-63
SO$_4^{2-\,e)}$		52	48	13	16	41	32	26	23-44
DOC [f]		44	69	–	–	–	60	–	–

[a] Abbreviations are: LRF: lowland rain forest and LMRF: lower montane rain forest.

[b] Collectors were placed below a single beech tree.

[c] Values refer to the median coefficient of variation of 23 sampling months.

[d] Ranges of CVs in Whelan et al. (1998) are for individual collection periods of 9 to 17 days length.

[e] Value in Zimmermann et al. (2007) refers to total S.

[f] Value in Zimmermann et al. (2007) refers to total C.

The high spatial variability of solute deposition patterns in a tropical montane forest [*Zimmermann et al.* 2007] is likely the result of the very heterogeneous canopy structure with a high abundance of epiphytes [*Fleischbein et al.*, 2005] and large accumulations of organic matter. The comparison of solute deposition CVs among the variety of forests (Table 3.6) indicates factors other than structural properties must have a strong influence on solute deposition patterns. *Seiler and Matzner* [1995] found that canopy uptake of NH_4^+ and NO_3^- can counteract the amplifying effect of dry deposition on the spatial variability. Moreover, as for throughfall amounts, the duration of the study is of crucial importance, in that short term studies (< 3 months), or investigations based on few events tend to report higher coefficients of variation [*Lawrence and Fernandez*, 1993]. Furthermore, meteorological variables influence the spatial variability of solute deposition, which is discussed in the next section.

3.4.3 Seasonal dynamics of spatial throughfall patterns

The influence of antecedent wetness conditions (Table 3.3) partly explains the observed increase in variability of solute deposition patterns from EWS to WS (Table 3.2, Figure 3.3). Interestingly, half of the solutes in our study showed a negative correlation between spatial variability and ADP, which suggests factors other than dry deposition [*Raat et al.*, 2002] increase the spatial variability of throughfall solute fluxes. We suppose that in case of successive leaching and washoff, as it typically occurs during the progressing wet season in many tropical forests [e.g. *Germer et al.*, 2007], for certain nutrients only "hotspots" remain to be leached. These "hotspots" (e.g. accumulation of decaying organic material in the canopy) in the otherwise heavily leached canopy environment would create a high spatial variability.

For SO_4^{2-} and DOC our data show that high solute concentrations in rainfall might have a homogenizing effect on throughfall solute deposition patterns (Table 3.3). The latter effect is presumably enhanced by biomass burning, which is an important source of black carbon, S, K, NH_4^+ and NO_3^- in aerosols in the Amazon region [*Maenhaut et al.*, 1996; *Guyon et al.*, 2003; *Andreae et al.*, 2004]. We assume that we could detect this effect on throughfall spatial variability only for SO_4^{2-} and DOC because foliar uptake of NH_4^+ and NO_3^- is frequent and K^+ has a very high deposition ratio [*Parker*, 1983; Figure 3.2, this study]. A similar relationship between ion concentration in rainfall and deposition variability was shown by NO_3^- and SO_4^{2-} in a mixed-hardwood forest [*Puckett*, 1991].

3.4.4 Temporal persistence of spatial throughfall patterns
3.4.4.1 Throughfall quantity

The proportion of collectors that deviated significantly in one direction from the median seems to be high (Figure 3.4) compared to 31–46% in two coniferous forests and one deciduous forest in the Pacific Northwest, USA [*Keim et al.*, 2005] and 48% (based on the standard deviation) in a Douglas fir stand in the Netherlands [*Raat et al.*, 2002]. In contrast, *Zimmermann et al.* [2007] found a similar high proportion of 68% in an Ecuadorian tropical montane forest, although a direct comparison with the Ecuadorian forest is restricted due to different numbers of sampling occasions (n=14 events in this study vs. n=5 events in *Zimmermann et al.*, 2007]. Random sub-samples of five events from our dataset indicated that the extreme and general persistence of throughfall was higher in the tropical montane forest.

The contrasting temporal stability of throughfall patterns during EWS and WS (Figure 3.5) might be influenced by a synchronous growth activity at the onset of the rainy season, which occurs in many tropical forest ecosystems with a distinct dry season [*Wright*, 1991; *van Schaik et al.*, 1993; *Coley and Barone*, 1996; *Leigh*, 1999; *Bach*, 2002]. In this context, *Wright* [1991] observed that the short bursts of vegetative growth during leaf flush were followed by long quiescent periods, which might favor a higher stability during the WS. The vegetative growth patterns may also explain the relative importance of Δ day vs. the meteorological event parameters as predictors for r_s. I.e. Δ day represents a strong predictor for r_s during the EWS because of marked changes in the canopy, whereas during time periods of low vegetative activity meteorological event parameters become more important. During both EWS and WS, we identified rainfall intensities as the most influential meteorological parameters for the prediction of r_s (Figure 3.5), hence, we suppose that the rainfall intensity has an effect on leaf positions (e.g. leaves bend over during high intensity rain and the location of drip points changes).

The relatively high stability of throughfall patterns during the WS (Figure 3.5b) may have ecological consequences in that moisture gradients at the forest floor influence root water uptake [*Bouten et al.*, 1992], nitrification-denitrification rates [*Carnol and Ineson*, 1999; *Raat et al.*, 2002] and even arthropod distributions [*Kaspari and Weiser*, 2000]. Based on our results (Figure 3.5, Table 3.2) we suggest that forest environments that experience deciduousness show a lower temporal stability of throughfall patterns due to seasonal changes of canopy properties. Therefore, spatial CVs might be lower than in forest ecosystems with aseasonal climates or natural forests dominated by evergreen trees.

3.4.4.2 Solute deposition

For most solutes the proportion of collectors that showed a mean $\tilde{D}_{i,E}$ significantly different from zero was higher than in temperate coniferous and deciduous forests [*Raat et al.*, 2002; *Staelens et al.*, 2006a]. It is important to note that the overall persistence of solute deposition patterns depends not only on the proportion of collectors that deviate constantly in one direction from the median but also on the distance of the mean $\tilde{D}_{i,E}$ from the median; the latter metric, however, is difficult to compare with other studies because it depends on how the time stability plot is computed.

Given the large collecting area of the troughs used in this study, which results in the sampling of more integrated solute deposition signals, it is rather surprising that for some solutes a relatively large proportion of points received constantly either less or more than the median amount of deposition (e.g. Mg^{2+}, Ca^{2+} and Cl^{-} during the EWS and H^{+} during the WS, Figure 3.6). The latter relationship between sampling support and spatial heterogeneity implies that the spatial pattern has at least a moderate spatial extent (i.e. >1m). It is, therefore, possible that the time stability patterns of certain solutes influence soil water nutrient patterns. Although the transfer of the solute deposition pattern to the soil solution is influenced by many processes, e.g. NH_4^+, NO_3^- and SO_4^{2-} soil water patterns are known to be altered by other processes such as plant uptake, immobilization in the mineral soil and biochemical transformations [*Seiler and Matzner*, 1995; *Manderscheid and Matzner*, 1995].

The predictions of r_s among events, however, indicate a relatively weak temporal stability of most solute deposition patterns (Figure 3.7). The low stability of those patterns may be caused by rapid plant growth at the beginning of the rainy season [*Wright*, 1991; *van Schaik et al.*, 1993] and changing meteorological conditions (Table 3.1) that influence solute deposition patterns (Table 3.3). We suggest that the overall decreasing importance of Δ day (Table 3.4) reflects the change in vegetative activity patterns and the change of the relationship between Δ day and dry deposition with the progressing wet season.

In summary, the predictions of r_s are in line with the findings obtained from the time stability plots, even though the former analysis does not distinguish between general and extreme persistence. The weak temporal stability of solute deposition patterns in our research area impedes the formation of persistent (i.e. throughout a whole rainy season) "hot" and "cold spots" and therefore the establishment of solute deposition-induced biochemical microhabitats in the soil. In this context, *Barthold et al.* [2008] explained the equal distribution of exchangeable K in the topsoil across a 1500 ha tropical forest area with the homogenizing effect of throughfall deposition and litter leachate. Other authors detected relationships between tree distribution and soil nutrient patterns and suggested that geological processes and topographic variations rather than direct plant-soil-interactions are the most

likely explanation for the variation in soil nutrient patterns [*John et al.*, 2007]. The results of our study with respect to the stability of throughfall deposition patterns would support this suggestion.

3.5 Conclusions

(1) The spatial variability of throughfall in the open tropical rain forest was at the lower end of values reported from other tropical forest sites, but higher than in most temperate forests. The lower variability in temperate forest ecosystems reflects more the structural differences of natural vs. managed forest ecosystems than ecosystem-inherent characteristics.

The spatial variability of solute deposition in the open tropical rain forest ranks on an intermediate position in a range of tropical and temperate forest ecosystems. This suggests that the diversity of tree species and the heterogeneity of solute deposition are not linearly correlated.

(2) Most solutes showed a higher spatial variability during the later stage of the wet season. Antecedent dry periods influenced the spatial variability of NH_4^+, K^+, Cl^-, SO_4^{2-} and DOC in that the length of the dry period and the heterogeneity of the solute deposition pattern correlated negatively. High solute concentrations in rainfall had a homogenizing effect on the deposition of SO_4^{2-} and DOC. The latter effect might be enhanced by biomass burning.

(3) The temporal stability of throughfall patterns was low during the early wet season, but gained in stability as the wet season progressed. Rapid plant growth at the beginning of the wet season and subsequent quiescent periods, a widespread phenomenon in tropical forest ecosystems with a pronounced seasonality, may explain the spatio-temporal patterns of throughfall. The relatively high stability of throughfall patterns during later stages of the wet season may influence processes at the forest floor and in the soil.

The deposition patterns for most solutes were only stable on a short-term scale, but not throughout the wet season. This weak stability impedes the formation of solute deposition-induced biochemical microhabitats in the soil.

3.6 Acknowledgements

Wilcke and one anonymous reviewer provided constructive, meticulous and thoughtful reviews of an earlier draft.

Rainfall redistribution in a tropical forest: spatial and temporal patterns.

Alexander Zimmermann [1], Beate Zimmermann[2], Helmut Elsenbeer[1, 2]

[1] Institute of Geoecology, University of Potsdam, Karl-Liebknecht-Str. 24-25, 14476 Potsdam, Germany

[2] Smithsonian Tropical Research Institute, Apartado 0843-03092, Balboa, Ancón, Panama

Abstract   The investigation of throughfall patterns has received considerable interest over the last decades. And yet, the geographical bias of pertinent previous studies and their methodologies and approaches to data analysis cast a doubt on the general validity of claims regarding spatial and temporal patterns of throughfall. We employed 220 collectors in a 1-ha plot of tropical rainforest and sampled throughfall during a period of 14 months. Our analysis of spatial patterns is based on 60 datasets, whereas the temporal analysis comprises 91 events. Both datasets show skewed frequency distributions. When skewness arises from large outliers, the classical, non-robust variogram estimator overestimates the sill variance, and in some cases even induces spurious autocorrelation structures. In these situations, robust variogram estimation techniques offer a solution. Throughfall in our plot typically displayed no or only weak spatial autocorrelations. In contrast, temporal correlations were strong, that is, wet and dry locations persisted over consecutive wet seasons. Interestingly, seasonality, and hence deciduousness, had no influence on spatial and temporal patterns. We argue that if throughfall patterns are to have any explanatory power with respect to patterns of near-surface processes, data-analytical artifacts must be ruled out lest spurious correlation be confounded with causality; furthermore, temporal stability over the domain of interest is essential.

4.1 Introduction

Spatial patterns of several hydrological and biogeochemical processes at the forest floor have been linked to throughfall patterns, such as the distribution of soil water content [*Schume et al.*, 2003], seepage water and ion fluxes [*Manderscheid and Matzner*, 1995], decomposition of organic material [*Möttönen et al.*, 1999], root water uptake [*Bouten et al.*, 1992], and root growth [*Ford and Deans*, 1978]. The verdict is, however, not unequivocal. *Raat et al.* [2002] and *Shachnovich et al.* [2008] found no relationship between throughfall patterns and the distribution of the soil water content, which they attributed to the homogenizing effect of the forest floor. Nonetheless, this list hints at the potential impact of throughfall patterns on hydrological and biological processes in forest ecosystems. It appears that the strength of the link between throughfall and processes at or below the forest floor critically depends on the spatial patterns of throughfall and its temporal persistence.

Spatial patterns are, of course, intimately linked to spatial variability, which by all accounts is rather high for throughfall [*Levia and Frost*, 2006], though large differences exist among forest ecosystems; latitudinal and management gradients may explain some of them [*Lloyd and Marques*, 1988; *Hölscher et al.*, 1998; *Möttönen et al.*, 1999; *Keim et al.*, 2005; *Holwerda et al.*, 2006]. Throughfall measurements in managed temperate forests, for example, vary from 0 to 100 % of incident precipitation [*Lloyd and Marques*, 1988], whereas a range of 0 to 200 % is representative for many tropical forests [*Lloyd and Marques*, 1988; *Holwerda et al.*, 2006]. Some forests, however, exhibit even more extreme distributions with a range between 0 and 1000 % [*Cavelier et al.*, 1997]. Such skewed frequency distributions emerge because some leaf morphologies, e.g. leaves with drip tips, and canopy structures, e.g. drip points on inclined branches, favor the concentration of throughfall; consequently, other below-canopy areas must be drier. As to spatial structure expressed in terms of autocorrelation, the reported correlation lengths vary as widely as the few forest ecosystems investigated. Some researchers found no autocorrelation over the studied lag distances [*Loustau et al.*, 1992; *Bellot and Escarre*, 1998], whereas others detected spatial correlations in the range of 3 to 10 m [*Möttönen et al.*, 1999; *Keim et al.*, 2005; *Staelens et al.*, 2006b]. Surprisingly, *Loescher et al.* [2002] detected autocorrelation of throughfall measurements over a distance of 43 m in a wet tropical forest, which they attributed to canopy gaps and individual tree crowns. It is tempting to interpret this broad range of recorded autocorrelation patterns as a reflection of differences in forest structure. And yet, the high variability of throughfall at small spatial scales should focus attention on the appropriateness of the design [*Skøien and Blöschl*, 2006] and the data-analytical tools [*Zimmermann et al.*, 2008b] on which those correlation lengths depend.

Temporal persistence seems to be required to initiate moisture gradients strong and persistent enough to trigger biotic and abiotic responses. The results of the few studies dealing with the temporal persistence of throughfall patterns vary from no persistent between-storm throughfall patterns [*Lin et al.*, 1997] to stability over several months [*Raat et al.*, 2002; *Staelens et al.*, 2006b; *Zimmermann et al.*, 2008a].

This brief overview points to rather diverging results, and the lack of explanations for observed throughfall autocorrelation structures and temporal persistence, despite their relevance for a range of biotic and abiotic processes [*Keim et al.*, 2005], motivated us to seek answers to the following research questions:

1) Do putative spatial and temporal patterns of throughfall reflect a natural phenomenon or the choice of variogram estimators?

2) Does the redistribution of rain in a heterogeneous tropical rainforest canopy result in a detectable throughfall autocorrelation structure over the studied lag distances?

3) Do throughfall measurements show temporal persistence?

To answer these questions is not only important for several aspects in hydrology but may equally influence the work of biogeochemists and ecologists as near surface water in forests controls key chemical reactions (e.g. nitrification-denitrification rates [*Raat et al.*, 2002]) and plant growth (e.g. survival of seedlings [*Engelbrecht and Kursar*, 2003]).

4.2 Materials and methods
4.2.1 Site description

We investigated throughfall patterns in a 1-ha plot located in the Lutz Creek Catchment (9° 9' N, 79° 51' W) on Barro Colorado Island, Panama (Fig. 4.1). The island was isolated from the main land during the creation of Lake Gatun, which is part of the Panama Canal. The area is characterized by a rough topography with steep slopes of up to 40° [*Dietrich et al.*, 1982]. The 1-ha plot, however, is situated on a more gentle north-west facing hillside with an inclination of $13.1 \pm 7.3°$ (mean $\pm$ 1sd, 10 by 5 m grid, n=210). The climate of Barro Colorado is characterized by distinct wet and dry seasons. The wet season lasts approximately from May to mid-December. Total annual rainfall averages 2651 ± 441 mm (mean $\pm$ 1sd, n = 83, data from 1925 to 2007, Smithsonian Tropical Research Institute, Environmental Science Program). The vegetation is classified as tropical semi-deciduous moist forest [*Foster and Brokaw*, 1982]. Ten percent of the canopy tree species are dry-season deciduous [*Croat*, 1978]. Deciduousness in the area is a complex phenomenon; some trees can be leafless for several weeks to months every year, while others drop their leaves only in particular dry years [*Foster and Brokaw*, 1982]. Because a few tree species lose their leaves in June – July, deciduousness is not a mere dry-season phenomenon, which adds another

aspect to the within-canopy dynamics. The forest in the study area is secondary growth of more than 100 years of age with an unevenly distributed understory. Stand height is 25-35 m with few emergents approaching 45 m. The stand characteristics in our plot (Table 4.1) closely resemble data of other tree censuses in the area [*Thorington et al.*, 1982]. Canopy openness is an exception in that our measurements show a higher variability compared to another study from Barro Colorado Island in which canopy gaps were excluded [*Harms et al.*, 2004].
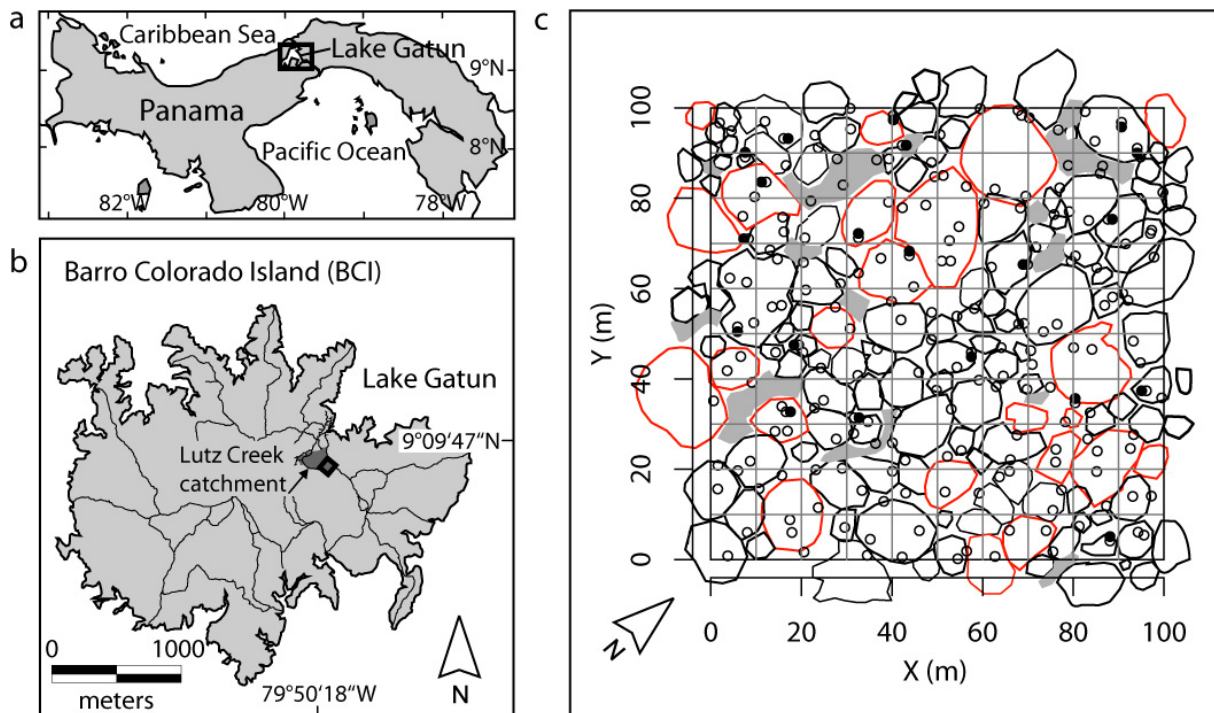
Figure 4.1: Location of the research area in Panama (a) and on Barro Colorado Island (b). The lines refer to the trail system and the square indicates the location of the sampling area. The close-up view (c) shows the structure of the tree crowns in the sampling area, red outlines refer to trees that are dry season deciduous, and gray areas indicate locations of small-scale disturbances due to tree and branch fall. Areas that do not belong to any of the former categories contain trees with indistinguishable crowns (e.g. due to lianas). The map is based on an aerial photograph from April 2008 and ground survey data (for details on the crown photograph we refer to *Jansen et al.* [2008]). Locations of throughfall sampling points and the square subplots are also shown; open circles refer to locations that were chosen according to the design-based component, whereas solid circles mark locations selected by the model-based component of the applied sampling scheme.

Table 4.1: Stand characteristics of the 1-ha study area.[a]

Number of stems, 1 cm $\leq$ dbh < 5 cm	1779
Number of stems, 5 cm $\leq$ dbh < 10 cm	658
Number of stems, 10 cm $\leq$ dbh < 20 cm	278
Number of stems, 20 cm $\leq$ dbh < 40 cm	143
Number of stems, 40 cm $\leq$ dbh < 60 cm	37
Number of stems, dbh $\geq$ 60 cm[b]	24
Number of tree species, dbh $\geq$ 5 cm	98
Basal area, dbh $\geq$ 5 cm, (m^2)	35.3
Canopy tree crown diameter (mean $\pm$ 1sd, m, n=131)	9.7 $\pm$ 4.5
Canopy openness (median $\pm$ MAD, %, n=200)	3.0 $\pm$ 4.1

[a] Abbreviations are: dbh, diameter at breast height; sd, standard deviation; MAD, median absolute deviation from the median

[b] The maximum dbh is 130 cm.

4.2.2 Sampling and instrumentation

Our throughfall sampling scheme comprises a design-based and a model-based sampling component (Fig. 4.1c). The design-based component consists of a stratified simple random sampling with compact geographical stratification [*de Gruijter et al.*, 2006]. We divided our 1-ha plot into 100 square subplots of 10 m side length. In each of these subplots, which represent the strata, we randomly allocated two throughfall sampling points. We then chose 20 of these sampling points at random, and selected an additional sampling location 1 m away in a random direction. This model-based component increased the number of sampling points at short lag distances, which is important for estimating the shape of the variogram model near the origin.

Throughfall samples were collected on an event basis from August 2007 to October 2008 (n = 91 events; Appendix, Table 4.A1). The sampling covered both peaks of the 2007 and 2008 wet season and the dry and subsequent transition season in 2008. Events were separated by at least two hours without rain and had to accumulate at least 0.6 mm of rainfall with a minimum mean intensity of 1.2 mm h^{-1}. According to this definition 198 events occurred during the study period. Logistical constraints and small scale variability of rainfall did not permit the sampling of all events. Rainfall was continuously recorded with two Hobo$^{®}$ tipping bucket rain gauges (orifice of 182 cm^2, 0.2 mm tip resolution); additionally, we used 5 manual read out collectors (orifice of 113 cm^2). All rainfall was recorded in a clearing 300 m from the throughfall sampling site. The throughfall collectors (n = 220) consisted of a 2-l polyethylene sampling bottle and a funnel. The receiving area of each collector was 113 cm^2;

hence, total sampling area in the 1-ha plot summed up to 2.49 m^2. A polyethylene net with 0.5 mm mesh width on the bottom of the funnel prevented measuring errors due to organic material and small animals.

4.2.3 Measurement of canopy openness

In order to facilitate the interpretation of throughfall data we measured canopy openness at all design-based throughfall sampling positions (n=200). These measurements are based on hemispherical photographs, which we analyzed with Gap Light Analyzer 2.0 [*Frazer et al.*, 1999]. We used the full spectral resolution (RGB images) because the use of all three bands results in more discernable detail in sunlit image areas [*Jonckheere et al.*, 2005]. The hemispherical photographs were acquired using a Nikon Coolpix 4500 digital camera with a Nikon FC-E8 0.21x fish-eye lens. The camera was mounted on a tripod in approximately 0.5 m height and leveled horizontally. We performed all photographs under overcast conditions to minimize the anisotropy of the sky radiance. All photographs were taken between the 21st and 24th September 2007. For each of the photographs we determined the canopy openness of 6 different zenith angles: 1.9°, 3.8°, 5.0°, 7.5°, 10° and 20°. We then determined which of the different image sections correlated best with our throughfall measurements. For this analysis we used only events that were sampled in a time frame of less than a month from the date of canopy photography to minimize bias due to changing canopy structures. We found that the angle of 5.0° showed the best results; hence we used canopy openness data of this image section for further calculations.

4.2.4 Analysis of throughfall data
4.2.4.1 Software

For all calculations, we used both MatLab$^®$ and the language and environment of R, version 2.2.6. [*R Development Core Team*, 2004], and here primarily the libraries geoR [*Ribeiro and Diggle*, 2001] and gstat [*Pebesma*, 2004]. For calculating experimental variograms with the estimator proposed by *Genton* [1998], we applied the Fortran code of *Rousseeuw and Croux* [1993].

4.2.4.2 The data

For the analysis of the spatial correlation of throughfall measurements we used the first 60 events of the study period. We chose this subset of events because it comprises all seasonal changes of the canopy; hence, we expected that the analysis of further events would

not provide new insights. The data set for spatial analysis consists of 13200 observations of which 44 (0.33 %) are missing values.

The analysis of the temporal correlation of throughfall measurements is based on the whole data set (n = 91 events) which contains 20020 observations including 94 (0.47 %) missing values. The analysis of temporal correlations requires data that is independent of event size; therefore we used standardized throughfall, $\widetilde{T}$, which we calculated as:

$$\widetilde{T}_{c_i,E_i} = \left(\frac{T_{c_i,E_i} - median(T_{E_i})}{MAD(T_{E_i})} \right) \qquad (4.1)$$

where T_{c_i,E_i}, i = 1,2,…,n denotes throughfall at collector c_i and event E_i, i = 1,2,...,n; $median(T_{E_i})$ is the median throughfall of all collectors during event E_i, and $MAD(T_{E_i})$ is the median absolute deviation from the median based on all collectors during event E_i.

4.2.4.3 Models to describe spatial and temporal correlation

Our objective is to obtain variogram models that describe the spatial and temporal dependence among throughfall measurements. The calculation of spatial and temporal variograms differs insofar as our analysis of spatial data is based on omnidirectional variograms, whereas we used a directional variogram to describe the temporal correlation of throughfall measurements (Fig. 4.2). Apart from this difference all steps in the exploratory and geostatistical analysis are very similar, thus we do not describe the analytical procedure separately.
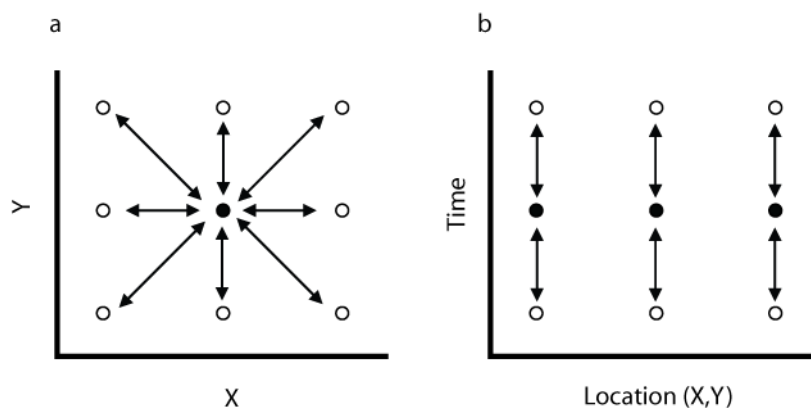

Figure 4.2: Schematic illustration of the approach for variogram modeling in space (a) and time (b). We used omnidirectional variograms to investigate spatial patterns, whereas our temporal analysis is based on directional variograms. For reasons of clarity we show only lag pairs (arrows) of selected data (solid points).

The variogram models have to take into account that throughfall data can be asymmetric. In general, we can distinguish two cases of asymmetry [*Lark*, 2000; *Kerry and Oliver*, 2007a, b]. First, asymmetry can arise from a long tail of values in the underlying (primary) process. Second, data with outliers might be regarded as the superposition of two distinct processes in which outliers that belong to another (secondary) process contaminate the underlying distribution. In both cases, the overall data distribution may appear strongly skewed.

Since the effect of a skewed underlying distribution on the variogram differs from that of single outliers, data processing and variogram modeling should account for these differences [*Kerry and Oliver*, 2007a, b]. In case of a skewed underlying distribution, it is recommended to transform the data, whereas the presence of outliers in the data should be tackled either by their removal or the use of robust variogram estimators [e.g. *McBratney and Webster*, 1986; *Lark*, 2000; *Kerry and Oliver*, 2007a, b].

In throughfall datasets we expect to find large outliers in the spatial but also in the temporal domain. Outliers in the spatial domain occur due to sampling locations beneath drip points of leaves or inclined stems. In the temporal domain we expect these points to be responsible for outlying values because drip points are not active during all events; hence, it is likely that these points show large temporal fluctuations with throughfall magnitude. Since outliers in both domains might not approach the center of the distribution even after transformation, we have to decide whether or not to remove them. At first glance, drip points could be considered a contaminating process. In practice, however, there is no threshold to separate these points from the underlying process. In fact, there is no evidence that drip points belong to another population as the redistribution of rainfall represents a continuous process in which the concentration of throughfall at some points results in depletion elsewhere. In cases where outlier removal is not possible without risking the exclusion of genuine observations, *Lark* [2000] recommended to use robust estimators. We therefore consider robust variogram estimators in addition to *Matheron's* [1962] estimator, and we assess the results by means of cross-validation as proposed by *Lark* [*2000*] and *Kerry and Oliver* [2007a, b]. Since departure from normality of the underlying distribution may introduce bias into robust estimators [*Lark, 2000*], we perform a comprehensive exploratory data analysis and transform data if necessary prior to variogram estimation.

4.2.4.4 Exploratory data analysis

Our exploratory data analysis and the following geostatistical analysis consist of several steps. To provide a brief overview of our data analytical methods we summarize important steps and decisions in a flowchart (Fig. 4.3). For exploratory data analysis we first

visualized the univariate data distribution by diagnostic plots (histograms, quantile-quantile plots, box plots), and calculated the coefficient of skewness. To determine the need for transformation, we used the octile skew [*Brys et al.*, 2003], denoted "$skew_8$", which is a measure of the asymmetry of the first (O_1) and seventh octile (O_7) of the data about the median:

$$skew_8 = \frac{(O_7 - median) - (median - O_1)}{(O_7 - O_1)}.$$ (4.2)

The advantage of the octile skew compared to the conventional coefficient of skew lies in its insensitivity to extreme values. We used this robust approach to accommodate any outliers that may inflate the coefficient of skewness even though the underlying distribution has a Gaussian shape. Since in this case the skewness cannot be removed by data transformation [*Kerry and Oliver*, 2007b], we wanted to transform our data only if the underlying distribution departs from normality. A rule of thumb [*Rawlins et al.*, 2005] suggests to transform the data if the octile skew is larger than 0.2 or smaller than -0.2. We applied this rule and transformed the data if necessary to square roots or to common logarithms (log_{10}). Since the spatial data contained zero values and the temporal data comprised negative numbers (Eq. 4.1) we added a constant of 1 and 3 to the data, respectively, to make all values just positive prior to transformation.

In order to explore in detail the influence of extreme values on the experimental variograms, we also displayed the bivariate data distribution by means of **h**-scattergrams [*Webster and Oliver*, 2001]. These are scatterplots of point pairs separated by a fixed distance, which are produced for a number of lag classes. Outliers may appear in some, but not necessarily all, of those classes. Where they occur, non-robust semivariance estimates are potentially too large. Besides this benefit of **h**-scattergrams in displaying extreme values, they can also be used to assess the plausibility of the effective range of a variogram model [*Zimmermann et al.*, 2008b].

Since a geostatistical analysis requires second-order stationarity, we produced diagnostic plots (plots of the data, which were divided into quintiles; plots of the data versus the coordinates) to explore the data for non-stationarity of the mean that may be caused by local trends according to

$$z(\mathbf{x}) = \mu(\mathbf{x}) + \varepsilon(\mathbf{x}),$$ (4.3)

where $z(\mathbf{x})$ is the observed variable at location $\mathbf{x}$, $\mu(\mathbf{x})$ is the local mean, i.e. it represents a deterministic drift of the variable at location $\mathbf{x}$, and $\varepsilon(\mathbf{x})$ is the random component at location

x that should be normally distributed with zero mean and that satisfies the second-order stationarity.
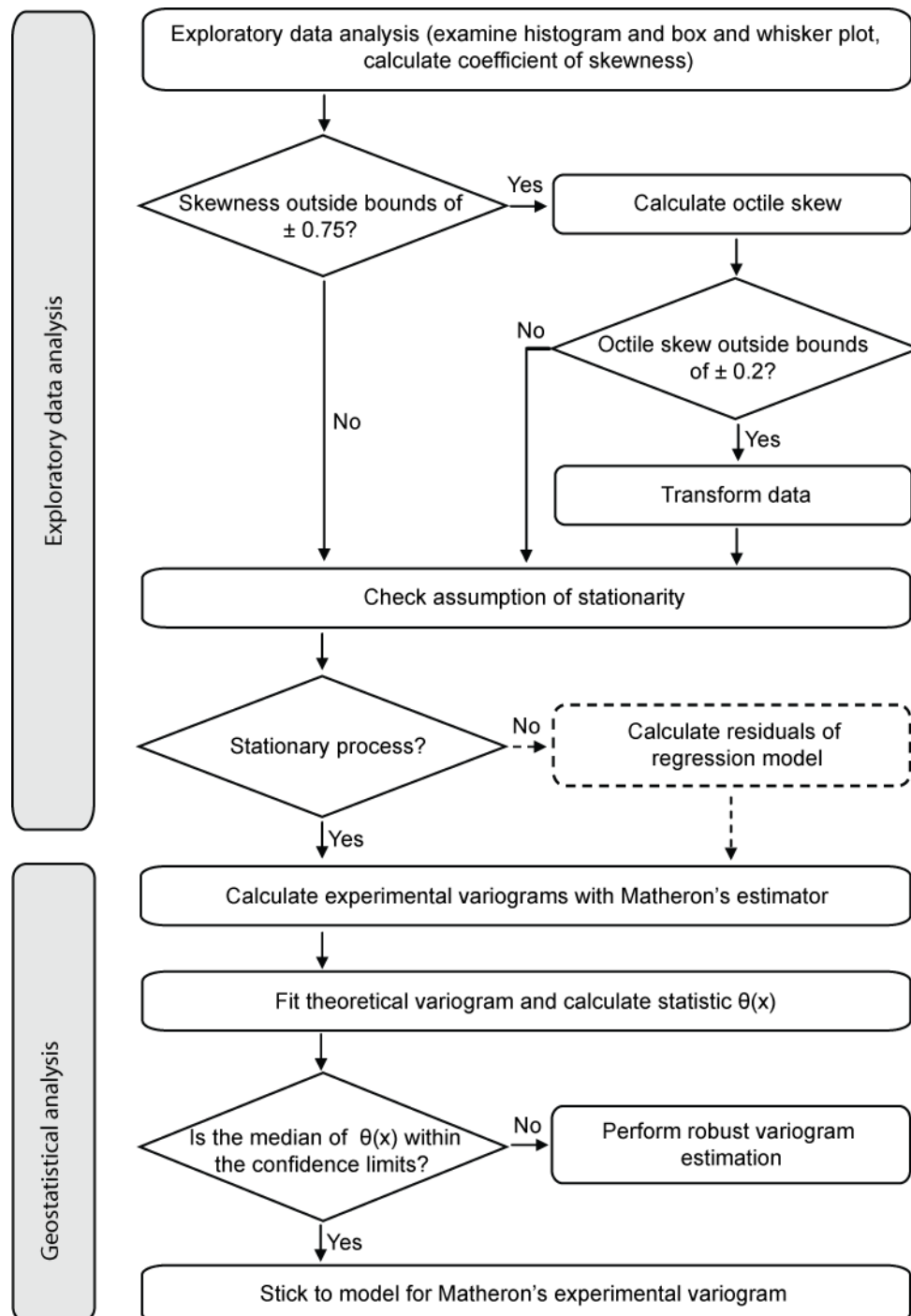
Figure 4.3: Summary of main steps and decisions involved in analyzing our throughfall data, which incorporates the recommendations for analyzing spatial data as given in *Kerry and Oliver* [2007a] and *Zimmermann et al.* [2008b]. The dashed box highlights an operation not applicable to our data, i.e. the assumption of second-order stationarity was valid for our throughfall datasets. If Matheron's estimator performs satisfactorily in studies of spatial structure, we recommend estimating the variogram parameters by residual maximum likelihood, particularly in the framework of spatial prediction.

4.2.4.5 Geostatistical analysis

First we calculated experimental variograms using the estimator due to *Matheron* [1962]:

$$2\hat{\gamma}_M(\mathbf{h}) = \frac{1}{N(\mathbf{h})} \sum_{i=1}^{N(\mathbf{h})} \{z(\mathbf{x}_i) - z(\mathbf{x}_i + \mathbf{h})\}^2, \tag{4.4}$$

where $z(\mathbf{x}_i)$ is the observed value at location $\mathbf{x}_i$, and $N(\mathbf{h})$ are the pairs of observations that are separated by lag $\mathbf{h}$. To ensure that the selection of lag classes does not unduly influence the variogram, we used regular lag classes. That is, for the spatial analysis we calculated the semivariance at 2-m lags with a lag tolerance of 0.99 m over half the maximum separation distance; we only used a semivariance estimate if its number of contributing point pairs was at least 30. For the temporal analysis we calculated the semivariance at 1-day lags, but in contrast to the spatial analysis, we used semivariance estimates to a distance of up to 70 % of the temporal extent because of the continuous large number of point pairs in these lag classes (>1700 point pairs). Four variogram models (exponential, Gaussian, spherical, pure nugget) were fitted to the experimental variograms by ordinary least squares, and we selected the model which had the minimum average sum of squares from the fit.

Observations that qualify as outliers originating from a contaminating process potentially cause an overestimation of the sill variance. *Lark* [2000] showed how cross-validation (or a validation subset) helps to assess the applicability of the standard variogram estimator by using a statistic $\theta(\mathbf{x})$:

$$\theta(\mathbf{x}) = \frac{\{z(\mathbf{x}) - \hat{Z}(\mathbf{x})\}^2}{\sigma_{\mathbf{K},\mathbf{x}}^2}, \tag{4.5}$$

where $z(\mathbf{x})$ is the observed value at location $\mathbf{x}$, $\hat{Z}(\mathbf{x})$ is the kriged estimate and $\sigma_{\mathbf{K},\mathbf{x}}^2$ the kriging variance. If kriging errors follow a Gaussian distribution, $\theta(\mathbf{x})$ will be distributed as χ^2 with one degree of freedom. Since the median of the standard χ^2 distribution with one degree of freedom is 0.455, the median of $\theta(\mathbf{x})$ is also 0.455 when a variogram appropriate for interpolating intrinsic data is used. A sample median significantly ($\alpha = 0.05$) less than 0.455 suggests that kriging overestimates the variance, whereas one which is greater than 0.455 underestimates the variance. In order to compute confidence limits for the median of $\theta(\mathbf{x})$ for our datasets, we proceeded as follows. First, we performed 1000 unconditional simulations to predict the values of throughfall magnitude. Second, we used cross-validation to assess each

simulation using the statistic $\theta(\mathbf{x})$; that is to say we computed the median of $\theta(\mathbf{x})$. Third, we determined the 2.5 % and 97.5 % percentiles of the $\theta(\mathbf{x})$-median distribution to approximate 95 % confidence limits. For datasets whose median of $\theta(\mathbf{x})$ was outside those limits for the variograms based on the Matheron estimator, we calculated robust experimental variograms proposed by *Cressie & Hawkins* [1980], *Dowd* [1984], and *Genton* [1998].

The Cressie – Hawkins' estimator is given by:

$$2\hat{\gamma}_{CH}(\mathbf{h}) = \frac{\left\{ \dfrac{1}{N(\mathbf{h})} \sum_{i=1}^{N(\mathbf{h})} \left| z(\mathbf{x}_i) - z(\mathbf{x}_i + \mathbf{h}) \right|^{\frac{1}{2}} \right\}^4}{0.457 + \dfrac{0.494}{N(\mathbf{h})} + \dfrac{0.045}{N^2(\mathbf{h})}} \ . \tag{4.6}$$

The Dowd estimator is

$$2\hat{\gamma}_D(\mathbf{h}) = 2.198 \left\{ median\left(\left| y_i(\mathbf{h}) \right| \right) \right\}^2 , \tag{4.7}$$

where $y_i(\mathbf{h}) = z(\mathbf{x}_i) - z(\mathbf{x}_i + \mathbf{h}), i = 1,2,...,N(\mathbf{h})$; and Genton's estimator is given by

$$2\hat{\gamma}_G(\mathbf{h}) = \left(2.219 \left\{ \left| y_i(\mathbf{h}) - y_j(\mathbf{h}) \right|; i < j \right\}_{\binom{H}{2}} \right)^2 , \tag{4.8}$$

with $y_i(\mathbf{h})$ defined as for equation (4.7) and $H =$ integer part $(n/2) + 1$, $n = N(\mathbf{h})$.

Because the robust estimators listed above differ in their susceptibility to skewness in the underlying distributions, and particularly in their resistance to outliers, *Lark* [2000] recommended the same cross-validation procedure as described above to choose among them. He suggested to use the estimator with the $\theta(\mathbf{x})$-median closest to the expectation of 0.455, and to use the efficient Genton's estimator if none of the robust estimators are markedly better by this criterion. We adopted this recommendation; for an in-depth discussion of robust variogram estimation we refer to *Lark* [2000].

4.3 Results
4.3.1 Event characteristics

During the 14-month study period we sampled 91 events, which yielded 1089 mm of throughfall (Appendix, Table 4.A1). These 91 events vary greatly with respect to throughfall magnitude (0.1 – 77.4 mm), storm intensity (maximum 30-minute rainfall intensity between

$0.6 - 74.8$ mm h^{-1}), and antecedent wetness conditions (antecedent rainfall of previous 3 days between $0 - 88.4$ mm). Since our dataset not only comprises 46 % of all rain events during the study period but also covers consecutive wet seasons and one dry season, we assume that our data reflects the variety of meteorological characteristics typical for the research area.

4.3.2 Spatial analysis
4.3.2.1 Exploratory data analysis

For the sampled events, a correlation exists between the magnitude of an event and the octile skew (Fig. 4.4a) that decreases asymptotically with increasing event size. As a consequence, the shape of the underlying distribution of throughfall magnitude, which is taken into account when calculating the octile skew (Eq. 4.2), changes from strongly right-skewed for small events to Gaussian for large rain storms (Fig. 4.4b). This shift of frequency distributions coincides with a decline of spatial variability with increasing throughfall magnitude, as the median absolute deviation (MAD)/median ratio depends on median throughfall magnitude (Fig. 4.4a inlet; Appendix, Table 4.A1).
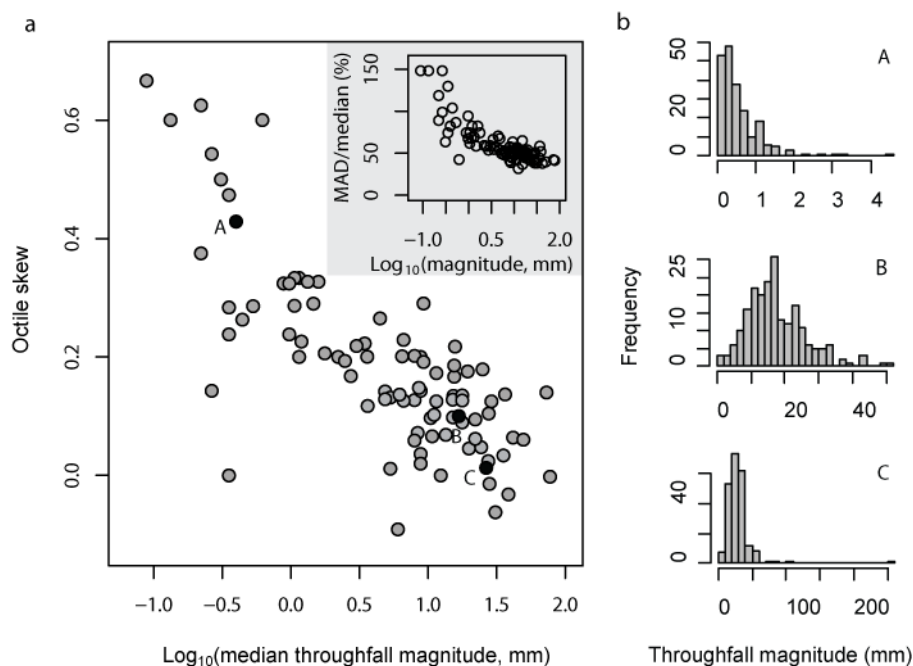
Figure 4.4: The octile skew as a function of median throughfall magnitude (a). Octile skew and throughfall magnitude are non-linearly correlated (Spearman rank correlation coefficient, $\rho = -0.73$, $p < 0.001$, n=91). The black circles represent events along a gradient of throughfall magnitudes, whose frequency distributions are shown at the right-hand side of this figure (b). The frequency distributions of examples A (event 43), B (event 22), and C (event 16) exhibit distinct octile skews (A: high; B and C: low) and skews (A and C: high; B: low). The inlet shows the MAD (median absolute deviation)/median throughfall ratio as a function of the median throughfall.

A closer examination of our data (Fig. 4.4a; Appendix, Table 4.A1) reveals the processes that produce distinct shapes of throughfall frequency distributions. Small events often exhibit both a high octile skew (> 0.2) and a high skew (> 1.5); hence, their skewness is produced by an actually skewed underlying distribution, and not only by single outliers. We attribute the underlying skewness to the patchiness of throughfall as a function of vegetation density; that is to say, many outliers in small events originate from spots with high canopy openness (Fig. 4.5). Canopy openness, however, does not explain all outlying values. That is, during some small events we observed drip from big leaves, which we consider responsible for highly outlying values regardless of canopy closure above the sampling point (Fig. 4.5b).
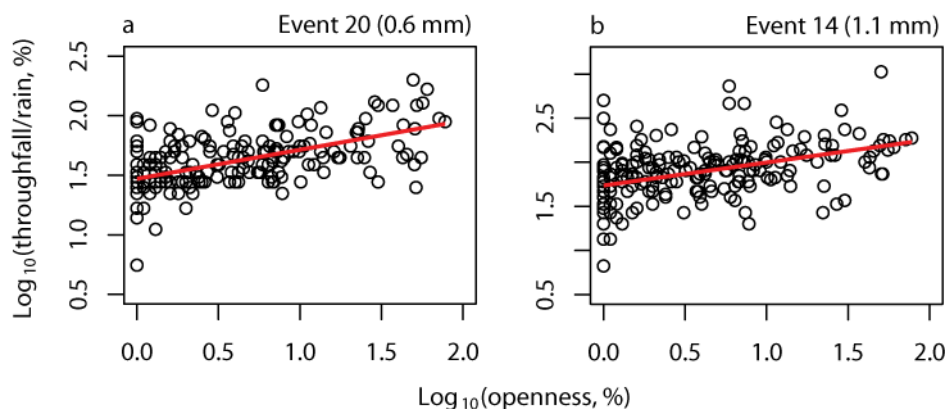
Figure 4.5: Exemplary relationships between canopy openness (%) and relative throughfall (throughfall / rainfall, %) for two small events, event 20 (a) and event 14 (b). The lines indicate linear regression models (event 20: $r^2 = 0.29$, $p < 0.001$, $n = 200$; event 14: $r^2 = 0.17$, $p < 0.001$, $n = 200$).

Many larger events belong to another type of frequency distribution (Fig. 4.4b, example C) that shows a low octile skew (< 0.2) but a high skewness (> 1.5). Their high skewness results from a few outliers far from the centre of the data. Our field observations indicate that some of these outliers originate from stemflow drip points and leaf drip tips, which concentrate water to amounts of up to 1000 % of incident precipitation. The low underlying skew of large events indicates the diminishing influence of canopy openness on the throughfall frequency distribution. The correlation of canopy openness and throughfall magnitudes corroborates this observation in that the importance of canopy openness as a predictor of throughfall magnitude decreases with increasing event size (Fig. 4.6).

Even though drip points clearly distort the univariate distribution, their influence on the experimental variogram depends on the lag classes in which they occur as can be illustrated with two examples (Fig. 4.7). Event 22, which is slightly skewed (Appendix, Table 4.A1), displays no outliers in its bivariate distribution, whereas event 16 comprises one large outlier. This gets conspicuous at lag distances of more than 4 m (Fig. 4.7); hence, we expect the experimental variogram to be sensitive to this value at the 4 – 8 m lag. Event 16 was not

Figure 4.6: Canopy openness as a predictor of throughfall magnitude (as Spearman rank correlation coefficients) plotted against throughfall magnitude. The line indicates a linear regression model ($r^2 = 0.64$, $p < 0.001$, $n = 30$). Note: only events that were sampled in a time frame of less than a month from the date of canopy photography were used for this analysis.

transformed because the octile skew was below 0.2; however, even after a $\log_{10}$-transformation, outliers were still present in 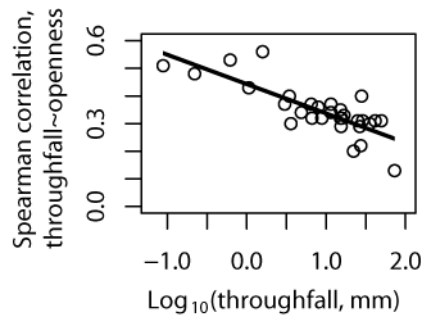the data as revealed by diagnostic plots. The latter example shows that the octile skew in general successfully indicates transformation needs. This statistical criterion, however, can not replace a careful examination of the data, and in some cases a transformation might be reasonable even though the octile skew is below 0.2 or above -0.2 (e.g. event 50; Appendix, Table 4.A1).

4.3.2.2 Geostatistical analysis

According to the $\theta(\mathbf{x})$-statistic [*Lark*, 2000], the non-robust Matheron estimator (Eq. 4.4) overestimated the semivariance in 55 % of the analyzed datasets ($n = 60$ events) as a consequence of outliers in the data (Appendix, Table 4.A2). In these cases, we applied robust estimators and found that none of them behaved superior, though Dowds' and Gentons' estimator were often closer to the expectation of the median of $\theta(\mathbf{x})$ than the Cressie-Hawkins estimator.

When we computed the semivariance for each pair of points, x_i and x_j as

$$\gamma(x_i, x_j) = \frac{1}{2}\{z(\mathbf{x}_i) - z(\mathbf{x}_j)\}^2, \tag{4.9}$$

and plotted these values as boxplots against lag distance classes, which produces a graph called the "variogram cloud" [*Webster and Oliver*, 2001] (Fig. 4.8a), it became obvious that a single extreme outlier has a strong influence on the shape of that cloud. In our example (event 16), the first extremely large semivariance values occur around the 8 – 10 m lag (Fig. 4.8a); not surprisingly, the Matheron experimental variogram starts to overestimate the semivariance at precisely the same distance classes (Fig. 4.8b). The resulting seemingly strong autocorrelation structure vanishes when experimental variograms are based on robust estimators (Fig. 4.8b). A transformation of datasets that display extreme outliers (Fig. 4.4, example C) appears to be only partly successful. Transformations reduce the influence of outliers on the semivariance cloud (Fig. 4.8c), and non-robust estimates of the experimental
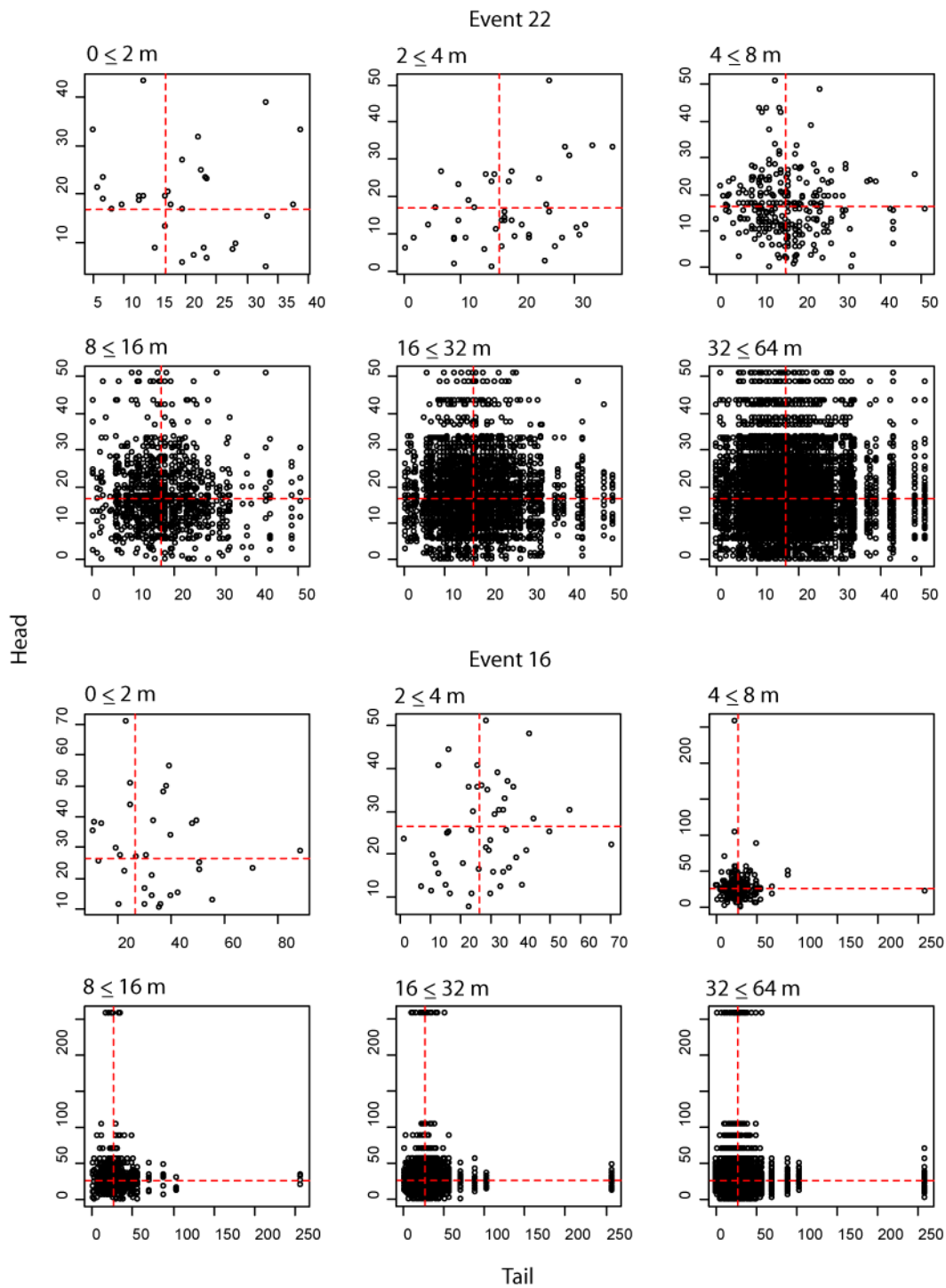
Figure 4.7: Examples of **h**-scattergrams that reveal contrasting bivariate data distributions (events 22 and 16) for selected lag classes. The plots show all pairs of throughfall measurements at locations **x** separated by a certain lag-distance class (shown at the top of each graph); the value at the start of the distance vector **h**, $z(\mathbf{x})$, is called the tail value, and the value at the end of the distance vector, $z(\mathbf{x}+\mathbf{h})$, is the head value. The vertical and horizontal red lines correspond to the population median.

variogram do not produce any artificial autocorrelation structure. According to the $\theta(\mathbf{x})$-statistic [*Lark*, 2000], however, Matheron's estimator still overestimates the semivariance,

which is reflected in the considerable difference between sill variances calculated with non-robust and robust variogram estimators (Fig. 4.8d).

The variogram analysis for the subset of 60 events showed a consistent pattern, that is to say, throughfall displayed either weak or no spatial autocorrelations over the studied lag distances (Appendix, Table 4.A2; Fig. 4.9). Since all 60 events exhibited similar throughfall autocorrelation patterns, we rule out any influence of deciduousness on these patterns.
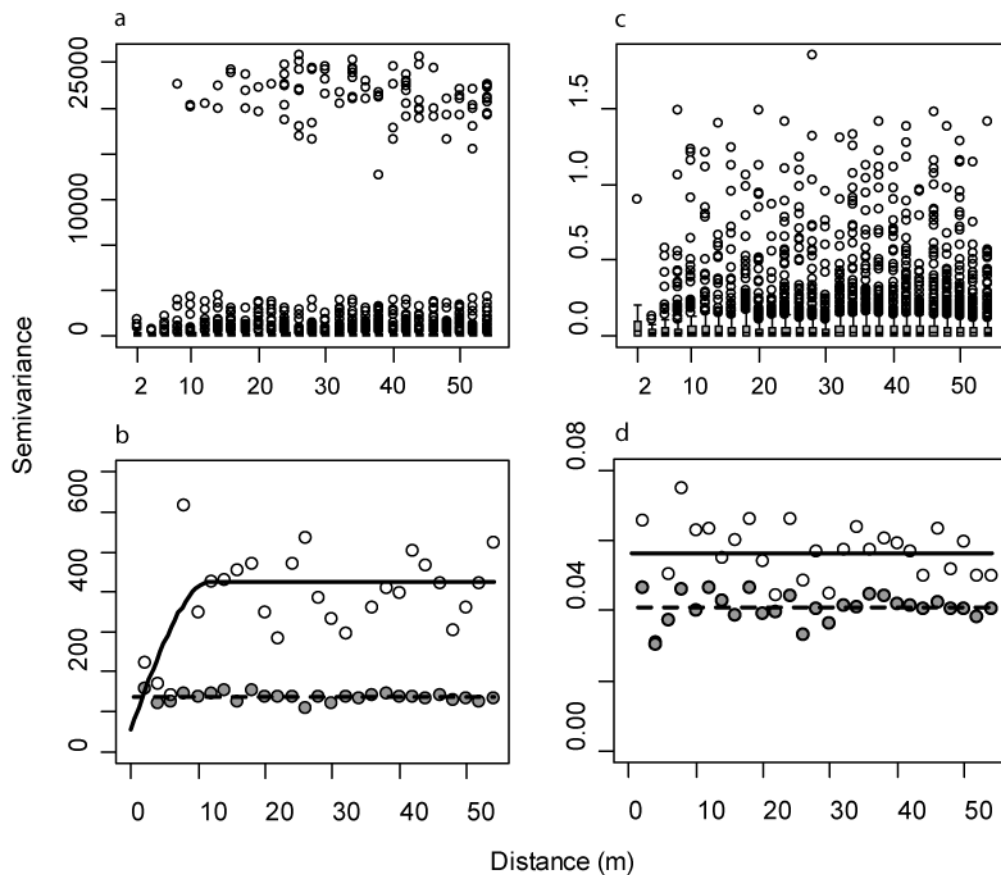
Figure 4.8: Boxplots of semivariances for all point pairs (Eq. 4.9) plotted against lag distance classes for two examples: raw data of event 16 (a) and log-transformed data of the same event (c). The corresponding experimental and theoretical variograms based on the non-robust Matheron estimator (Eq. 4.4) (open circles, solid line, respectively), and the robust estimator due to Genton (Eq. 4.8) (solid circles, dashed line, respectively) are shown below (b and d).
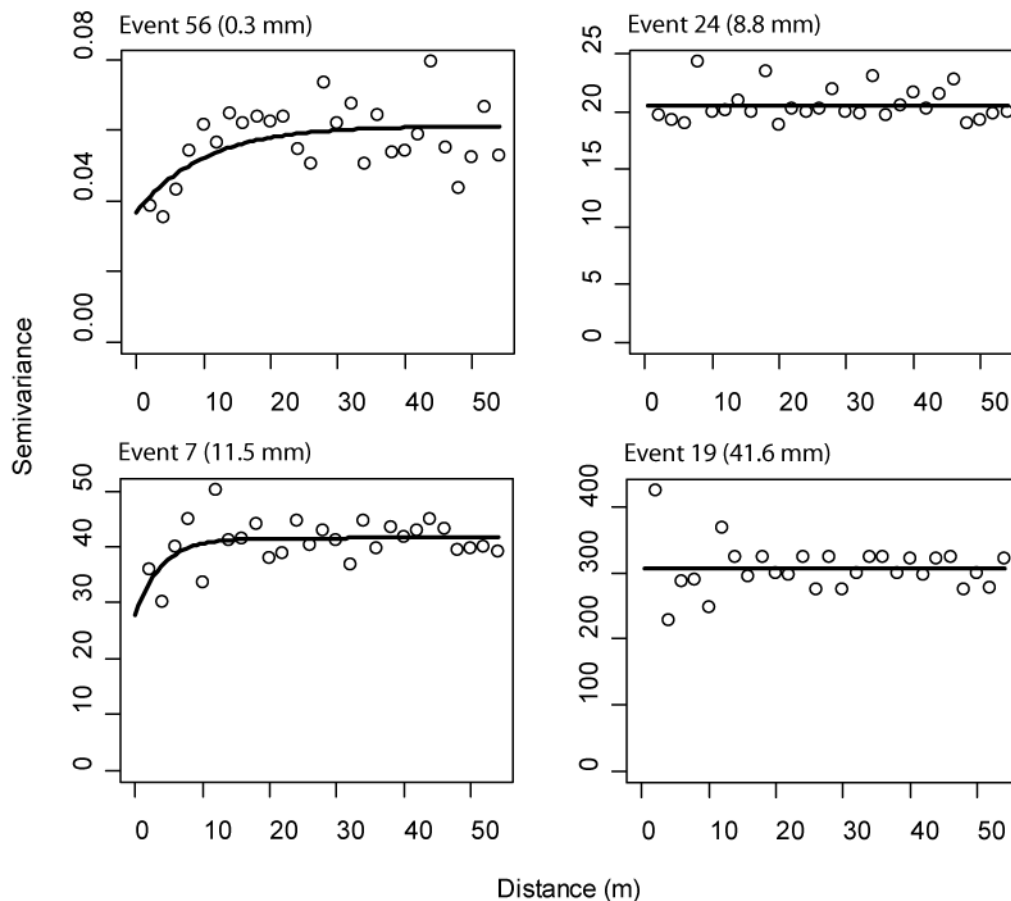
Figure 4.9: Exemplary variograms across a range of throughfall magnitudes. The left panels show events with a weak throughfall autocorrelation structure, whereas the right panels illustrate variograms with a pure nugget structure. The latter case was detected in 82% of all events.

4.3.3 Temporal analysis
4.3.3.1 Exploratory data analysis

Similar to the spatial data, the temporal data set shows large outlying values. This is not surprising in view of our observations that drip points are not active during all events. Their irregular activation results in large temporal fluctuations of the standardized throughfall (Fig. 4.10). Since these outlying values result in both a large skewness (5.88) and a large octile skew (0.2), we $\log_{10}$-transformed the data for further analysis. These data still show some outlying values (skew: 0.32; octile skew: 0.01). They are, however, not particularly numerous; for instance, if we considered all values beyond 1.5 and 3 times the interquartile range from the upper quartile as outliers, the rate of contamination would be 0.0093 and 0.0022 (Fig. 4.11).

To investigate whether our data show local trends we first produced several diagnostic plots (e.g. plots of the data versus the time of sampling) which displayed no trend in the data. Furthermore, we checked if correlations of throughfall measurements between events show

similar trends over time regardless of the season. For this analysis we compared events sampled during the transition from dry to wet season (the time of leaf flush) with events that occurred during the peak of the rainy season 2007. This comparison is based on 14 events in both periods of similar throughfall magnitude (Wilcoxon rank sum test, p = 0.98, n = 14). Surprisingly, we did not detect any differences between measurements of the two sampling intervals (Fig. 4.12). This result indicates that deciduousness does not influence temporal correlations of throughfall measurements in our sampling area.
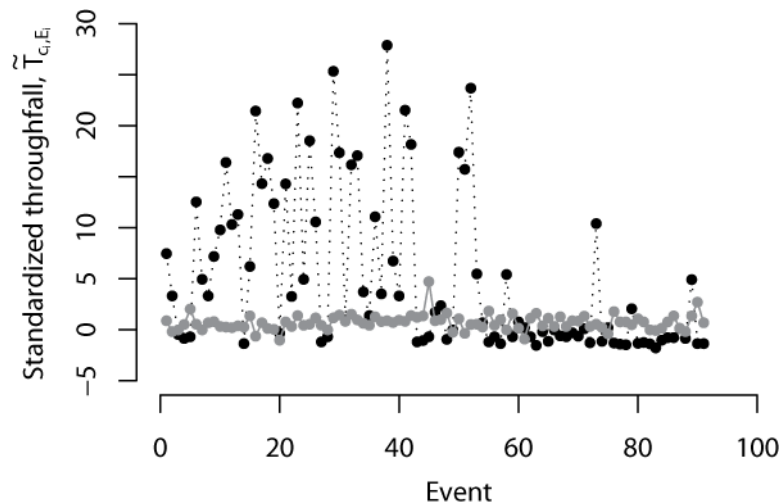
Figure 4.10: Fluctuations of the standardized throughfall, $\widetilde{T}_{c_i, E_i}$, through time at two selected sampling locations. The black dots and the dotted line illustrate the temporal behavior of a drip point, whereas the gray dots and the solid line refer to a sampling location where no drip was detected. Note the disappearance of the drip point after event 60.
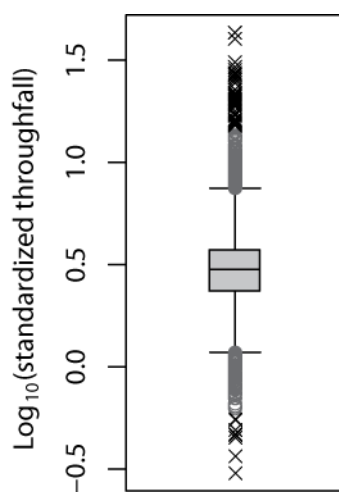
Figure 4.11: Box-and-whisker plot of the throughfall data used for estimating the temporal variogram (n = 19926). The box contains the middle 50 % of the data, the horizontal line in this box refers to the median. The whiskers illustrate the distance of 1.5 times the interquartile range from the quartiles. Data points beyond this distance are shown as gray circles, and crosses indicate values with a distance of three times the interquartile range from the quartiles.
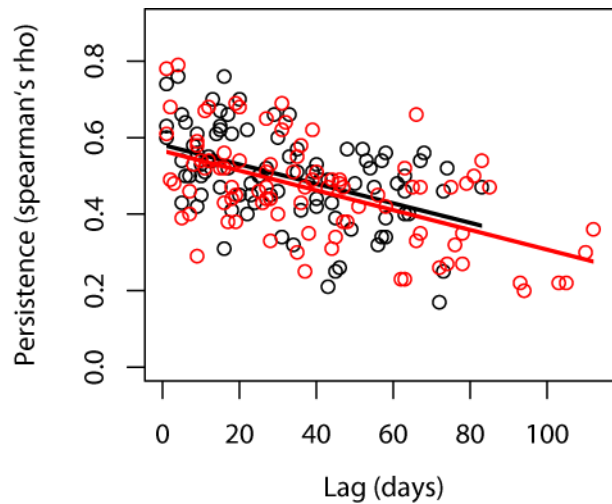
Figure 4.12: The persistence of throughfall measurements between event pairs (n = 14 events, n = 91 pairs) as a function of the temporal lag between events for the peak of the rainy season 2007 (black circles) and for the transition from dry to wet season 2008 (red circles). The persistence is expressed with Spearman rank correlation coefficients, ρ. The lines indicate linear regression models, the black line refers to the 2007 data (r^2 = 0.2, p < 0.001, n = 91), whereas the red line relates to the 2008 data (r^2 = 0.31, p < 0.001, n = 91).

4.3.3.2 Geostatistical analysis

Though the transformed data exhibit only a few outliers that skew the distribution rather modestly, the $\theta(\mathbf{x})$-statistic [*Lark*, 2000] indicated that the non-robust Matheron estimator overestimated the semivariance (median of $\theta(\mathbf{x})$ = 0.303). Hence, we applied robust estimators and found that *Dowd's* [1984] estimator provided satisfactory results (median of $\theta(\mathbf{x})$ = 0.451). Interestingly, our results show that even a very low fraction of outlying values (< 1 % of the data) influences the sill variance of *Matheron's* [1962] estimator; the shape of the variogram, however, displays almost no difference between non-robustly and robustly estimated temporal variograms (Fig. 4.13).

Our data show that throughfall exhibits long-term persistence, that is, measurements at individual sampling points correlate over consecutive wet seasons (Fig. 4.13, Table 4.2). The variogram indicates that these correlations vanish after one year. This long-term persistence preserves the spatial variability of throughfall through time which is reflected in large differences between dry and wet sampling points. The driest locations in our study area received only 16 % of rainfall, whereas extreme wet spots accumulated up to 350 % of rainfall during the 14-month sampling period.
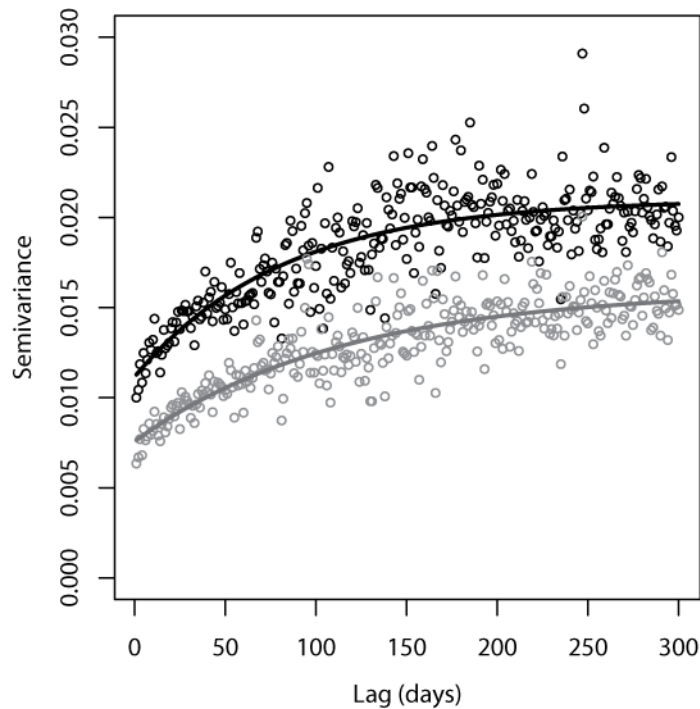
Figure 4.13: Experimental and theoretical variograms for the temporal dataset (n=91 events, n=19926 observations) based on the non-robust Matheron estimator (Eq. 4.4) (black circles, black line, respectively), and the robust estimator due to Dowd (Eq. 4.7) (gray circles, gray line respectively). Details of the theoretical variogram model for the latter estimator are given in Table 4.2.

Table 4.2: Variogram model parameters for temporal data [a].

Model	Exponential
Nugget	0.008
Sill	0.016
Range (days)	115
Effective range[b] (days)	344

[a] Model fitted to the experimental variogram which was estimated with Dowds estimator.

[b] The effective range, R_{eff}, for an exponential model is calculated as: R_{eff} = range*3.

4.4 Discussion

4.4.1 A call for robust variogram estimation techniques

The majority of throughfall studies report asymmetric frequency distributions [*Ford and Deans*, 1978; *Lloyd and Marques*, 1988; *Bellot and Escarre*, 1989; *Kostelnik et al.*, 1989; *Cavelier et al.*, 1997; *Hölscher et al.*, 1998; *Germer et al.*, 2006; *Holwerda et al.*, 2006]. Only a few studies in temperate forests detected Gaussian behavior of throughfall quantity [Loustau et al., 1992; Möttönen et al., 1999; Keim et al., 2005]. Our data indicate that throughfall frequency distributions can be positively skewed for different reasons. Small events show a high skew (Fig. 4.4b, Example A) because throughfall mainly consists of the free throughfall component (Fig. 4.5a), which originates from rain falling in gaps without striking the canopy [*Gash*, 1979; *Loustau et al.*, 1992]. As soon as rainfall magnitude increases, free throughfall alone does not account for all outlying values (Fig. 4.6) because water on leaves begins to

coalescence and drip occurs (Fig 4.5b). Large positive skewness and a large spatial variability of small events have been detected by many studies regardless of forest type [*Bellot and Escarre*, 1989; *Staelens et al.*, 2006b]. In contrast, many large events show a high skew (Fig. 4.4b, Example C) due to a few outliers caused by drip points. *Lloyd and Marques* [1988] detected a similar structure in the throughfall frequency distribution of a Brazilian tropical forest and noted the influence of drip points. If the latter are absent, however, large events tend to show a low skewness and a relatively low spatial variability [*Bellot and Escarre*, 1989; *Loustau et al.*, 1992; *Staelens et al.*, 2006b], which is also reflected in our data where large events have low octile skews (Fig. 4.4a) and a low MAD/median throughfall ratio (Fig. 4.4a, inlet).

Our results and the above list of studies provide evidence that a positive skew of throughfall frequency distributions is the rule rather than the exception, particularly in tropical forests [*Lloyd and Marques*, 1988]. Interestingly, our data show that sampling locations which represent outliers in the spatial domain are also responsible for extreme values in the temporal domain because outlying values at these points do not occur in every event (Fig. 4.10). Extreme values in both domains influence the non-robust variogram estimator (spatial data: Fig. 4.8; temporal data: Fig. 4.13) because they cause an overestimation of the sill variance (Fig. 4.8 and 4.13) and in some cases they even induce spurious autocorrelation structures (Fig. 4.7 and 4.8). Theoretical studies of the influence of outliers on the variogram showed that the size of the dataset is less important than the rate of contamination [*Kerry and Oliver*, 2007b]. Our results confirm these theoretical findings and provide evidence that even very low rates of contamination (< 1 % of the data) potentially distort non-robust variogram estimates (Fig. 4.8 and 4.13). This problem cannot be solved by common transformations, such as square root- or $\log_{10}$-transformation (Fig. 4.8 and 4.13), because some outliers in our throughfall datasets, e.g. those originating from drip points, are too far from the centre of the data. Therefore, in many cases the use of robust variogram estimators to model spatial throughfall data appears inevitable if one wants to avoid the arbitrary decision of removing outliers prior to geostatistical analysis. It must be re-emphasized, however, that an underlying Gaussian distribution is of particular importance for robust variogram estimation so as to avoid bias [*Lark*, 2000]. Our study demonstrates that different processes induce distinct throughfall frequency distributions and that data treatment has to account for these differences; that is, many small throughfall events have to be transformed to square roots or logarithms before geostatistical analysis, whereas large events often require robust variogram estimation.

In the presence of outliers, we mainly chose the robust estimators proposed by *Dowd* [1984] (Eq. 4.7) and *Genton* [1998] (Eq. 4.8), a choice that is justified by the behavior of their influence functions [*Hampel et al.*, 1986]. The performance of these functions can be

described by several measures; one such is the gross error sensitivity [*Genton*, 1998; *Lark*, 2000]. This measure indicates that only Dowd's and Genton's estimator are B-robust, that is, the estimators have a bounded asymptotic bias. Matheron's (Eq. 4.4) and the Cressie-Hawkins' estimator (Eq. 4.6), in contrast, are not B-robust because the effect of an outlying value $x = z(\mathbf{x}_i) - z(\mathbf{x}_i + \mathbf{h})$ is proportional to x^2 and $x^{0.5}$ over all x, respectively [*Lark*, 2000]. Another important measure of robustness is the breakdown point [*Hampel*, 1971]. Dowd's and Genton's estimator show a large robustness as their breakdown point is 0.5 (the maximum of any estimator), which means that half of the pair differences, $y_i(\mathbf{h})$, may be replaced by arbitrary large or small values before the estimators $\hat{\gamma}_D(\mathbf{h})$ and $\hat{\gamma}_G(\mathbf{h})$ collapse [*Lark*, 2000]. In comparison, the Cressie-Hawkins estimator is not robust by this commonly used criterion in robust statistics as its breakdown point is zero [*Genton*, 1998; *Lark*, 2000].

To summarize, we wish to highlight two critical steps in a geostatistical investigation of throughfall data. First, a careful exploratory data analysis is necessary to determine transformation needs, and to detect outliers in the dataset in order to understand their influence on the estimated covariance functions. In particular, the analysis of the bivariate distribution by means of **h**-scattergrams [*Webster and Oliver*, 2001] is a useful tool as it reveals in which lag classes outliers appear and hence, in which lag class the standard estimator (Eq. 4.4) potentially overestimates the variogram (Fig. 4.7 and 4.8). Second, the $\theta(\mathbf{x})$-statistic [*Lark*, 2000] is a valuable criterion to assess the applicability of the standard variogram estimator (Eq. 4.4); furthermore, it can be used to eventually choose among robust estimators [*Lark*, 2000]. The choice of the variogram estimator depends on the characteristics of the data, because the difference between the Cressie-Hawkins' estimator [*Cressie & Hawkins*, 1980] and the other robust estimators, $\hat{\gamma}_D(\mathbf{h})$ and $\hat{\gamma}_G(\mathbf{h})$, is not always of practical importance as outliers in real datasets are not unbounded [*Lark*, 2000]. Throughfall datasets that contain extreme outlying values, however, may call for highly robust variogram estimators such as Dowd's [*Dowd*, 1984] and Genton's [*Genton*, 1998] estimator. Surprisingly, robust variogram estimation techniques, which have been widely used in hydrology and soil science [e.g. *Shouse et al.*, 1990; *Mohanty et al.*, 1991; Woodbury and Sudicky, 1991; *Lark*, 2002; *Sobieraj et al.*, 2004], have yet to be applied in studies that deal with throughfall patterns. Unfortunately, some throughfall studies [e.g. *Shachnovich et al.*, 2008] do not provide sufficient information on the uni- and bivariate distributions, which casts doubt on the choice of the non-robust estimator (Eq. 4.4).

4.4.2 An attempt to separate spatial patterns from spatial illusions: insights from a global comparison

A comparison of a variety of forest ecosystems reveals large differences of throughfall autocorrelation patterns (Table 4.3). Large variations in sampling scale triplets [*Blöschl and Sivapalan*, 1995; *Blöschl*, 1999] (Table 4.3), however, do not exactly facilitate the interpretation of these patterns. Ideally, sampling and modeling scales are commensurate with the scales of variation of the variable of interest [*Blöschl*, 1999; *Skøien and Blöschl*, 2006]. Since most throughfall studies [*Bellot and Escarre*, 1989; *Loustau et al.*, 1992; *Keim et al.*, 2005; *Staelens et al.*, 2006b] detected a large spatial variation over small scales, an adequate sampling scheme would involve a small spacing, small support, and a sufficiently large extent to cover typical forest structures. When sampling scales do not match the scale of the process in question, they will affect the estimated autocorrelation structure; for instance, large spacings led to overestimation of the correlation length [*Russo and Jury*, 1987; *Skøien and Blöschl*, 2006]. Therefore, the speculation of *Loescher et al.* [2002] that "large tree canopies and gaps are the source of much of the spatial variance in throughfall volume" does not necessarily explain the observed range. It is more likely that the large throughfall correlation length of more than 40 m [*Loescher et al.*, 2002] reflects the large spacing of the sampling points (Table 4.3).

Webster and Oliver [2001] demonstrated that experimental variograms based on fewer than 50 data are often erratic. They recommended using no fewer than 100, and ideally 150 observations, for a reliable variogram if the variation is isotropic. We support this recommendation and suggest analyzing variograms of several events; if consistent autocorrelation patterns emerge [*Keim et al.*, 2005], an erratic variogram structure can be ruled out. This implies that conclusions drawn from a single variogram based on fewer than 100 observations [e.g., *Loescher et al.*, 2002; *Staelens et al.*, 2006b] have to be interpreted with a grain of salt.

Keim et al. [2005] noted that the throughfall correlation length corresponds roughly to one crown diameter. Our data (Fig. 4.9; Appendix, Table 4.A2) do not support this suggestion. We suppose that tree canopy structures may indeed influence throughfall autocorrelation patterns, but in areas with a highly variable understory those patterns are likely to disappear because in thick understory throughfall is redistributed before it eventually reaches the forest floor, whereas in locations with a sparse understory it is not. This supposition, however, can not be tested yet because only few studies provide sufficient data [*Möttönen et al.*, 1999; Keim et al., 2005]; that is, other study sites [*Bellot and Escarre*, 1989; *Loustau et al.*, 1992] cannot be compared because their low number of throughfall sampling

locations alone (Table 4.3) could be responsible for the detected pure nugget autocorrelation structure.

Table 4.3: Comparison of sampling designs and throughfall autocorrelation ranges from studies conducted in a variety of forest ecosystems.

Reference	Location	Forest type	A_{dom}[a] (m^2)	N[b]	Support[c] (cm^2)	Spacing[d]	Effective range[e] (m)
Bellot and Escarre, 1989	NE Spain	Holm-oak forest	950	50	?	4.4	pure nugget
Keim et al., 2005	W USA	60 yr old conifer forest	225	94	9.2	1.5	5[f]
Keim et al., 2005	W USA	Old conifer forest	900	94	9.2	3.1	5[f]
Keim et al., 2005	W USA	60 yr old deciduous forest	304	94	9.2	–	10[f]
Loescher et al., 2002	Costa Rica	Tropical rainforest	25600	56	95	21.4	43[g]
Loustau et al., 1992	S France	18 yr old pine stand	2500	52	707	6.9	pure nugget
Möttönen et al., 1999	E Finland	150 - 200 yr old Scots pine forest	10000	181	50	7.4	9
Shachnovich et al., 2008	Israel	40 yr old pine forest	70	20	55	1.9	?
Staelens et al., 2006b	Belgium	85 yr old beech tree	225	50	158	2.1	3–4
Staelens et al., 2006b	Belgium	85 yr old beech tree	225	48	460	2.2	no stable sill
This study	Panama	Tropical rainforest	10000	220	113	6.7	pure nugget[h]

[a] Size of sampling area.

[b] Number of sampling locations

[c] Receiving area of collector.

[d] The spacing, L_s, is calculated according to *Skøien and Blöschl* [2006], that is, $L_s = (A_{dom}/N)^{0.5}$.

[e] The effective range, R_{eff}, is calculated as: exponential model: $R_{eff} = range*3$, Gaussian model: $R_{eff} = range*3^{0.5}$, spherical model: $R_{eff} = range$

[f] *Keim et al.* [2005] estimated the range visually from the experimental variogram, no variogram model was fitted.

[g] We report ranges as given by the authors, however, *Loescher et al.* [2002] might have reported the distance parameter of the covariance function instead of the effective range.

[h] We detected a pure nugget structure in 82 % of the analyzed events, the remaining events showed weak structures (i.e. high nugget /sill ratios) with highly variable effective ranges.

4.4.3 Temporal persistence of throughfall: long-term datasets and long-term persistence

The majority of studies that investigated the persistence of throughfall detected a temporal stability over several months [*Raat et al.*, 2002; *Staelens et al.*, 2006b; Zimmermann et al., 2007, 2008a]; our results are no exception (Fig. 4.13; Table 4.2). They also imply that wet and dry areas persist over consecutive wet seasons, which may have some ecological relevance because moisture gradients at the forest floor influence, for instance, root water uptake [*Bouten et al.*, 1992], nitrification-denitrification rates [*Carnol and Ineson*, 1999; *Raat et al.*, 2002] and arthropod distributions [*Kaspari and Weiser*, 2000].

A comparison of our experimental setup with a range of studies that investigated the persistence of throughfall measurements in temperate [*Raat et al.*, 2002; *Keim et al.*, 2005; *Staelens et al.*, 2006b] and tropical forests [*Zimmermann et al.*, 2007, 2008a] reveals large differences with respect to design criteria (e.g. number of sampling points and occasions) and data-analytical methods. To our knowledge this study is the first attempt to describe the temporal persistence of throughfall with variograms. Since reliable variogram analyses require relatively large datasets, benefits have to justify the expense necessary to acquire such datasets. So far, various versions of time stability plots have been used to analyze temporal persistence of throughfall [*Raat et al.*, 2002; *Keim et al.*, 2005; *Staelens et al.*, 2006b; *Zimmermann et al.*, 2007, 2008a]. These graphs plot standardized throughfall for all sampling points and occasions in order to illustrate whether spots receiving large or small throughfall volumes persist over time [Keim et al., 2005]. Their main drawback is that unlike temporal variograms they do not reveal the length of the time period over which throughfall measurements are correlated (Fig. 4.13; Table 4.2). Another disadvantage of time stability plots is that they do not differentiate between temporal lags. Therefore, these plots can not be used for the analysis of long-term datasets because as soon as temporal correlations vanish they will detect a lower persistence. In other words, the quality of temporal variograms usually improves with increasing duration of throughfall monitoring due to an increase in contributing point pairs per lag, while time stability plots deteriorate when the observation period exceeds the range of temporal correlations.

Regardless of methodological differences, a comparison of studies which monitored throughfall over several months [*Raat et al.*, 2002; *Staelens et al.*, 2006b; Zimmermann et al., 2008a] reveals that deciduous forests in the temperate zone exhibit a relatively low temporal persistence of throughfall measurements. This can be explained by seasonal variations in canopy foliation [*Staelens et al.*, 2006b]. In contrast, temperate coniferous forests display a relatively high persistence of throughfall measurements [*Raat et al.*, 2002]. Deciduousness, however, is not restricted to high latitudes, and some tropical forests show a lower persistence

of throughfall during leaf flushes [*Zimmermann et al.*, 2008a]. Nonetheless, our results (Fig. 4.12 and 4.13) indicate that phenological dynamics are not necessarily influential. The proportion of deciduous trees and the occurrence of some palm species (e.g. *Orbignya phalerata* Mart.), which are known to strongly affect the redistribution of rainfall due to their seasonal leaf growth and conducive morphology [*Germer et al.*, 2006], may help to explain the diversity of temporal persistence in tropical forests.

4.5 Conclusions

We summarize our results by answering the research questions posed in the introduction:

1) Throughfall datasets show frequently a large positive skew. Outliers in both the spatial and the temporal domain influence the standard, non-robust variogram estimator, which primarily results in an overestimation of the sill variance and, to some extent, in spurious autocorrelation structures. Common transformations are important for reducing the underlying skewness but can not guarantee satisfactory results in cases where outliers are far from the centre of the data. In addition to a thorough exploratory data analysis, we propose to apply the θ-statistic [*Lark*, 2000] to assess the need for robust variogram estimation when modeling spatial throughfall data. In the presence of outliers, Dowd's [*Dowd*, 1984] and Genton's [*Genton*, 1998] estimators were chosen most frequently by this criterion, which can be explained by their B-robustness and high breakdown points.

2) The redistribution of rainfall in our study area, a 1-ha plot of tropical forest, results in rather weak or non-detectable throughfall autocorrelation patterns over the studied lag distances. We speculate that this weak or pure nugget spatial structure of throughfall is typical in areas with highly variable understory vegetation because at some locations throughfall is redistributed several times before it eventually reaches the forest floor, whereas in other areas it is not.

3) Throughfall measurements show a high temporal persistence, and wet and dry areas, respectively, outlast consecutive wet seasons. Seasonality, and hence deciduousness, seems to have no influence on temporal autocorrelations in our research area. Wet spots accumulated up to 350 % of incident rainfall, whereas the driest points received only 16 % of rainfall during the 14 month study period. The long-term persistence of this spatial heterogeneity may influence biogeochemical processes at the forest floor. This study introduces variogram analysis as a useful tool to assess the temporal persistence of throughfall measurements.

We hope that our work will stimulate research on throughfall spatial and temporal patterns in other places. To improve the understanding of rainfall redistribution in forest

ecosystems and its influence on near-surface processes, we have to improve the comparability among study sites. Therefore, we propose to standardize the sampling scale triplet, which ideally involves plots of 1-ha and a sufficient number of sampling locations, particularly at small lag distances.

4.6 Acknowledgements

4.7 Appendix

Table 4.A1: Event characteristics and summary statistics for throughfall data (n=220).

Event	Date (dd-mm-yy)	Median (mm)	MAD[a] (mm)	MAD[a]/ Median ratio (%)	Skewness	Octile skew[b]
1	23-08-07	28.1	10.8	38.5	1.19	-0.01
2	25-08-07	15.7	8.2	52.2	1.05	$0.22^{sqr)}$
3	31-08-07	1.6	1.3	82.4	2.58	$0.33^{sqr)}$
4	02-09-07	0.2	0.3	118.6	3.80	$0.38^{sqr)}$
5	03-09-07	0.1	0.1	148.3	2.65	$0.67^{sqr)}$
6	05-09-07	11.5	6.6	57.0	3.71	0.13
7	08-09-07	11.5	5.9	51.3	0.98	0.17
8	09-09-07	35.4	15.7	44.5	1.05	0.03
9	11-09-07	15.5	7.2	46.6	1.70	0.17
10	12-09-07	8.0	3.9	49.4	2.58	0.13
11	13-09-07	15.2	7.5	49.7	4.86	0.10
12	14-09-07	22.1	9.2	41.5	2.86	0.09
13	15-09-07	29.0	14.7	50.9	3.30	0.12
14	17-09-07	1.1	0.7	61.8	4.86	$0.29^{log)}$
15	19-09-07	3.4	2.3	66.5	2.14	$0.22^{log)}$
16	24-09-07	26.5	10.8	40.8	6.95	0.01
17	25-09-07	4.9	2.6	53.9	4.55	0.14
18	27-09-07	15.3	5.6	36.5	4.60	0.13
19	30-09-07	41.6	15.7	37.9	3.23	0.06
20	02-10-07	0.6	0.3	42.4	1.96	$0.60^{log)}$
21	03-10-07	25.0	11.8	47.2	4.28	0.18
22	07-10-07	16.8	7.9	46.8	0.94	0.10
23	12-10-07	49.5	19.7	39.7	6.66	0.06
24	17-10-07	8.8	3.9	44.5	1.00	0.14
25	18-10-07	27.4	11.8	43.0	5.56	0.02
26	19-10-07	6.5	3.3	51.3	2.79	$0.20^{sqr)}$
27	21-10-07	3.0	1.8	58.9	1.44	$0.22^{sqr)}$
28	24-10-07	6.6	3.3	49.4	1.39	0.13
29	25-10-07	3.6	2.0	54.6	8.17	0.20
30	26-10-07	72.9	30.8	42.2	5.60	0.14
31	29-10-07	6.6	3.3	49.4	1.08	$0.23^{sqr)}$
32	30-10-07	5.3	2.6	49.4	5.51	0.13
33	31-10-07	17.7	9.2	51.9	5.50	0.09
34	03-11-07	77.4	32.1	41.5	0.36	0.00
35	04-11-07	1.5	0.9	58.4	1.73	$0.29^{log)}$
36	05-11-07	8.8	4.6	51.9	3.01	$0.20^{sqr)}$

[a] MAD: median absolute deviation.

[b] If the octile skew was > 0.2 we transformed the data (unless otherwise noted); transformations are indicated for all events used for spatial analysis (event 1-60): [sqr] denotes to square root transformation, whereas [log] indicates log_{10} transformation.

Table 4.A1 continued: Event characteristics and summary statistics for throughfall data (n=220).

Event	Date (dd-mm-yy)	Median (mm)	MAD[a] (mm)	MAD[a]/ Median ratio (%)	Skewness	Octile skew[b]
37	07-11-07	6.0	2.9	48.0	1.58	-0.09
38	09-11-07	38.5	20.0	52.0	9.85	-0.03
39	10-11-07	15.1	9.8	65.0	1.60	0.13
40	12-11-07	10.4	5.0	47.7	1.48	0.10
41	13-11-07	2.7	1.5	53.8	7.01	0.17
42	14-11-07	17.7	8.5	48.2	6.73	0.13
43	23-02-08	0.4	0.3	82.4	2.92	$0.43^{sqr)}$
44	21-03-08	1.0	0.9	94.3	3.96	$0.24^{sqr)}$
45	25-03-08	0.1	0.2	148.3	5.31	$0.60^{sqr)}$
46	10-04-08	8.4	3.3	39.0	1.31	0.07
47	29-04-08	5.3	2.6	49.4	1.36	0.01
48	30-04-08	27.6	13.4	48.6	2.26	0.10
49	08-05-08	12.4	3.9	31.8	1.67	0.00
50	11-05-08	4.9	3.3	67.4	5.73	$0.13^{log)}$
51	26-05-08	17.7	7.9	44.5	4.68	0.13
52	27-05-08	9.3	5.2	56.5	7.19	$0.29^{log)}$
53	05-06-08	30.9	11.8	38.1	0.95	-0.06
54	07-06-08	8.0	3.3	41.2	1.24	0.06
55	12-06-08	1.2	1.0	82.4	3.16	$0.23^{log)}$
56	14-06-08	0.3	0.4	148.3	2.69	0.14
57	18-06-08	0.4	0.3	74.1	2.17	0.00
58	25-06-08	8.8	3.9	44.5	1.26	0.04
59	30-07-08	1.1	0.8	68.4	8.70	$0.33^{log)}$
60	31-07-08	19.5	10.5	53.9	1.08	0.18
61	02-08-08	0.3	0.2	63.5	2.58	0.50
62	03-08-08	0.2	0.2	89.0	2.44	0.63
63	06-08-08	3.6	2.1	57.9	1.38	0.12
64	07-08-08	6.2	3.3	53.0	1.51	0.14
65	09-08-08	19.9	9.8	49.4	1.44	0.05
66	14-08-08	0.3	0.3	98.8	5.91	0.54
67	16-08-08	4.5	3.1	70.5	2.85	0.27
68	17-08-08	0.4	0.3	74.1	7.86	0.47
69	21-08-08	8.0	4.6	57.7	2.18	0.20
70	22-08-08	15.5	7.9	50.8	0.80	0.19
71	23-08-08	36.5	21.3	58.4	0.85	0.14
72	24-08-08	2.2	1.3	59.3	6.62	0.20
73	25-08-08	9.3	5.9	63.5	3.78	0.19
74	28-08-08	0.5	0.5	86.5	3.77	0.29
75	02-09-08	2.5	1.4	58.2	5.17	0.19

[a] MAD: median absolute deviation.

[b] If the octile skew was > 0.2 we transformed the data (unless otherwise noted); transformations are indicated for all events used for spatial analysis (event 1-60): $^{sqr)}$ denotes to square root transformation, whereas $^{log)}$ indicates log_{10} transformation.

Table 4.A1 continued: Event characteristics and summary statistics for throughfall data (n=220).

Event	Date (dd-mm-yy)	Median (mm)	MAD[a] (mm)	MAD[a]/ Median ratio (%)	Skewness	Octile skew
76	03-09-08	1.3	0.9	69.2	1.18	0.33
77	06-09-08	1.1	0.8	68.4	1.09	0.20
78	12-09-08	8.6	3.9	45.9	1.30	0.15
79	13-09-08	8.8	3.9	44.5	2.43	0.02
80	18-09-08	24.3	11.8	48.5	0.94	0.05
81	20-09-08	1.1	0.8	74.1	1.88	0.33
82	24-09-08	13.4	6.8	50.7	2.43	0.07
83	25-09-08	22.1	9.8	44.5	2.81	0.06
84	26-09-08	0.9	0.7	74.1	1.93	0.32
85	28-09-08	0.4	0.5	103.8	6.03	0.26
86	30-09-08	0.4	0.5	129.7	2.50	0.24
87	02-10-08	10.7	5.9	55.1	3.28	0.07
88	06-10-08	0.4	0.3	74.1	5.25	0.28
89	09-10-08	11.1	4.6	41.5	2.10	0.10
90	19-10-08	1.0	0.7	67.4	2.06	0.32
91	20-10-08	1.8	1.3	74.1	2.06	0.21

[a] MAD: median absolute deviation.

Table 4.A2: Results of variogram analysis.

Event	Estimator[a]	Model[b]	Nugget/sill ratio (%)	Effective range[c] (m)	Median of $\theta(x)$
1	G	Nug	100.00	–	0.369
2	M	Nug	100.00	–	0.425
3	D	Gau	71.91	90.64	0.410
4	M	Nug	100.00	–	0.360
5	M	Exp	75.03	9.81	0.563
6	G	Nug	100.00	–	0.422
7	M	Exp	73.23	9.81	0.457
8	M	Nug	100.00	–	0.347
9	D	Nug	100.00	–	0.438
10	G	Nug	100.00	–	0.435
11	G	Nug	100.00	–	0.494
12	D	Nug	100.00	–	0.450
13	M	Exp	77.28	49.06	0.361
14	M	Nug	100.00	–	0.324

[a] Experimental variogram estimators proposed by Matheron (M), Cressie-Hawkins (CH), Dowd (D) and Genton (G)

[b] selected theoretical variogram model; Exp: exponential, Gau: Gaussian, Sph: spherical, Nug: nugget

[c] The effective range, R_{eff}, is calculated as: exponential model: R_{eff} = range*3, Gaussian model: R_{eff} = range*$3^{0.5}$, spherical model: R_{eff} = range

Table 4.A2 continued: Results of variogram analysis.

Event	Esti-mator[a]	Model[b]	Nugget/sill ratio (%)	Effective range[c] (m)	Median of $\theta(x)$
15	M	Nug	100.00	–	0.400
16	G	Nug	100.00	–	0.411
17	D	Nug	100.00	–	0.438
18	G	Nug	100.00	–	0.413
19	G	Nug	100.00	–	0.377
20	M	Nug	100.00	–	0.425
21	G	Nug	100.00	–	0.466
22	M	Nug	100.00	–	0.432
23	D	Nug	100.00	–	0.383
24	M	Nug	100.00	–	0.356
25	D	Nug	100.00	–	0.331
26	D	Nug	100.00	–	0.417
27	M	Nug	100.00	–	0.369
28	M	Nug	100.00	–	0.393
29	CH	Exp	80.92	39.25	0.431
30	D	Nug	100.00	–	0.438
31	D	Nug	100.00	–	0.373
32	CH	Nug	100.00	–	0.515
33	D	Sph	80.99	13.08	0.468
34	M	Nug	100.00	–	0.420
35	M	Nug	100.00	–	0.445
36	M	Nug	100.00	–	0.352
37	M	Nug	100.00	–	0.362
38	CH	Nug	100.00	–	0.451
39	M	Gau	79.80	33.99	0.345
40	G	Nug	100.00	–	0.436
41	CH	Nug	100.00	–	0.474
42	D	Exp	59.76	9.81	0.434
43	D	Nug	100.00	–	0.343
44	M	Nug	100.00	–	0.357
45	M	Nug	100.00	–	0.369
46	D	Nug	100.00	–	0.400
47	M	Nug	100.00	–	0.335
48	M	Nug	100.00	–	0.382
49	D	Gau	80.23	11.33	0.404
50	M	Nug	100.00	–	0.451

[a] Experimental variogram estimators proposed by Matheron (M), Cressie-Hawkins (CH), Dowd (D) and Genton (G)

[b] selected theoretical variogram model; Exp: exponential, Gau: Gaussian, Sph: spherical, Nug: nugget

[c] The effective range, R_{eff}, is calculated as: exponential model: $R_{eff} = range*3$, Gaussian model: $R_{eff} = range*3^{0.5}$, spherical model: $R_{eff} = range$

Table 4.A2 continued: Results of variogram analysis.

Event	Esti-mator[a]	Model[b]	Nugget/sill ratio (%)	Effective range[c] (m)	Median of $\theta(x)$
51	G	Nug	100.00	–	0.445
52	D	Nug	100.00	–	0.385
53	M	Nug	100.00	–	0.354
54	M	Nug	100.00	–	0.401
55	M	Nug	100.00	–	0.502
56	CH	Exp	57.47	19.62	0.586
57	D	Nug	100.00	–	0.380
58	D	Sph	76.76	9.81	0.403
59	G	Nug	100.00	–	0.427
60	M	Nug	100.00	–	0.415

[a] Experimental variogram estimators proposed by Matheron (M), Cressie-Hawkins (CH), Dowd (D) and Genton (G)

[b] selected theoretical variogram model; Exp: exponential, Gau: Gaussian, Sph: spherical, Nug: nugget

[c] The effective range, R_{eff}, is calculated as: exponential model: R_{eff} = range*3, Gaussian model: R_{eff} = range*$3^{0.5}$, spherical model: R_{eff} = range

Summary and conclusions

5.1 The variability of throughfall and its chemical composition

The redistribution of rainfall in forest canopies is highly variable in space. The tropical forests, which I studied in this thesis, displayed an even more pronounced variability of throughfall than what was found in temperate forest ecosystems. This result, however, may not solely reflect ecosystem-inherent characteristics. More likely, it also reflects different management practices [*Zimmermann et al.*, 2008a]. Natural forest ecosystems as the investigated tropical rainforests seem to experience a more complex pattern of throughfall spatial distribution than managed forests.

Tropical montane forests with their high epiphyte coverage and large, patchy, accumulations of canopy soils [*Bruijnzeel and Proctor*, 1995; *Nadkarni et al.*, 2004] seem to occupy the far end of this variability. In general, comparisons among several tropical forests revealed large differences in the variability of throughfall [*Zimmermann et al.*, 2008a]. These differences reflect distinct biotic and abiotic factors; furthermore, they mirror differences in sampling schemes. Among the biotic determinants are forest stand properties such as crown architecture types, spatial arrangement of trees, occurrence of gaps, and epiphyte coverage [*Crockford and Richardson*, 2000; *Levia and Frost*, 2006; *Zimmermann et al.*, 2007], whereas rainfall magnitude turns out to be the most influential abiotic factor [*Rodrigo and Ávila*, 2001; *Staelens et al.*, 2006b; *Zimmermann et al.*, submitted]. Many studies used the coefficient of variation (CV) as a simple measure of the spatial variability of throughfall, which usually decreases to a constant level with an increasing number of sampling occasions [*Holwerda et al.*, 2006]. Therefore, differences in both study durations and the numbers of sampled events hamper site comparisons.

The particularly high variability of small throughfall events results from relatively large throughfall values measured in open spots [*Zimmermann et al.*, submitted] that cause a skewed underlying distribution. In contrast, large throughfall events often display a low underlying skewness and a low spatial variability if robust measures (e.g. MAD/median ratio) are considered [*Zimmermann et al.*, submitted]. In large throughfall events, however, drip points can be responsible for a few large outliers that considerably distort the overall data distribution and inflate non-robust measures of variability such as the CV.

The variability of solute concentrations and solute deposition frequently exceeds the variability of throughfall volumes [e.g. *Staelens et al.*, 2006a; *Zimmermann et al.*, 2007, 2008a], but does not reveal clear differences between tropical and temperate forest ecosystems. In other words, biodiversity is not necessarily reflected in the heterogeneity of

solute deposition [*Zimmermann et al.*, 2008a]. This finding implies that other factors than structural properties of forests strongly influence solute deposition patterns. Some of these factors are, for instance, forest pests [*Lawrence and Fernandez*, 1993], retention of solutes in the canopy [*Seiler and Matzner*, 1995], solute concentration in rainfall, antecedent dry period, and duration of the study [*Zimmermann et al.*, 2008a].

5.2 Spatial patterns of throughfall

Throughfall in the investigated Panamanian tropical lowland rain forest displayed only weak or pure nugget autocorrelation structures over the studies lag distances [*Zimmermann et al.*, submitted]. That is to say, the large differences among several throughfall measurements evolve already at small spatial scales. Deciduousness of canopy trees does not influence these patterns, which may indicate that the structural properties of the understory have an overriding influence on these patterns.

The proper modeling of the autocorrelation structure by variogram analysis critically depends on a thorough exploratory data analysis as the shape of the frequency distribution strongly affects the suitability of available geostatistical tools. Whereas transformations are required to handle skewness in the underlying distribution [*Kerry and Oliver*, 2007a], robust variogram estimation offers a solution in cases where a few large outliers distort the overall data distribution [*Zimmermann et al.*, submitted].

Throughfall studies published so far that investigated autocorrelation structures exclusively used the classical, non-robust variogram estimator [*Loustau et al.*, 1992; *Bellot and Escarre*, 1998; *Möttönen et al.*, 1999; *Gómez et al.*, 2002; *Loescher et al.*, 2002; *Keim et al.*, 2005; *Staelens et al.*, 2006b; *Shachnovich et al.* 2008]. For datasets that contain large outliers but have a low underlying skewness, the application of the classical estimator frequently causes the overestimation of the sill variance and, in some cases, even induces spurious autocorrelation structures. Apart from this analytical problem, the sampling schemes of some investigations [e.g. *Loescher et al.*, 2002] do not match the spatial scale of the process in question. Some few sophisticated studies provide evidence that throughfall shows a high spatial variability over short distances [*Möttönen et al.*, 1999; *Keim et al.*, 2005]; hence, sampling schemes should account for this small-scale variability. The large variety of applied sampling procedures hampers inter-site comparisons; in particular, the low number of data used in some studies on throughfall spatial structure [e.g. *Loustau et al.*, 1992; *Bellot and Escarre*, 1998; *Shachnovich et al.* 2008] casts a doubt on the validity of their conclusions.

5.3 Temporal persistence of throughfall and its chemical composition

The studies in Ecuador, Brazil and Panama provide evidence that throughfall measurements show temporal persistence over several months. Results from Panama indicate that deciduousness does not influence the temporal persistence, and wet and dry locations outlast consecutive wet seasons. This finding may be of interest for ecological studies that investigate the influence of microhabitats on plants (e.g. seedling survival) and animals (e.g. arthropod distributions). In contrast, seasonal variation seems to influence the temporal stability of throughfall measurements at the Brazilian research site. These differences probably depend on growth patterns; particularly the growth dynamics of some palm species seem to be influential [*Germer et al.*, 2006].

The results from the study site in Panama show that variogram analysis may be a valuable tool to investigate temporal patterns of throughfall, particularly for long-term studies [*Zimmermann et al.*, submitted]. In spite of the immense size of the temporal dataset, extreme values continue to affect the non-robust variogram estimator; this obvious independence of sample size on the effect of outliers on the variogram corroborates findings from simulation studies [*Kerry and Oliver*, 2007b]. Therefore, large datasets require the same careful exploratory data analysis as do smaller ones.

Throughfall solute concentrations and solute deposition show a much lower temporal persistence than throughfall measurements [*Zimmermann et al.*, 2007, 2008a]. This relatively low persistence results from the multitude of factors that influence solute concentrations and deposition. For instance, the results from Brazil indicate that solute deposition can be influenced by antecedent rainfall, rainfall intensity, and solute concentrations in rainfall. All these factors display a high temporal variability, which accounts for the low temporal persistence of solute deposition. The low persistence of solute deposition is likely to homogenize soil chemical properties.

5.4 Suggestions for future research and research concepts

Since the description of throughfall and solute deposition patterns requires large datasets, many studies encounter logistical and financial constraints. It is unlikely that a single research initiative offers the opportunity to investigate throughfall and throughfall chemistry patterns in a variety of ecosystems. Therefore, we need standardized sampling scale triplets, which would ideally involve research plots of 1-ha and a sufficient number of collectors, particularly at small lag distances (in total probably more than 200 sampling locations). The relatively large plot size of 1-ha ensures the inclusion of many tree crowns which is particularly important at research sites with a large variability of crown architecture types.

The research would not have to be coordinated; the standardized sampling scale triplet alone would guarantee comparability and hence greatly advance the understanding of factors that influence spatial and temporal patterns of throughfall and its chemistry.

The next step is to link these patterns with near-surface processes in forest ecosystems. So far only few researchers investigated spatial patterns spanning several processes simultaneously [e.g. *Möttönen et al.*, 1999]. Future efforts could start with describing the link between throughfall and soil moisture by taking advantage of the relatively long-term stability of throughfall at many sites [e.g. *Raat et al.*, 2002; *Zimmermann et al.*, submitted]. A potential sampling protocol would involve sampling of throughfall for a period of 1-week, then a 1-week period with no sampling activity in which all samplers need to be removed, and finally a soil moisture measurement exactly at the locations of the antecedent throughfall collection. Another step further would be to measure the saturated hydraulic conductivity at these points, which would provide information if throughfall induces preferential flow at certain locations. Of course, these invasive measurements could be accompanied by soil sampling to measure, for instance, soil chemical properties and root densities. Such multi-component (throughfall, near surface and upper soil column) and multi-variable (e.g. throughfall magnitude, saturated hydraulic conductivity, root density, soil nutrient status) investigations could greatly enhance the understanding of near-surface processes in forest ecosystems and may provide some surprising and many interesting results.

References

Andreae, M.O., E.V. Browell, M. Garstang, G.L. Gregory, R.C. Harriss, G.F. Hill, D.J. Jacob, M.C. Pereira, G.W. Sachse, A.W. Setzer, P.L. Silva Dias, R.W. Talbot, A.L. Torres, and S.C. Wofsy (1988), Biomass-burning emissions and associated haze layers over Amazonia, *J. Geophys. Res.*, *93*, 1509–1527.

Andreae, M.O., D. Rosenfeld, P. Artaxo, A.A. Costa, G.P. Frank, K.M. Longo, and M.A.F. Silva-Dias (2004), Smoking rain clouds over the Amazon, *Science*, *303*, 1337–1342.

Andreae, M.O., R.W. Talbot, H. Berresheim, and K.M. Beecher 1990. Precipitation chemistry in central Amazonia, *J. Geophys. Res.*, *95*, 987–999.

Artaxo, P., J.V. Martins, M.A. Yamasoe, A.S. Procópio, T.M. Pauliquevis, M.O. Andreae, P. Guyon, L.V. Gatti, and A.M.C. Leal (2002), Physical and chemical properties of aerosols in the wet and dry seasons in Rondônia, Amazonia, *J. Geophys. Res.*, *107*, 8081, doi: 10.1029/2001JD000666.

Bach, C.S. (2002), Phenological patterns in monsoon rainforests in the Northern Territory, Australia, *Austral. Ecology*, *27*, 477–489.

Barthold, F.K., R.F. Stallard, and H. Elsenbeer (2008), Soil nutrient – landscape relationships in a lowland tropical rainforest in Panama, *For. Ecol. Manage.*, *255*, 1135–1148, doi: 10.1016/j.foreco.2007.09.089.

Beier, C., K. Hansen, and P. Gundersen (1993), Spatial variability of throughfall fluxes in a spruce forest, *Environ. Pollut.*, *81*, 257–267.

Bellot, J., and A. Escarre (1998), Stemflow and throughfall determination in a resprouted Mediterranean holm-oak forest, Ann. Sci. For., *55*, 847–865.

Bland, J.M., and S.M. Kerry (1998), Weighted comparisons of means, *Br. Med. J.*, *316*, 129.

Blöschl, G. (1999), Scaling issues in snow hydrology, *Hydrol. Process.*, *13*, 2149–2175.

Blöschl, G., and M. Sivapalan (1995), Scale issues in hydrological modelling – A review, *Hydrol. Process.*, 9, 251–290.

Bouten, W., T.J. Heimovaara, and A. Tiktak (1992), Spatial patterns of throughfall and soil water dynamics in a Douglas fir stand, *Water Resour. Res.*, *28*, 3227–3233.

Bruijnzeel, L.A. (1991), Nutrient input-output budgets of tropical forest ecosystems: A review, *J. Trop. Ecol.*, *7*, 1–24.

Bruijnzeel, L.A., and L.S. Hamilton (2000), *Decision Time for Cloud Forests*, IHP Humid Tropics Program Series, 13, IHP-UNESCO, Paris.

Bruijnzeel, L.A., and J. Proctor (1995), Hydrology and biogeochemistry of tropical montane

cloud forests: what do we really know?, in *Tropical Montane Cloud Forests*, edited by L.S. Hamilton, J.O. Juvik, and F.N. Scatena, pp. 38–78, Ecological Studies, Springer-Verlag, New York.

Brys, G., M. Hubert, and A. Struyf (2003), A comparison of some new measures of skewness, in *Developments in Robust Statistics*, edited by R. Dutter, P. Filzmoser, U. Gather, and P.J. Rousseeuw, pp. 98–113, Physica-Verlag Heidelberg, Germany.

Carlyle-Moses, D.E., J.S.F Laureano, A.G. Price (2004), Throughfall and throughfall spatial variability in Madrean oak forest communities of northeastern Mexico, *J. Hydrol.*, *297*, 124–135, doi: 10.1016/j.jhydrol.2004.04.007.

Carnol, M., and P. Ineson (1999), Environmental factors controlling NO_3^- leaching, N_2O emissions and numbers of NH_4^+ oxidisers in a coniferous forest soil, *Soil Biol. Biochem.*, *31*, 979–990.

Cavelier, J., M. Jaramillo, D. Solis, and D. de León (1997), Water balance and nutrient inputs in bulk precipitation in tropical montane cloud forest in Panama, *J. Hydrol.*, *193*, 83–96.

Clark, K.L., N.M. Nadkarni, D. Schaefer, and H.L. Gholz (1998), Atmospheric deposition and net retention of ions by the canopy in a tropical montane forest, *J. Trop. Ecol.*, *14*, 27–45.

Coley, P.D., and J.A. Barone (1996), Herbivory and plant defenses in tropical forests, *Annu. Rev. Ecol. Syst.*, *27*, 305–335.

Cressie, N., and D. Hawkins (1980), Robust estimation of the variogram, *Math. Geol.*, *12*, 115–125.

Croat, T.B. (1978), *Flora of Barro Colorado Island*, 943 pp., Stanford Univ. Press, Stanford, California, USA.

Crockford, R.H., and D.P. Richardson (2000), Partitioning of rainfall into throughfall, stemflow and interception: effect of forest type, ground cover and climate, *Hydrol. Process.*, *14*, 2903–2920.

Crockford, R.H., D.P. Richardson, and R. Sageman (1996), Chemistry of rainfall, throughfall and stemflow in a eucalypt forest and a pine plantation in south-eastern Australia: 2. Throughfall, *Hydrol. Process.*, *10*, 13–24.

Cronan, C.S. (1980), Solution chemistry of a New Hampshire subalpine ecosystem: a biogeochemical analysis, *Oikos*, *34*, 272–281.

de Gruijter, J.J., D.J. Brus, M.F.P. Bierkens, and M. Knotters (2006), Sampling for Natural Resource Monitoring, 332 pp., Springer, Berlin, Heidelberg.

Dietrich, W.E., D.M. Windsor, and T. Dunne (1982), Geology, Climate, and Hydrology of

Barro Colorado Island, in *The Ecology of a Tropical Forest: Seasonal Rhythms and Long Term Changes*, edited by E.G. Leigh et al., pp. 21–46, Smithsonian Institution, Washington DC.

Dingman, S.L. (1994), *Physical Hydrology*, Prentice-Hall Inc., Upper Saddle River, NY.

Dowd, P.A. (1984), The variogram and kriging: robust and resistant estimators, in *Geostatistics for Natural Resources Characterization*, edited by G. Verly et al., pp. 91–106, D. Reidel, Dordrecht.

Duijsings, J.J.H.M., J.M. Verstraten, and W. Bouten (1986), Spatial variability in nutrient deposition under an oak/beech canopy, *Z. Pflanzenernähr. Bodenk.*, *149*, 718–727.

Efron, B., and R.J. Tibshirani (1993), *An Introduction to the Bootstrap*, Chapman & Hall, San Francisco.

Elsenbeer, H., D. Lorieri, and M. Bonell, Mixing model approaches to estimate storm flow sources in an overland flow-dominated tropical rain forest catchment, *Water Resour. Res.*, *31*, 2267–2278.

Engelbrecht, B.M.J., and T.A. Kursar (2003), Comparative drought-resistance of seedlings of 28 species of co-occurring tropical woody plants, *Oecologia, 136*, 383–393.

Filoso, S., M.R. Williams, and J.M. Melack (1999), Composition and deposition of throughfall in a flooded forest archipelago, *Biogeochemistry, 45*, 169–195.

Fleischbein, K., W. Wilcke, R. Goller, J. Boy, C. Valarezo, W. Zech, and K. Knoblich (2005), Rainfall interception in a lower montane forest in Ecuador: effects of canopy properties, *Hydrol. Process., 19*, 1355–1371, doi: 10.1002/hyp.5562.

Fleischbein, K, W. Wilcke, C. Valarezo, W. Zech, and K. Knoblich (2006), Water budgets of three small catchments under montane forest in Ecuador: experimental and modelling approach, *Hydrol. Process., 20*, 2491–2507.

Ford, E.D., and J.D. Deans (1978), The effects of canopy structure on stemflow, throughfall and interception loss in a young Sitka spruce plantation, *J. Appl. Ecol., 15*, 905–917.

Forti, M.C., and L.M. Moreira-Nordemann (1991), Rainwater and throughfall chemistry in a "terra firme" rain forest: Central Amazonia, *J. Geophys. Res., 96*, 7415–7421.

Forti, M.C., and C. Neal (1992a), Spatial variability of throughfall chemistry in a tropical rainforest (Central Amazonia, Brazil), *Sci. Total Environ., 120*, 245–259.

Forti, M.C., and C. Neal (1992b), Hydrochemical cycles in tropical rainforests: an overview with emphasis on Central Amazonia, *J. Hydrol.*, 134, 103–115.

Foster, R.B., and N.V.L. Brokaw (1982), Structure and History of the Vegetation of Barro Colorado Island, in *The Ecology of a Tropical Forest: Seasonal Rhythms and Long Term Changes*, edited by E.G. Leigh et al., pp. 67–81, Smithsonian Institution, Washington DC.

References

Frazer, G.W., C.D. Canham, and K.P. Lertzman (1999), Gap Light Analyzer (GLA), Version 2.0: Imaging software to extract canopy structure and gap light transmission indices from true-color fisheye photographs, Simon Frazer University, BC, Canada, and the Institute of Ecosystem Studies, Millbrook, New York, USA.

Gash, J.H.C. (1979). An analytical model of rainfall interception by forests, *Quart. J. R. Met. Soc.*, *105*, 43–55.

Genton, M.G. (1998), Highly robust variogram estimation, *Math. Geol.*, *30*, 213–221.

Germer, S., H. Elsenbeer, and J.M. Moraes (2006), Throughfall and temporal trends of rainfall redistribution in an open tropical rainforest, south-western Amazonia (Rondônia, Brazil), *Hydrol. Earth Syst. Sc.*, *10*, 383–393.

Germer, S., C. Neall, A.V. Krusche, S.C. Gouveia, H. Elsenbeer (2007), Seasonal and within-event dynamics of rainfall and throughfall chemistry in an open tropical rainforest in Rondonia, Brazil, *Biogeochemistry*, *86*, 155–174, doi: 10.1007/s10533-007-9152-9.

Gómez, J.A., K. Vanderlinden, J.V. Giráldez, and E. Fereres (2002), Rainfall concentration under olive trees, *Agric. Water Manag.*, 55, 53–70.

Guevara-Escobar, A., E. González-Sosa, C. Véliz-Chávez, E. Ventura-Ramos, and M. Ramos-Salinas (2007), Rainfall interception and distribution patterns of gross precipitation around an isolated *Ficus benjamina* tree in an urban area.

Guyon, P., B. Graham, G.C. Roberts, O.L. Mayol-Bracero, W. Maenhaut, P. Artaxo, and M.O. Andreae (2003), In-canopy gradients, composition, sources, and optical properties of aerosol over the Amazon forest, *J. Geophys. Res.*, *108*, 4591, doi: 10.1029/2003JD003465.

Hafkenscheid, R. (2000), *Hydrology and Biogeochemistry of Tropical Montane Rain Forests of Contrasting Stature in the Blue Mountains, Jamaica*, Ph.D. thesis, Free University of Amsterdam.

Hambuckers, A., and J. Remacle (1993), Relative importance of factors controlling the leaching and uptake of inorganic ions in the canopy of a spruce forest, *Biogeochemistry*, *23*, 99–117.

Hampel, F.R. (1971), General qualitative definition of robustness, *Ann. Math. Statist.*, *42*, 1887–1896.

Hampel, F.R., E.M. Ronchetti, Rousseuw, P.J., and W.A. Stahel (1986), *Robust Statistics: the Approach Based on Influence Functions*, 502 pp., John Wiley & Sons, New York.

Hansen, K., G.P.J. Draaijers, W.P.M.F. Ivens, P. Gundersen, and N.F.M. Leeuwen (1994), Concentration variation in rain and canopy throughfall collected sequentially during individual rain events. *Atmos. Environ.*, *28*, 3195–3205.

Harms, K.E., J.S. Powers, and R.A. Montgomery (2004), Variation in small sapling density,

understory cover, and resource availability in four neotropical forests, *Biotropica*, *36*, 40–51.

Helvey, J.D., and J.H. Patric (1965), Canopy and litter interception of rainfall by hardwoods of Eastern United States, *Water Resour. Res.*, *1*, 193–206.

Henderson, A., S.P. Churchill, and J.L. Luteyn (1991), Neotropical plant diversity, Nature, 351, 21–22.

Hölscher, D., T.D.A. Sá, R.F. Möller, M. Denich, and H. Fölster (1998), Rainfall partitioning and related hydrochemical fluxes in a diverse and in a mono specific (*Phenakospermum guyannense*) secondary vegetation stand in eastern Amazonia, *Oecologia*, *114*, 251–257.

Holwerda, F., F.N. Scatena, and L.A. Bruijnzeel (2006), Throughfall in a Puerto Rican lower montane rain forest: A comparison of sampling strategies, *J. Hydrol.*, *327*, 592–602.

Homeier, J. (2004), *Baumdiversität, Waldstruktur und Wachstumsdynamik Zweier Tropischer Bergregenwälder in Ecuador und Costa Rica*, Dissertationes Botanicae, *391*, University of Bielefeld, Germany

Insightful Corporation (2001a), S-Plus 6 for Windows Guide to Statistics, Volume 1, Insightful Corporation, Seattle, Washington

Insightful Corporation (2001b), S-Plus 6 for Windows Guide to Statistics, Volume 2, Insightful Corporation, Seattle, Washington

Jackson, I.J. (1971), Problems of throughfall and interception assessment under tropical forest, *J. Hydrol.*, *12*, 234–254.

Jansen, P.A., S.A. Bohlman, C.X. Garzon-Lopez, H. Olff, H.C. Muller-Landau, and J.S. Wright (2008), Large-scale spatial variation in palm fruit abundance across a tropical moist forest estimated from high-resolution areal photographs, *Ecography*, *31*, 33–42, doi: 10.1111/j.2007.0906-7590.05151.x

Johansson, D. (1974), Ecology of vascular epiphytes in West African rain forest, *Acta Phytographica Suecica*, *59*, 1–129.

John, R., J.W. Dalling, K.E. Harms, Y.B. Yavitt, R.F. Stallard, M. Mirabello, S.P. Hubbell, R. Valencia, H. Navarrete, M. Vallejo, and R.B. Foster (2007), Soil nutrients influence spatial distributions of tropical tree species, *Proc. Natl. Acad. Sci.*, *104*, 864–869, doi: 10.1073/pnas0604666104.

Jonckheere, I., K. Nackaerts, B. Muys, and P. Coppin (2005), Assessment of automatic gap fraction estimation of forests from digital hemispherical photography, *Agr. Forest Meteorol.*, *132*, 96–114, doi:10.1016/j.agrformet.2005.06.003

Jordan, C., F. Golley, J. Hall, and J. Hall (1980) Nutrient scavenging of rainfall by the canopy of an Amazonian rain forest, *Biotropica*, *12*, 61–66.

Kaspari, M., and M.D. Weiser (2000), Ant activity along moisture gradients in a neotropical

forest, *Biotropica*, *32*, 703–711.

Keim, R.F., A.E. Skaugset, and M. Weiler (2005), Temporal persistence of spatial patterns in throughfall, *J. Hydrol.*, *314*, 263–274, doi: 10.1016/j.jhydrol.2005.03.021.

Kerry, R., and M.A. Oliver (2007a), Determining the effect of asymmetric data on the variogram. I. Underlying asymmetry, *Comp. & Geosci.*, 33, 1212–1232, doi: 10.1016/j.cageo.2007.05.008.

Kerry, R., and M.A. Oliver (2007b), Determining the effect of asymmetric data on the variogram. II. Outliers, *Comp. & Geosci.*, 33, 1233–1260, doi: 10.1016/j.cageo.2007.05.009.

Kimmins, J.P. (1973), Some statistical aspects of sampling throughfall precipitation in nutrient cycling studies in British Columbian coastal forests, *Ecology*, *54*, 1008– 1019.

Köhler, L., C. Tobón, K.F.A. Frumau, and L.A. (Sampurno) Bruijnzeel (2007), Biomass and water storage dynamics of epiphytes in old-growth and secondary montane cloud forest stands in Costa Rica, *Plant Ecol.*, *193*, doi: 10.1007/s11258-006-9256-7.

Kostelnik, K.M., J.A. Lynch, J.W. Grimm, and E.S. Corbett (1989), Sample size requirements for estimation of throughfall chemistry beneath a mixed hardwood forest, *J. Environ. Qual.*, *18*, 274–280.

Laclau, J.P., J. Ranger, J.P. Bouillet, J.D. Nzila, and P. Deleporte (2003), Nutrient cycling in a clonal stand of Eucalyptus and an adjacent savanna ecosystem in Congo - 1. Chemical composition of rainfall, throughfall and stemflow solutions, *For. Ecol. Manage.*, *176*, 105–119.

Langusch, J-J., W. Borken, M. Armbruster, N.B. Dise, and E. Matzner (2003), Canopy leaching of cations in Central European forest ecosystems - a regional assessment, *J. Plant Nutr. Soil Sci.*, *166*, 168–174.

Lark, R.M. (2000), A comparison of some robust estimators of the variogram for use in soil survey, *Europ. J. Soil Sci.*, *51*, 137–157.

Lark, R.M. (2002), Modelling complex soil properties as contaminated regionalized variables, *Geoderma*, *106*, 173–190.

Lawrence, G.B., and I.J. Fernandez (1993), A reassessment of areal variability of throughfall deposition measurements, *Ecol. Appl.*, *3*, 473–480.

Leigh, E.G. (1999), *Tropical Forest Ecology. A View From Barro Colorado Island*, pp. 149– 178, Oxford University Press, New York, Oxford.

Levia, D.F., and E.E. Frost (2003), A review and evaluation of stemflow literature in the hydrological and biogeochemical cycles of forested and agricultural ecosystems, *J. Hydrol.*, *274*, 1–29.

Levia, D.F., and E.E. Frost (2006), Variability of throughfall volume and solute inputs in wooded ecosystems, *Prog. Phys. Geog.*, *30*, 605–632, 10.1177/0309133306071145.

Levings, S.C., and D.M. Windsor (1984), Litter moisture content as a determinant of litter arthropod distribution and abundance during the dry season on Barro Colorado Island, Panama, *Biotropica, 16*, 125–131.

Levings, S.C., and D.M. Windsor (1996), Seasonal and Annual Variation in Litter Arthropod Populations. in *The Ecology of a Tropical Forest: Seasonal Rhythms and Long-term Changes*, edited by Leigh, E.G. et al., pp. 355–388, Smithsonian Institution Press, Washington, DC.

Lin, T-C., S.P. Hamburg, H-B. King, and Y-J. Hsia (1997), Spatial variability of throughfall in a subtropical rain forest in Taiwan, *J. Environ. Qual., 26*, 172–180.

Liu, W., J.E.D. Fox, and Z. Xu, (2002), Nutrient fluxes in bulk precipitation, throughfall and stemflow in montane subtropical moist forest on Ailao Mountains in Yunnan, south-west China, *J. Trop. Ecol., 18*, 527–548.

Lloyd, C.R., and A.O. Marques (1988), Spatial variability of throughfall and stemflow measurements in Amazonian rainforest, *Agr. Forest Meteorol., 42*, 63–73.

Loescher, H.W., J.S. Powers, and S.F. Oberbauer (2002), Spatial variation of throughfall volume in an old-growth tropical wet forest, Costa Rica, *J. Trop. Ecol., 18*, 397–407, doi: 10.1017/S0266467402002274.

Loustau, D., P. Berbigier, A. Granier, and F.E.H. Moussa (1992), Interception loss, throughfall and stemflow in a maritime pine stand. I. Variability of throughfall and stemflow beneath the pine canopy, *J. Hydrol., 138*, 449–467.

Lovett, G.M., and D.A. Schaefer (1992), Canopy interactions of Ca^{2+}, Mg^{2+} and K^+., in *Atmospheric Deposition and Forest Nutrient Cycling*, edited by Johnson, D.W., and S.E. Lindberg, pp. 253–275, Ecological Studies, 91, Springer Verlag, New York.

Lovett, G.M., A.W. Thompson, J.B. Anderson, and J.J. Bowser (1999), Elevational patterns of sulfur deposition at a site in the Catskill Mountains, New York, *Atmos. Environ., 33*, 617–624.

Lu, D. (2005), Integration of vegetation inventory data and Landsat TM image for vegetation classification in the western Brazilian Amazon, *For. Ecol. Manage., 213*, 369–383, doi: 10.1016/j.foreco.2005.04.004.

Maenhaut, W., G. Koppen, and P. Artaxo, (1996), Long-term Atmospheric Aerosol Study in Cuiabá, Brazil: Multielemental Composition, Sources, and Impact of Biomass Burning, in *Biomass Burning and Global Change*, edited by Levine, J.S., pp. 637–652, Massachusetts Institute of Technology, Cambridge.

Manderscheid, B, and E. Matzner (1995), Spatial and temporal variation of soil solution chemistry and ion fluxes through the soil in a mature Norway spruce (*Picea abies* (L.) Karst.) stand, *Biogeochemistry, 30*, 99–114.

Matheron, G. (1962), *Traité de Géostatistique Appliqué*, Tome 1. Memoires du Bureau de Recherches Géologiques et Minières, Paris.

McBratney, A.B., and R. Webster (1986), Choosing functions for semi-variograms of soil properties and fitting them to sampling estimates, *Journal of Soil Science*, *37*, 617–639.

Mohanty, B.P., R.S. Kanwar, and R. Horton (1991), A robust-resistant approach to interpret spatial-behavior of saturated hydraulic conductivity of a glacial till soil under no-tillage system, *Water Resour. Res.*, *27*, 2979–2992.

Möttönen, M., E. Järvinen, T.J. Hokkanen, T. Kuuluvainen, and R. Ohtonen (1999), Spatial distribution of soil ergosterol in the organic layer of a mature Scots pine (*Pinus sylvestris* L.) forest, *Soil Biol. Biochem.*, *31*, 503–516, doi: 10.1016/S0038-0717(98)00122-9.

Myers, N., R.A. Mittermeier, C.G. Mittermeier, G.A.B. da Fonseca, and J. Kent (2000), Biodiversity hotspots for conservation priorities, *Nature*, *403*, 853–858.

Nadkarni, N.M. (1986), The nutritional effects of epiphytes on host trees with special reference to alteration of precipitation chemistry, *Selbyana*, *9*, 44–51.

Nadkarni, N.M., D. Schaefer, T.J. Matelson, and R. Solano (2004), Biomass and nutrient pools of canopy and terrestrial components in a primary and secondary montane cloud forest, Costa Rica, *Forest Ecol. Manage.*, *198*, 223–236.

Neary, A.J., and W.I. Gizyn (1994), Throughfall and stemflow chemistry under deciduous and coniferous forest canopies in south-central Ontario, *Can. J. Forest Res.*, *24*, 1089–1100.

Nye, P.H. (1961), Organic matter and nutrient cycles under moist tropical forest, *Plant Soil*, *13*, 333–346.

Parker, G.G. (1983), Throughfall and stemflow in the forest nutrient cycle, *Adv. Ecol. Res.*, *13*, 53–133.

Paulsch, A. (2002), *Development and application of a classification system for undisturbed and disturbed tropical montane forests based on vegetation structure*, Ph.D. thesis, University of Bayreuth, Germany.

Pebesma, E.J. (2004), Multivariable geostatistics in S: the gstat package. *Comp. & Geosci.*, *30*, 683–691.

Pedersen, L.B. (1992), Throughfall chemistry of Sitka spruce stands as influenced by tree spacing, *Scand. J. Forest Res.*, *7*, 433–444.

Pires, J.M., Prance, G.T., 1986. The Vegetation Types of the Brazilian Amazon, in *Key Environments: Amazônia*, edited by Prance, G.T., and T.M. Lovejoy, pp 109–129, Pergamon, Oxford.

Puckett, L.J. (1991), Spatial variability and collector requirements for sampling throughfall

volume and chemistry under a mixed hardwood canopy, *Can. J. For. Res.*, *21*, 1581–1588.

Raat, K.J., G.P.J. Draaijers, M.G. Schaap, A. Tietema, and J.M. Verstraten (2002), Spatial variability of throughfall water and chemistry and forest floor water content in a Douglas fir forest stand, *Hydrol. Earth Syst. Sc.*, *6*, 363–374.

Rawlins, B.G., R.M. Lark, K.E. O'Donnell, A.M. Tye, and T.R. Lister (2005), The assessment of point and diffuse metal pollution of soils from an urban geochemical survey of Sheffield, England, *Soil Use and Management*, *21*, 353–362.

R Development Core Team (2004), R: A language and environment for statistical computing. R Foundation for Statistical Computing, Vienna, Austria.

R Development Core Team (2007), R: A language and environment for statistical computing, R Foundation for Statistical Computing, Vienna, Austria. URL http://www.R-project.org.

Ribeiro, P.J., and P.J. Diggle (2001), GeoR: a package for geostatistical analysis. R-NEWS Vol 1, No 2. (URL: http://cran.r-project.org/doc/Rnews)

Robson, A.J., C. Neal, G.P. Ryland, and M. Harrow (1994), Spatial variations in throughfall chemistry at the small plot scale, *J. Hydrol.*, *158*, 107–122.

Rodrigo, A., and A. Ávila (2001), Influence of sampling size in the estimation of mean throughfall in two Mediterranean holm oak forests, *J. Hydrol.*, *243*, 216–227.

Rollenbeck, R., J. Bendix, P. Fabian, J. Boy, H. Dalitz, P. Emck, M. Oesker, and W. Wilcke (2007), Comparison of different techniques for the measurement of precipitation in tropical montane rain forest regions, *J. Atmos. Ocean. Tech.*, *24*, 156-168.

Rousseeuw, P.J., and C. Croux (1993), Alternatives to the median absolute deviation, *J. Am. Stat. Assoc.*, *88*, 1273–1283.

Russo, D., and W.A. Jury (1987), A theoretical study of the estimation of the correlation scale in spatially variable fields. 1. Stationary fields. *Water Resour. Res.*, *23*, 1257–1268.

Scatena, F.N. (1990), Watershed scale rainfall interception on two forested watersheds in the Luquillo mountains of Puerto Rico, *J. Hydrol.*, *113*, 89–102.

Schellekens, J., F.N. Scatena, L.A. Bruijnzeel, A.J. Wickel (1999), Modelling rainfall interception by a lowland tropical rain forest in northeastern Puerto Rico, *J. Hydrol.*, *225*, 168–184.

Schume, H., G. Jost, and K. Katzensteiner (2003), Spatio-temporal analysis of the soil water content in a mixed Norway spruce (*Picea abies* (L.) Karst.) – European beech (*Fagus sylvatica* L.) stand, *Geoderma*, *112*, 273–287.

Seiler, J., and E. Matzner (1995), Spatial variability of throughfall chemistry and selected soil properties as influenced by stem distance in a mature Norway spruce (*Picea-abies*, Karst) stand, *Plant Soil*, *176*, 139–147.

Shachnovich, Y., P.R. Berliner, and P. Bar (2008), Rainfall interception and spatial distribution of throughfall in a pine forest planted in an arid zone, *J. Hydrol.*, *349*, 168–177, doi: 10.1016/j.jhydrol.2007.10.051.

Shapiro, S.S., and M.B. Wilk (1965), An analysis of variance test for normality (complete samples). *Biometrika*, *52*, 591–611.

Shouse, P.J., T.J. Gerik, W.B. Russell, and D.K. Cassel (1990), Spatial distribution of soil particle size and aggregate stability in a clay soil, *Soil Science*, 149, 351–360.

Skøien, J. O., and G. Blöschl (2006), Scale effects in estimating the variogram and implications for soil hydrology, *Vadose Zone J.*, *5*, 153–167.

Sobieraj, J.A., H. Elsenbeer, and G. Cameron (2004), Scale dependency in spatial patterns of saturated hydraulic conductivity, *Catena*, *55*, 49–77, doi: 10.1016/S0341-8162(03)00090-0.

Soil Survey Staff (2003), *Keys to Soil Taxonomy*, US Government Printing Office, Washington, DC.

Staelens, J., A.D. Schrijver, and K. Verheyen (2007), Seasonal variation in throughfall and stemflow chemistry beneath a European beech (Fagus sylvatica) tree in relation to canopy phenology, *Can. J. For. Res.*, *37*, 1359–1372, doi: 10.1139/XO7-003.

Staelens, J., A.D. Schrijver, K. Verheyen, and N.E.C. Verhoest (2006a), Spatial variability and temporal stability of throughfall deposition under beech (*Fagus sylvatica* L.) in relation to canopy structure, *Environ. Pollut.*, 142, 254–263, doi: 10.1016/j.envpol.2005.10.002.

Staelens, J., A.D. Schrijver, K. Verheyen, and N.E.C. Verhoest (2006b), Spatial variability and temporal stability of throughfall water under a dominant beech (*Fagus sylvatica* L.) tree in relationship to canopy cover, *J. Hydrol.*, *330*, 651–662, doi: 10.1016/j.jhydrol.2006.04.032.

Stallard, R.F., and J.M. Edmond (1981), Geochemistry of the Amazon. 1. Precipitation chemistry and the marine contribution to the dissolved load at the time of peak discharge, *J. Geophys. Res.*, *86*, 9844–9858.

Steinhardt, U. (1979), Untersuchungen über den Wasser- und Nährstoffhaushalt eines andinen Wolkenwaldes in Venezuela, *Göttinger Bodenkundliche Berichte*, *56*, 1–185.

Stout, B.B., and R.J. McMahon (1961), Throughfall variation under tree crowns, *J. Geophys. Res.*, *66*, 1839–1843.

Thimonier, A. (1998), Measurement of atmospheric deposition under forest canopies: some recommendations for equipment and sampling design, *Environ. Monitor. Assess.*, *52*, 353–387.

Thorington, R.W., B. Tannenbaum, A. Tarak, and R. Rudran (1982), Distribution of Trees on

Barro Colorado Island: A Five-Hectare Sample, in *The Ecology of a Tropical Forest: Seasonal Rhythms and Long Term Changes*, edited by E.G. Leigh et al., pp. 83–94, Smithsonian Institution, Washington DC.

Tobón, C., J. Sevink, and J.M. Verstraten (2004), Solute fluxes in throughfall and stemflow in four forest ecosystems in northwest Amazonia, *Biogeochemistry*, *70*, 1–25.

Tukey Jr., H.B. (1970), The leaching of substances from plants, *Annu. Rev. Plant Physiol*, *31*, 305–324.

Vachaud, G., A.P.D. Silans, P. Balabanis, and M. Vauclin (1985), Temporal stability of spatially measured soil water probability density function, *Soil Sci. Soc. Am. J.*, *49*, 822–828.

van Schaik, C.P., J.W. Terborgh, and S.J. Wright (1993), The phenology of tropical forests: Adaptive significance and consequences for primary consumers, *Annu. Rev. Ecol. Syst.*, *24*, 353–377.

Venables, W.N., and B.D. Ripley (2002), *Modern applied statistics with S*, 4th ed., Springer

Veneklaas, E.J. (1990), Nutrient fluxes in bulk precipitation and throughfall in two montane tropical rainforests, Columbia, *Journal of Ecology*, *78*, 974–992.

Veneklaas, E.J., and R. Van Ek (1990), Rainfall interception in two tropical montane rain forests, Columbia., *Hydrol. Process.*, *4*, 311–326.

Vernimmen, R.R.E., L.A. Bruijnzeel, A. Romdoni, and J. Proctor (2007), Rainfall interception in three contrasting lowland rain forest types in Central Kalimantan, Indonesia, *J. Hydrol.*, *340*, 217–232, doi: 10.1016/j.jhydrol.2007.04.009.

Webster, R., and M.A. Oliver (2001), *Geostatistics for Environmental Scientists*, John Wiley & Sons, Chichester, UK.

Whelan, M.J., L.J. Sanger, M. Baker, and J.M. Anderson (1998), Spatial patterns of throughfall and mineral ion deposition in a lowland Norway spruce (*Picea abies*) plantation at the plot scale, *Atmos. Environ.*, *32*, 3493–3501.

Wilcke, W., S. Yasin, C. Valarezo, and W. Zech (2001), Change in water quality during the passage through a tropical montane rain forest in Ecuador, *Biogeochemistry*, *55*, 45–72.

Wilcke, W., S. Yasin, U. Abramowski, C. Valarezo, and W Zech (2002), Nutrient storage and turnover in organic layers under tropical montane rain forest in Ecuador, *Eur. J. Soil Sci.*, *53*, 15-27.

Woodbury, A.D., and E.A. Sudicky (1991), The geostatistical characteristics of the Borden aquifer. *Water Resour. Res.*, *27*, 533–546.

Wright, S.J. (1991), Seasonal drought and the phenology of understory shrubs in a tropical moist forest, *Ecology*, *72*, 1643–1657.

Zeng, G.M., G. Zhang, G.H. Huang, J.M. Jiang, and H.L. Liu (2005), Exchange of Ca^{2+}, Mg^{2+}

and K$^+$ and uptake of H$^+$, NH$_4^+$ for the subtropical forest canopies influenced by acid rain in Shaoshan forest located in Central South China, *Plant Science*, *168*, 259–266.

Zimmermann, B., H. Elsenbeer, and J.M. De Moraes (2006), The influence of land-use changes on soil hydraulic properties: Implications for runoff generation, *For. Ecol. Manage.*, *222*, 29–38, doi: 10.1016/j.foreco.2005.10.070.

Zimmermann, A., S. Germer, C. Neill, A.V. Krusche, and H. Elsenbeer (2008a), Spatio – temporal patterns of throughfall and solute deposition in an open tropical rain forest, *J. Hydrol.*, *360*, 87–102, doi: 10.16/j.jhydrol.2008.07.028.

Zimmermann, A., W. Wilcke, and H. Elsenbeer (2007), Spatial and temporal patterns of throughfall quantity and quality in a tropical montane forest in Ecuador, *J. Hydrol.*, 343, 80–96, doi: 10.1016/j.jhydrol.2007.06.012.

Zimmermann, B., E. Zehe, N.K. Hartmann, and H. Elsenbeer (2008b), Geostatistical analysis of soil hydraulic data – a discussion on assumptions, new methods and uncertainties, *Water Resour. Res.*, 44, W10408, doi: 10.1029/2007WR006604.

Zimmermann, A., Zimmermann, B., and H. Elsenbeer (submitted), Rainfall redistribution in a tropical forest: spatial and temporal patterns.

Zirlewagen, D., and K. von Wilpert (2001), Modeling water and ion fluxes in a highly structured, mixed species stand, *Forest Ecol. Manage.*, *143*, 27–37.

Zotz, G., and V. Thomas (1999), How much water is in the tank? Model calculations for two epiphytic bromeliads, *Annals of Botany*, *83*, 183–192.

CURRICULUM VITAE

Alexander Zimmermann

PERSONAL DETAILS

Profession	Geoecologist
Address	Hauptstrasse 5, 14476 Potsdam OT Marquardt, Germany
Phone	+49-(0)331-977-2047 (work, Potsdam, Germany)
	+507-67192130 (field site, Gamboa, Panama)
Email	zimmermann.alex@yahoo.de
Date and place of birth	08/11/1978 in Dresden, Germany
Nationality	German

EDUCATION

Since 03/2006	Ph.D. program in Geoecology, University of Potsdam, Germany
1999 – 2006	Diploma program in Geoecology, University of Potsdam, Germany
1992 – 1997	High school, Dresden, Germany

VOLUNTEER EXPERIENCE

09/1997 – 09/1998	UNESCO Biosphere Reserve "Oberlausitzer Heide- und Teich-landschaft", Germany (Civilian service).
01/1999 – 09/1999	Geo-engineering Company, IFB Eigenschenk & Partner, Dresden.
03/2002 – 04/2002	Forest Restoration Project, New Zealand Department of Conservation, Waitakere City, New Zealand

PROFESSIONAL EXPERIENCE

Since 05/2007	Research assistant, Institute of Geoecology, University of Potsdam

PUBLICATIONS

Zimmermann, B., Zimmermann, A., Lark, R.M., Elsenbeer, H. submitted. Sampling procedures for throughfall monitoring: A simulation study.

Zimmermann, A., Zimmermann, B., Elsenbeer, H. submitted. Rainfall redistribution in a tropical forest: spatial and temporal patterns.

Zimmermann, A., Germer, S., Neill, C., Krusche, A., Elsenbeer, H. 2008. Spatio–temporal patterns of throughfall and solute deposition in an open tropical rain forest, Journal of Hydrology. 360: 87–102. doi: 10.1016/j.jhydrol.2008.07.028.

Zimmermann, A., Wilcke, W., Elsenbeer, H. 2007. Spatial and temporal patterns of throughfall quantity and quality in a tropical montane forest in Ecuador, Journal of Hydrology. 343: 80–96. doi: 10.1016/j.jhydrol.2007.06.012.

CONFERENCE PRESENTATIONS

Zimmermann, A., Zimmermann, B., Elsenbeer, H. 2008. Rainfall Redistribution in a Tropical Forest: Spatial Patterns and Temporal Persistence, EOS Trans. AGU, 89(53), Fall Meet. Suppl., Abstract H14A-01 (INVITED).

Zimmermann, A., Turner, B.L., Elsenbeer, H. 2008. Solute dynamics in a near-surface flowpath-dominated forest catchment, EOS Trans. AGU, 89(53), Fall Meet. Suppl., Abstract H13I-05.

Zimmermann, A. 2007. Spatial and temporal patterns of throughfall amounts and solutes in a tropical montane forest – Comparisons with findings from lowland rain forests, EOS Trans. AGU, 88(23), Jt. Assem. Suppl., Abstract B43A–01 (The talk was honored with the AGU Outstanding Student Paper Award, Biogeosciences Section).

SKILLS

Fluency in R and S-Plus (statistical programming environments), MatLab, MS-Office, Adobe Photoshop/Illustrator, ArcGIS

LANGUAGES

German	Native language
English	Fluency
Russian	Elementary knowledge
Spanish	Elementary knowledge

FELLOWSHIPS & AWARDS

2004	Short Term Fellowship, Smithsonian Tropical Research Institute
2006 – 2007	Graduate school "Earth Surface Processes: Dynamics, Scales and Changing Environments"
2007	AGU Outstanding Student Paper Award, Biogeosciences Section, American Geophysical Union Joint Assembly, Acapulco, Mexico

RESEARCH INTERESTS

I am interested in hydrological processes at different scales; from plot scale to the small catchment scale. My research has always involved experimental hydrology, although I am equally fascinated by methodological questions. Currently, one part of my research activity focuses on spatial and temporal patterns of throughfall and solute deposition. I am particularly interested to compare these patterns among different forest ecosystems to answer the question whether forest structure influences near-surface hydrological and biogeochemical patterns.

The other part of my research efforts concentrates on sediment and solute transport in forest ecosystems. At the moment I investigate the transport of different phosphor fractions in throughfall, overland flow and stream flow.

Author's declaration

I prepared this dissertation without illegal assistance. The work is original except where indicated by reference in the text and no part of the dissertation has been submitted for any other degree. This dissertation has not been presented to any other University for examination, neither in Germany nor in another country.

Alexander Zimmermann

Gamboa, Panama, March 2009